Universidad de Valladolid

ESCUELA DE INGENIERÍAS INDUSTRIALES

DEPARTAMENTO DE INGENIERÍA QUÍMICA Y TECNOLOGÍA DEL MEDIO AMBIENTE

TESIS DOCTORAL:

Development of functionalized aerogels for applications as catalyst and hydrides matrix

Presentada por Luis Miguel Sanz Moral para optar al grado de doctor por la Universidad de Valladolid

Dirigida por:

Dr.- Ing. Ángel Martín Martínez

Universidad de Valladolid

ESCUELA DE INGENIERÍAS INDUSTRIALES

DEPARTAMENTO DE INGENIERÍA QUÍMICA Y TECNOLOGÍA DEL MEDIO AMBIENTE

TESIS DOCTORAL:

Desarrollo y funcionalización de aerogeles para aplicaciones en catálisis y confinamiento de hidruros

Presentada por Luis Miguel Sanz Moral para optar al grado de doctor por la Universidad de Valladolid

Dirigida por:

Dr.- Ing. Ángel Martín Martínez

Memoria para optar al grado de Doctor, con **Mención Doctor Internacional**,

presentada por el Ingeniero Químico:

Luis Miguel Sanz Moral

Siendo los tutores en la **Universidad de Valladolid**:

Dr. D. Ángel Martín Martínez

Y en el **Delft University of Technology** (Países Bajos):

Dr. Georgios Stefanidis

Valladolid, Septiembre de 2016

UNIVERSIDAD DE VALLADOLID

ESCUELA DE INGENIERÍAS INDUSTRIALES

Secretaría

La presente tesis doctoral queda registrada en el folio número _____
del correspondiente libro de registro número _____

Valladolid, a _____ de_____ de 2016

Fdo. El encargado del registro

Ángel Martín Martínez

Investigador Senior Ramón y Cajal

Departamento de Ingeniería Química y Tecnología del Medio Ambiente
Universidad de Valladolid

Certifica que:

LUIS MIGUEL SANZ MORAL ha realizado bajo su dirección el trabajo *"Development of functionalized aerogels for applications as catalyst and hydrides matrix"*, en el Departamento de Ingeniería Química y Tecnología del Medio Ambiente de la Escuela de Ingenierías Industriales de la Universidad de Valladolid. Considerando que dicho trabajo reúne los requisitos para ser presentado como Tesis Doctoral expresan su conformidad con dicha presentación.

Valladolid, a _____ de_____ de 2016

Fdo. Ángel Martín Martínez

Reunido el tribunal que ha juzgado la Tesis Doctoral titulada *"Development of functionalized aerogels for applications as catalyst and hydrides matrix"* presentada por el Ingeniero Químico Luis Miguel Sanz Moral y en cumplimiento con lo establecido por el Real Decreto 99/2011 de 28 de enero de 2011 acuerda conceder por_____ la calificación de _____.

Valladolid, a _____ de_____ de 2016

PRESIDENTE SECRETARIO

1er Vocal 2º Vocal 3er Vocal

INDEX

ÍNDICE

Abstract

Development of functionalized aerogels for applications as catalyst and hydrides matrix

Urban air pollution is a serious problem in many large cities in the world. In addition, the increasing share of solar and wind in the energetic mix and its fluctuating nature, demands the development of technologies for storage of energy in periods of excess supply, to use it during the periods of excess demand. Direct use of these energy forms on onboard applications is also not possible, and requires an intermediate form of energy storage.

Hydrogen is good as energy vector. Hydrogen based fuel cells are being developed using hydrogen storage systems based on compressed, liquefied and materials-bounded hydrogen. Compared to gas and liquid storage tanks, solid hydrides can store high amounts of hydrogen in small volumes, which is liberated by a reversible chemical reaction by thermolysis.

One of the technological challenges which restrain the development of hydrides for H_2 storage is the heat transfer inside the storage tanks. Microwaves seems to be a promising alternative to overcome this obstacle.

Another option for the improving of the kinetic decomposition of hydrides is the nanoconfinement of the hydride inside a micro or mesoporous material. By confining the hydride inside the porous host, hydride particle size is restrained to the pore size, and particle agglomeration and growth process, which could have an adverse effect on the kinetic decomposition, are avoided.

Finally the addition of a catalyst which accelerates the hydride decomposition also looks interesting.

In this thesis aerogels have been developed in order to serve as catalyst support and as matrix for hydrides.

First of all synthesis and supercritical drying of silica aerogels made via a sol–gel process were studied. Tetramethylortosilicate was used as precursor. Hydrolysis and poly-condensation steps were followed by carbon dioxide supercritical drying (T = 45°C; P = 10.5 MPa). The complete supercritical drying step was video recorded in order to study the evolution of the size of the gels, concluding that a noticeable shrinkage only takes place during the decompression of CO_2 at the end of the drying process, being the total shrinkage of 3–4%. The mass transfer mechanisms during drying have also been studied through analysis of the evolution transparency of the aerogels along the supercritical drying process. The mass transfer processing during drying was observed to be dominated by convection in the earliest stages, where a direct relationship between drying rate and CO_2 flow were found. In the later stages, diffusion of the remaining organic solvent through the alcogel determined the mass transfer process.

The next step was controlling the surface chemistry of silica aerogels by tuning from hydrophilic to hydrophobic functionalization. Tetramethylorthosilicate or a mix of the first one with, trimethylethoxysilane were used as precursors. The hydrolysis and poly-condensation steps

were followed by carbon dioxide supercritical drying (T = 45°C; P = 10.5 MPa). The resulting dry hydrophilic aerogels were subjected to a hydrophobic surface treatment. Functionalization was achieved by using supercritical carbon dioxide as solvent media for different silane functionalization reactants: trimethylethoxysilane, octyltrimethoxysilane and chlorotrimethylsilane. Effects of the working pressure and reagent concentration on the functionalization were analyzed using FT-IR spectroscopy and exposing the treated aerogels to saturated moisture conditions in order to study the mass increment during the humidification. Nitrogen adsorption measurements show a considerable drop on the specific areas (13–17%) and on the pore volumes which were reduced by 50% by the functionalization treatment. By modification of the operating pressure and variation of the functionalization agent employed, the degree of functionalization could be gradually increased up to the values of the aerogels synthesized as hydrophobic in the sol–gel phase.

After the synthesis and functionalization the aerogels were ready to be used in different fields. Effective routes to obtain more valuable products require the design of efficient catalysts. These novel structures require the integration of support active sites in a way that preserves their advantages and capabilities. Therefore the development of novel catalytic structures achieved by the integration of metallic nanoparticles evenly distributed in a mesoporous and high-surface aerogel appears as a promising alternative. Thus Pd nanoparticles were embedded on silica aerogel by using three different techniques. In each of them the metal was loaded in the matrix at different steps of the production: the direct synthesis, the wet impregnation and the supercritical impregnation of the previously dried aerogels. The resultant materials were characterized to analyze the differences depending on the applied technique for its impregnation. Atomic absorption, nitrogen physisorption, X-ray diffraction, infrared spectroscopy and transmission electron microscopy where performed. In all the techniques the concentration of metal was varied (from 0.13% to 1.61 wt%) by modifying the concentration of the suspension (Pd-polyvinylpyrrolidone nanoparticles used in the direct synthesis) or of the solution of the metallic precursor (palladium acetylacetonate), both in the organic solvent and the supercritical media. The characterization had generally shown a good distribution of the metallic particles in the matrix, and a negligible effect of the metal on the textural properties. Finally, considerable variations where observed on the silanol groups on the surface of the catalysts. These materials were tested in D-glucose hydrogenation, observing significant differences on the performance of the catalyst depending on the synthesis technique employed. Another field of study of application of the functionalized aerogels was for the nanoconfinement of hydrogen storage hydrides. Nonoconfinement of these compounds has proven to improve the decomposition kinetics and to reduce their thermolysis temperature. On the contrary, in

some cases nanoconfinement could reduce the thermal conductivity, creating significant temperature gradients along the sample. To avoid this disadvantage, a C/SiO_2 mesoporous matrix was synthesized by keeping very interesting physical properties (386 m^2/g and 1.41 cm^3/g), leaving space for the confinement of a hydride and tuning the global dielectric properties of the complex, making it susceptible to microwave heating. This idea was protected by a national patent. Ethane 1,2-diaminoborane was embedded on the matrix (11-31 wt%) by using wet impregnation method. Material characterization and H_2 liberation tests by conventional heating and microwaves were performed showing the great potential of this technology. In addition numerical simulation of the device under microwaves was performed to reach better understanding of the process.

Finally the potential commercialization of the product obtained in this last step of the thesis was explore by developing a business model which offers batteries of different powers by using hydrides for hydrogen storage and fuel cell to transform it into electricity.

Introduction

Hydrogen society: description and challenges.

The vertiginous growth of the world population and the residential distribution model mainly focused on large cities originate important challenges to the human race.

Urban air pollution is a serious problem in many large cities in the world. The intense and incessant traffic, coupled with factories that do not control their emissions, turns the air of cities around the world in real clouds of smog. The levels of particulate pollutants in many cases exceed the safety limit for human health set by OMS. What is more, this institution has classified diesel smoke as carcinogenic to humans.

Another aspect to take into account is the increasing share of solar and wind in the energetic mix and the COP21 agreement pave the way for a new family of technologies based on renewable energy. Since these renewable energy forms are by their nature fluctuating, it is necessary to develop technologies for storage of energy in periods of excess supply, to use it during the periods of excess demand. Direct use of these energy forms on onboard applications is also not possible, and requires an intermediate form of energy storage.

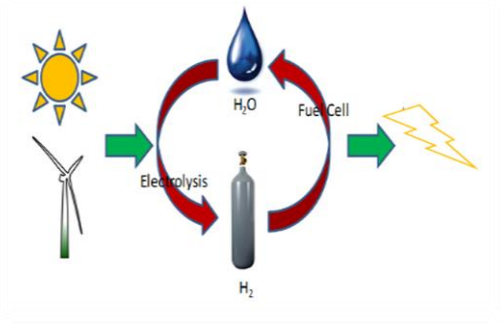

Figure 1.- hydrogen from renewable energy sources and society.

Many options have been explored, and hydrogen is one of the most promising alternatives to reach a sustainable society. Hydrogen is a good energy vector and avoids the emission of pollutants during its use in combustion or in a fuel cell. The challenge is being addressed using hydrogen storage systems based on compressed, liquefied and materials-bounded hydrogen[1]. Compared to gas and liquid storage tanks, solid hydrides can store high amounts of hydrogen in small volumes, which is liberated by a reversible chemical reaction by thermolysis.

One of the technological challenges which restrain the development of hydrides for H_2 storage is the heat transfer inside the storage tanks[2]. Great efforts have been made in order to overcome this challenge. Figure 2 shows one of the tanks developed as a part of the European research project “Nesshy”. The discs are made of compacted MgH_2 and Expanded Natural

Graphite. The heat is generated by an internal electric system (3 elements) and the cooling down is achived by forced air. This compex design is needed because the slow heat transfer and thermal inertia are important limitations of the storage tanks. However, this problem can be circumvented if heating energy is delivered directly to the material, and not by heat transfer through the storage tank. Application of microwaves offers this possibility.

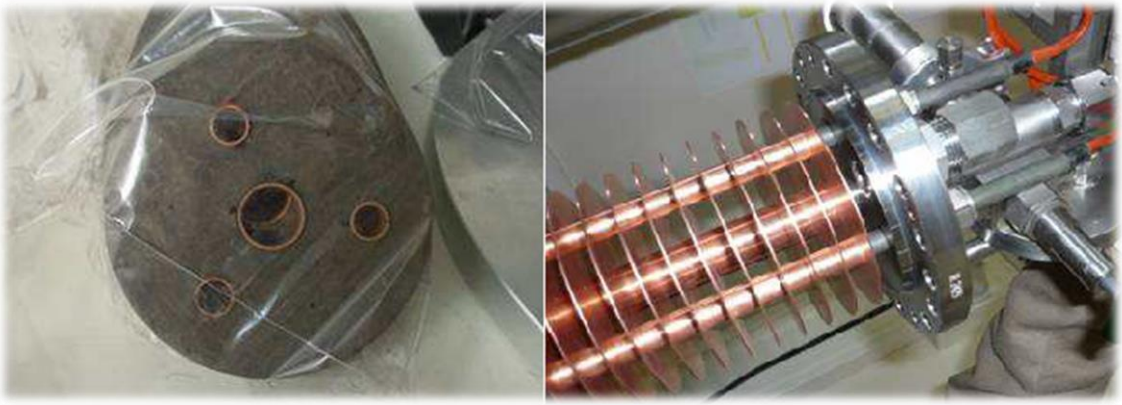

Figure 2.- Hydride tank developed by Nesshy.

Several metal hydrides decomposition under microwave irradiation were studied by Yuko Nakamori et al[3]. They concluded that the conductive lost and the particle size were the two most important parameters controlling the H_2 release. Ivaldete da Silva Dupim et al. showed that by particle size reduction a more effective heating of the particles was achieved by approximating the size of the particles to the penetration depth of the electromagnetic field in metallic powders. They obtained this size reduction by applying cold rolling[4]. Another technique is modifying the general dielectric properties of the complex by mixing with a hydride which actuates as a microwave absorber ($LiBH_4$)[5]. Huajun Zhang et al. propose the use of a honeycomb ceramic monolith coated with 0.54 wt% Ni (corresponding to 0.2 micron Ni thin layer) to hold the hydrides and allowed the rapid heating of the complex[6].

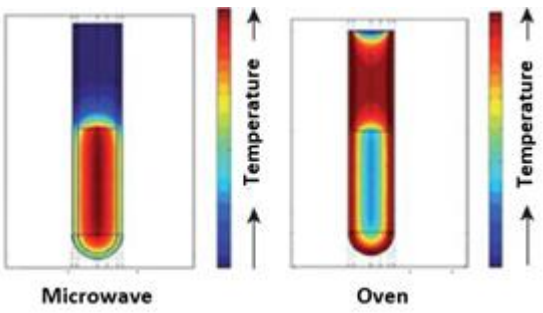

Figure 3.- Temperature gradients during heating with microwaves and traditional oven.

An alternative to improve the kinetic decomposition of hydrides is the nanoconfinement of the hydride inside a micro or mesoporous material. By confining the hydride inside the porous host, hydride particle size is restrained to the pore size, and particle agglomeration and growth process, which could have an adverse effect on the kinetic decomposition, are avoided. Moreover, some porous hosts, like carbon or silica mesoporous materials, chemically interact with different hydrides and destabilize it, further improving the decomposition kinetics. Payam Javadian et al. achived a temperature reduction of the decomposition of $0.7LiBH_4–0.3Ca(BH_4)_2$, by nanoconfining it in carbon aerogel scaffolds[7]. By combination of these effects, the decomposition temperature and release kinetics have been significantly improved[8].

Furthermore, the mesoporous host can be functionalized to provide additional properties to the material. In particular, it can be functionalized to enhance the absorption of microwave energy, and thus combine the main advantages of the two approaches: nanoconfinement and microwave heating. Indeed, a porous material with a high dielectric loss could confine the hydride and change the global dielectric properties of the complex. A material that fulfills this requirement is carbon, which can be manufactured as mesoporous carbon or as carbon aerogel. Some researchers have already confined hydrides into carbon scaffolds like $NaAlH_4$, $LiBH_4$[9] or $Mg(BH_4)_2$ [10,11]. But these carbon structures present a limitation which is its low pore volume that restricts the volume available for the confinement of hydride. Due to this limitation, the maximum hydride loadings achieved in carbon matrixes are between 15 and 30 wt%, which limits the hydrogen storage capacity below the requirements for practical applications. An alternative could be a hybrid material with leaves more pore space for the confinement of a hydride and tunes the global dielectric properties of the complex, making it susceptible of microwave heating.

Silica aerogel was already suggested as a very promising material for hydrides confinement due to its remarkable surface properties, and in particular to its high pore volumes that allow confining as much as a 60 wt% of hydride. Carbon/silica hybrid aerogels can combine favorable dielectric properties with high pore volumes. Carbon/silica porous materials can easily made by the carbonization of resorcinol–formaldehyde/silica aerogels, as described by Y. Kong et al.[12], keeping very interesting textural properties for encapsulation.

Aerogels: properties, synthesis and uses

Aerogels are micro-mesoporous materials with typical pore sizes of 10–100 nm, high surface areas (400–1500 m^2/g), low densities (typically 0.25–0.5 g/cm^3, although densities as low as

0.003 g/cm^3 can be achieved) and high porosities (92–98 %)[13]. This unique combination of characteristics, that confers very interesting properties to aerogels like a low thermal conductivity, ultra-low dielectric constant or low index of refraction, has given rise to a wide range of practical applications.

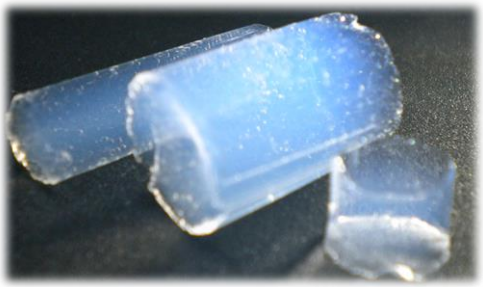

Figure 4.- silica aerogel cylindrical monoliths of different sizes.

The most developed application of aerogels, already in a commercial stage, is as high performance thermal insulating materials, which is favored by the low thermal conductivity of the material as well as by its low cost, low weight and high transparency to visible light[14]. Aerogels are also widely used as carrier materials, as their very high pore volumes (up to 4 cm^3/g) allow for loading capacities significantly above those of alternative porous materials, while their pore size characteristics provide favorable mass transfer conditions, with gas diffusion coefficients of the order of 0.1 cm^2/s, a similar order of magnitude as bulk gas diffusion coefficients[15]. Active compounds successfully loaded into aerogels include pharmaceuticals[16] and inorganic compounds[17]. The high thermal stability of silica aerogels, with melting temperatures above 1200 °C, makes them suitable for applications as catalyst supports in reactions performed at high temperatures, as for example hydrogenation reactions using palladium catalysts supported in aerogels[18]. Their surface activity, inferred by the abundance of hydroxyl groups that can be used as active sites for the incorporation of different functionalization agents[19], makes them useful as filters for volatile organics or for other applications in which an active surface is needed[20].

Aerogels are usually obtained through a two-step process: a sol–gel intertwining reaction, yielding a solid gel structure immersed in an alcohol solvent medium known as alcogel, and the removal of this solvent from the pores of this gel to produce a dry aerogel. The key process step that infers the unique textural properties of aerogels (high surface area, pore volume, pore size distribution…) is the solvent removal. This step can be difficult due to the surface tension of the liquid contained in the gel nanopores that infers a capillary pressure gradient during the formation of aerogels by drying of gels. Several techniques have been used in order

to dry the aerogels like atmospheric drying and freeze drying[21], but the most successful results have been obtained employing a supercritical drying technique[22], either with supercritical carbon dioxide or supercritical alcohol, that allows removing the solvent without formation of gas–liquid interfaces thus reducing the possible collapse of the pore structure of the aerogel during drying.

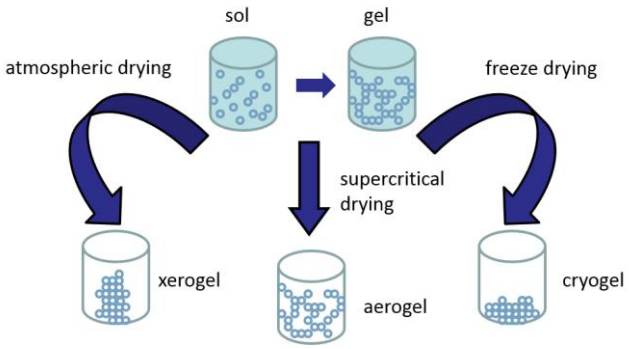

Figure 5.- silica gel synthesis and drying options.

Even employing supercritical drying methods, certain shrinkage of aerogels due to a partial collapse of their pore structure or other morphological variations is frequently observed after drying. This makes it difficult to obtain dry aerogels of a controlled, specified size. The effects of the aging and drying conditions on the properties of silica aerogels using supercritical alcohol drying have been studied by L. Kocon et al.[23] and Juncal Estella et al.[24] concluding that these conditions strongly influence the porous structure of silica gels, and that shrinkage during supercritical alcohol drying is mainly due to the restructuring of clusters. Using supercritical carbon dioxide for the drying, the impact of depressurizing rate on the porosity of resorcinol-formaldehyde gels has been investigated by G. Amaral-Labat et al.[25] and Orsolya Czakkel et al.[26], concluding that shrinkage always increased with increasing depressurizing rates. The results show that during the pressurization stage, the overall structure of the network remains unaffected by the rate of increase of pressure; on the other hand, depressurizing rate of the autoclave after drying has a significant influence on the final shrinkage, and hence on the resultant bulk density, surface area and pore volumes. Another point to consider is that if the diffusion time is not long enough, residual contents of solvent inside the aerogel could form a liquid phase during depressurization. Indeed, Zoran Novak et al.[27] claimed that cracks are caused by entering the two-phase region during the depressurization of the autoclave.

On the other hand, the precise characterization of the mass transfer mechanisms of aerogel drying is important for the evaluation of the minimum drying time required to achieve the

desired solvent residual content, which strongly influences the textural properties of the aerogel as concluded by García-González et al[28]. Most modeling studies of aerogel drying assume that drying is governed by the diffusion of organic solvent through aerogel pores. García-González et al. and P. Wawrzyniak et al.[29] studied the kinetic profile of the extraction curves of ethanol from silica aerogel, and correlated the results using the Fick's law in cylindrical coordinates. Novak et al. concluded that the diffusion coefficient was uniform throughout cylindrical aerogel samples. These authors observed significant discrepancies between model and experimental results during the first stages of drying, while a good agreement was attained in the latter stages. Based on these results, García-González et al. hypothesized that the process is governed by a mass transfer mechanism based on a combination of convection and diffusion, with an initial preponderance of convection and an increased contribution of diffusion to the process as drying time progresses and less solvent remains in the gels.

Aerogels functionalization: functionalization agents and methods

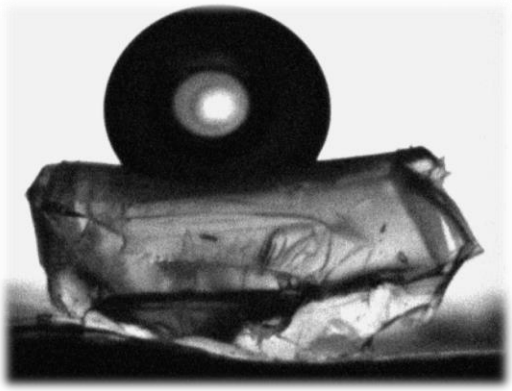

Figure 6.- water drop on the top of hydrophobic silica aerogel.

Common silica aerogels synthesized from precursors such as tetramethoxysilane or tetraethoxysilane are highly hydrophilic due to the abundance of hydroxyl surface groups in these aerogels. A collapse of the structure of such hydrophilic silica aerogels can be induced even by absorption of ambient humidity. In order to avoid this problem, or in cases in which a highly hydrophilic surface is not desirable, several surface modifications have been proposed. In general, the surface modification of silica alcogels occurs predominantly according to the following reaction:

$$xRE(OR')_n+yE(OR')_m+zH_2O\rightarrow R_qEO_p+wR'OH$$

Varying the functional groups (R) or the metal oxide (E) or the ratio between them can results in a number of interesting hybrid materials[30]. The main route for incorporation of these surface groups consists of adding different silica precursors. Suzana Štandeker et al. used methyltrimethoxysilane or trimethylethoxysilane in the standard sol–gel synthesis. This enables the adsorption of toxic organic compounds from water[31]. Suzana Štandeker et al. also prepared silica gels doped with mercapto functional groups in order to to remove Cu(II) and Hg(II) from aqueous solutions by mixing tetramethylorthosilicate, (3-mercaptopropyl)trimethoxysilane, methanol and water[32]. Different mix of tetramethylorthosilicate, tetraethylorthosilicate and vinyltriethoxysilane, phenyltrimethoxysilane, and phenyltriethoxysilane, were used by Naim Saad et al. in order to functionaliced the silica surface[33].

Another option is adding functionalizing agents in the liquid phase in which the sol–gel reaction takes place before drying[34]. Using this method, alcogels were functionalized by immersing them in chlorotrimethylsilane/ethanol/n-hexane solutions by Zhang et al[35]. Sung-Woo Hwang et al. also used trimethylchlorosilane, this time with isopropyl alcohol[36]. Joanna C.H. Wong et al. reached the hydrophobization of the surfaces by soaking the gels in a mixture of hexamethyldisilazane and heptane in an oven at 60°C for 24 h[37]. Anoher proposed agent was isooctyltrimethoxysilane in hexane bath, used by Maedeh Ramezani et al. to synthesise transparent superhydrophobic silica films[38]. K. Wörmeyer et al. functionalized the surface with a mono- and a tri-aminosilane in order to adsorpt CO_2, moisture and ethanol. They did it by placing the gels into an ethanol/aminosilane solution at 50°C. Gels were left at this temperature for 48 h for the aminosilane to be grafted to the surface of the gel. Afterwards, the functionalised gels were washed with ethanol[39]. A similar process was followed by Nick N. Linneen et al. by using toluene/aminosilane[40]. Sergey A. Lermontov et al. prepared prepare trifluoroacetylated aerogels by cogelation of (3-Aminopropyl)triethoxysilane with tetraethoxysilane, followed by trifluoroacetylation of free aminogroups[41]. Yannan Duan et al. studied the modification of silica particles using dimethoxy-methyl (3,3,3-trifluoropropyl) silane by three different methods during the gelation and after it. First, tetraethoxysilane and dimethoxy-methyl(3,3,3-trifluoropropyl)silane were mixed together in solution prior to hydrolysis and condensation, second dimethoxy-methyl(3,3,3-trifluoropropyl)silane was mixed with solution after tetraethoxy silane was completely hydrolyzed. Third, dimethoxy-methyl(3,3,3-trifluoropropyl)silane was added to alcogel and allowed to react with silica particles. They concluded that post-gelationmodification strategy works better for rendering silica aerogels more hydrophobic[42].

In some applications, it may be advantageous to switch from a hydrophilic to a hydrophobic surface functionalization of a finished, dry aerogel in different stages of the application. An example could be the deposition of an active compound inside the pores of the aerogel, which can be facilitated by the active surface hydroxyl groups of hydrophilic aerogel, followed by a use of this material in which the enhanced stability of a hydrophobic surface functionalization is required. Thus the development of methods for reversibly changing the surface functionalization of dry aerogels is of interest.

Some methods for a reversible hydrophobic surface modification of dry aerogels have been proposed. I. Smirnova et al. placed hydrophilic silica aerogels in a reactor and heated at 220°C. Methanol vapor was passed through the reactor for 13–40h. The resulting aerogels were extremely hydrophobic[43]. Other possibility is boiling and vaporizing the functionalization agent, and putting this vapor into contact with the aerogel. Babu S.K. Gorle et al. placed the silica aerogels in a reactor vessel and heated to 180°C while trimethylethoxysilane vapor continuously flows through the reactor. Typically it takes 48 h to ensure all of the free –OH groups are reacted although the reaction time for a specific aerogel depends on the amount of free –OH groups to be replaced by –O–Si–$(CH_3)_3$ groups[44]. A limitation of this method is the possible damage to the aerogel by condensation of the functionalization agent inside its pores. Even so, Jun Kyun Oh et al. silaniced dried hydrophilic silica aerogel by submerging then in a trimethylsilyl chloride solution. The hydrophobic aerogel thus obtained presented bacterial anti-adhesion properties[45]. Another possibility is putting into contact the aerogel with a solution of the functionalization agent in supercritical carbon dioxide. This facilitates the penetration of the functionalization agent into the pores of the aerogel thanks to the favorable transport properties in the supercritical fluid, and reduces the risk of damages to pore structure by condensation. Using this method, the surfaces of monolithic silica aerogels were rendered hydrophobic using hexamethyldisilazane as surface modification agent and supercritical-CO_2 as solvent by Kartal and Erkey[46]. Highly hydrophobic aerogels, with no modification of their optical properties, were obtained, and it was observed that the concentration of hexamethyldisilazane and the reaction time did not have a significant influence on the functionalization. Similarly, Concepción Domingo et al. measured the solubility of octyltriethoxysilane in sc-CO_2[47] and studied the functionalization of different porous materials by treatment with a solution of this precursor in the supercritical fluid[48]. M. Alnaief et al. studied the influence of performing the aerogel functionalization with amino groups at different steps of the synthesys: the functionalization of the dry silica aerogel by reaction in a gas phase, and functionalization of the gel in order to tune the adsorptive and

release properties of ketoprofen[49]. It also has to be considered that silane coating can be easily removed by heating the materials[50].

In applications of surface functionalization of pre-formed dry silica aerogels, it is important to achieve a good preservation of the properties of the aerogel after the functionalization treatment, and particularly of essential physical properties such as the available surface area and pore volume. Moreover, the possibilities to control the process in order to achieve different degrees of hydrophobicity tailored for specific applications are also relevant.

Particle deposition in silica aerogels: impregnation techniques

Silica aerogels present remarkable properties which make them suitable materials to incorporate controlled-size micro and nano particles, for example to prepare catalysts. As said before, the chemistry of aerogel surface can be controlled by using different alkyl–alkoxy/chloro silanes allowing to govern their grade of hydrophobicity[51]; in addition, the option of creating hybrid aerogels make almost all properties requirements achievable[52] .

Effective routes to obtain more valuable products require the design of efficient catalysts. These novel structures require the integration of support active sites in a way that preserves their advantages and capabilities. Therefore the development of novel catalytic structures achieved by the integration of metallic nanoparticles evenly distributed in a mesoporous and high-surface aerogel appears as a promising alternative.

By constrast, due to its breakability special techniques must be applied for their impregnation before or after the drying in order to avoid the capillarity forces which could damage the structure of the matrix. Nanometallic silver in silica aerogel matrix was prepared by placing the metal precursor in the synthesys media by Sandra Martínez et al[53]. A similar technique was used by Chien-Tsung Wang et al. in order to prepare iron oxide-silica aerogel. The resultant material was used as catalyst for methanol partial oxidation[54]. Ionic liquids have also been used by K. Anderson et al. as synthesis media. In this case the matrix was not cogelled with the metal precursor but with Pd colloid[55]. A. Navarrete et al. developed a new plasmonic composite by suspending Cu/ZnO catalyst in the gelation media[56]. Lindsey Sorensen et al. fabricated stable low-density silica aerogels containing luminescent ZnS capped CdSe quantum dots. The ZnS capped CdSe QDs of 6.0 and 2.5 nm dimension were prepared recapping CdOAc with (3-aminopropyl)triethoxysilane by ligand exchange in MeOH. This capping ligand has been shown to provide surface passivation and to couple covalently with the silica matrix[57]. Not only metals but also a colloidal mixture of activated carbon powders was added by M. Moner-Girona et al. in order to increases the elastic indentation recovery of the composite and reduce

shrinkage during supercritical drying[58]. Bullita et al. synthesized $ZnFe_2O_4$ nanoparticles on silica aerogel matrix by adding an ethanolic solution of the metal salts into the pre-hydrolyzed tetraethylorthosilicate[59]. S. Martínez et al. also embedded Ni and Pd nanoparticles on aerogels by impregnation of the gels followed by supercritical drying. The resultant catalysts were tested on the Mizoroki–Heck coupling reaction[60]. JF. Hund et al. formed metal clusters (Ag, Au) in a silica aerogel matrix by ɣ-irradiation of hydrogel precursors loaded with aqueous solutions containing Ag^+ or $[AuCl4]^-$ ions[61]. Cobalt catalysts supported on silica aerogel have been prepared by impregnation of the gels with an ethanolic solution of $Co(NO_3)_2$ $6H_2O$. The catalysts were active towards Fischer–Tropsch synthesis[62]. Finally supercritical CO_2 has been used as impregnation media and 1, 1, 1, 5, 5, 5-Hexafluoro-2, 4- pentanedione-palladium (2:1) as metal precursor[63]. Furthermore, the solubility of Palladium(II) acetylacetonate in supercritical CO_2 has been already studied, providing another Pd precursor which could be used in the supercritical impregnation (SCI) technique[64]. Benoît Heinrichs et al. prepared Pd/SiO_2-cogelled and impregnated aerogel catalysts after the drying[65] , concluding that the cogelled ones showed better resistance to sintering. Jinsoon Choi et al doped silica aerogels with Pt and Co by impregnation of the wet-gel obtaineing better distribution and textural properties than in the case of the cogelled ones[66]. Ll. Casas et al. prepared iron oxide nanoparticles hosted in silica aerogels. They added the iron presursor either to the silica gel or to the initial sol, observing that the magnetic properties of the nanoparticles can be controlled via synthesis conditions, matrix properties and thermal treatments[67].

Figure 7.- on the left, silica aerogel; at the center, silica arogel impregnated with ferrocene; on the right, silica aerogel impregnated with iron oxide.

This kind of catalyst could also be interesting for the improvement of the hydrides decomposition kinetics. A. Zaluska et al. concluded that an addition of a small amount of

catalyst (palladium or iron) offsets the negative effects of surface oxidation and eliminates the need for activation of MgH_2[68]. Concerning the support, M. Rueda et al. observed that the stabilization of AB into the silica aerogel microparticles, improves the release rate of hydrogen from AB[69]. Therefore a combination silica aerogel containening a small quantity of the metallic nanoparticules seems a promising material for hydrides catalyst.

[1] Zhou L, Progress and problems in hydrogen storage methods. Renew Sust Energ Rev 2005;9:395–408.

[2] Mazzucco A, Dornheim M, Sloth M, Jensen TR, Jensen JO, Rokni M. Bed geometries, fueling strategies and optimization of heat exchanger designs in metal hydride storage systems for automotive applications: A review. Int J Hhydrogen Energ, 2014;39:17054-7074.

[3] Nakamoria Y, Orimo S, Tsutaoka T. Dehydriding reaction of metal hydrides and alkali borohydrides enhanced by microwave irradiation. Applied Physics Letters 2006;88:112104.

[4] da Silva Dupim I, Ferreira Santos S, Huot J. Effect of Cold Rolling on the Hydrogen Desorption Behavior of Binary Metal Hydride Powders under Microwave Irradiation. Metals 2015;5:2021-2033.

[5] Leng HY, Wei J, Li Q, Chou KC. Effect of microwave irradiation on the hydrogen desorption properties of MgH2/LiBH4 composite. J Alloy Compd 2014;597:136–141.

[6] Zhang H, Geerlings H, Lin J, Chin WA. Rapid microwave hydrogen release from MgH2 and other hydrides. Int J Hydrogen Energ 2011;36:7580-7586.

[7] Javadian P, Sheppard DA, Buckley CE, Jensen TR. Hydrogen storage properties of nanoconfined LiBH4–Ca(BH4)2. Nano Energy 2015;11: 96–103.

[8] Nielsen TK, Besenbacherb F, Jensen TR. Nanoconfined hydrides for energy storage. Nanoscale 2011;3:2086–2098.

[9] Gao J, Ngene P, Herrich M, Xia W, Gutfleisch O, Muhler M, de Jong KP, de Jongh PE. Interface effects in NaAlH4ecarbon nanocomposites for hydrogen storage. Int J Hydrogen Energ 2014; 3 9;10175-10183.

[10] Yan Y, Au YS, Rentsch D, Remhof A, de Jongh PE, Züttel A. Reversible hydrogen storage in Mg(BH4)2/carbon nanocomposites. J Mater Chem A 2013;1:11177.

[11] Au YS, Yan Y, de Jong KP, Remhof A, de Jongh PE. Pore Confined Synthesis of Magnesium Boron Hydride Nanoparticles. J Phys Chem C 2014;118:20832–20839.

12 Kong Y, Zhong Y, Shen X, Cui S, Yang M, Teng K, Zhang J.Facile synthesis of resorcinol–formaldehyde/silica composite aerogels and their transformation to monolithic carbon/silica and carbon/silicon carbide composite aerogel. J. Non-Cryst. Solids 2012;354:3150–3155.

[13] Fricke J. Aerogels. Springer-Verlag, Berlin, 1986.

[14] Fricke J, Emmerling A, Aerogels – recent progress in production techniquesand novel applications. J. of Sol–Gel Science and Technology 1999;13:299–303.

[15] Stumpf C, Gässler K, Reichenauer G, Fricke J, Dynamic gas flow measurementson aerogels. J. of Non-Crystalline Solids 1992;145:180–184.

[16] Smirnova I, Mamic J, Arlt W, Adsorption of drugs on silica aerogels. Langmuir 20003;19:8521–8525.

[17] Goodwin TJ, Leppert VJ, Smith CA, Risbud SH, Nuemeyer M, Power PP, Lee HWH, Hrubesch LW, Synthesis of nanocrystalline gallium nitride in silicaaerogels. Applied Physics Letters 1996;69(21):3230–3232.

[18] Jespersen HT, Standeker S, Novak Z, Schaumburg K, Madsen J, Knez Z. Supercritical fluids applied to the sol–gel process for preparation of AERO-MOSILS/palladium particle nanocomposite catalyst. J Supercrit Fluid 2008;46:178–184.

[19] Sanz-Moral LM, Rueda M, Nieto A, Novak Z, Knez Z, Martín Á. Gradual hydrophobic surface functionalization of dry silica aerogels by reaction with silane precursors dissolved in supercritical carbon dioxide. J Supercrit Fluid 2013;84:74–79.

[20] Yoda S, Ohtake K, Takebayashi Y, SugetaT, SakoT, Sato T. Preparation of titania-impregnated silica aerogels and their application to removal of benzenein air. J. Materials Chemistry 2000;10:2151–2156.

[21] Smitha S, Shajesh P, Aravind PR, Kumar SR, Pillai PK, Warr-ier KGK. Effect of aging time and concentration of aging solution on the porositycharacteristics of subcritically dried silica aerogels. Micropor Mesopor Mat 2006;91: 286–292.

[22]Alain CR, Gérard MP. Chemistry of aerogels and their applications, Chem Rev

[23] Kocon L, Despetis F, Phalippou J. Ultralow density silica aerogels by alcohol supercritical drying. J. Non-Crystalline Solids 1998;225:96–100.

[24] Juncal E, Echeverría JC, Laguna M, Garrido JJ. Effects of aging and drying conditions on the structural and textural properties of silica gels, Micropor Mesopor Mat 2007;102:274–282.

[25] Amaral-Labat G, Szczurek A, Fierro V, Masson E, Pizzi A, Celzard A. Impact of depressurizing rate on the porosity of aerogels, Micropor Mesopor Mat 2012;152:240–245.

[26] Czakkel O, Nagy B, Geissler E, László K. In situ SAXZ investigation of structural changes in soft resorcinol-formaldehyde polymer gels during CO_2-drying. J Supercrit Fluid 2013;75:112–119.

[27] Novak Z, Knez Z. Diffusion of methanol-liquid CO_2 and methanol-supercritical CO_2 in silica aerogels, J. Non-Crystalline Solids 1997;221:163–169.

[28] García-González CA, Camino-Rey MC, Alnaief M, Zetzl C, Smirnova I. Supercritical drying of aerogels using CO_2: effect of extraction time on the end material textural properties. J Supercrit Fluid 2012;66:297–306.

[29] Wawrzyniak P, Rogacki G, Pruba J, Bartczak Z. Effective diffusion coefficient in the low temperature process of silica aerogel production. J. Non-CrystallineSolids 2001;285:50–56.

[30] Schubert U, Husing N, Lorenz A. Hybrid inorganic–organic materials by sol-gel processing of organofunctional metal alkoxides. Chem Mater 1995;7:2010–2027.

[31] Standeker S, Novak Z, Knez Z. Adsorption of toxic organic compounds from water with hydrophobic silica aerogels. J Colloid Interf Sci2007;310:362–368.

[32] Štandeker S, Veronovski A, Novak Z, Knez Ž. Silica aerogels modified with mercapto functional groups used for Cu(II) and Hg(II) removal from aqueous solutions. Desalination 269 (2011) 223–230

[33] Saad N, Al-Mawla M, Moubarak E, Al-Ghoul M, El-Rassy H. Surface-functionalized silica aerogels and alcogels for methylene blue adsorption. RSC Adv.2015;5:6111–6122

[34] Yokogawa H, Yokoyama M. Hydrophobic silica aerogels. J Non-Cryst Solids 1995;186:23–29.

[35] Wua G, Yu Y, Cheng X, Zhang Y. Preparation and surface modification mech-anism of silica aerogels via ambient pressure drying. Mater Chem Phys 2011;129:308–314.

[36] Hwang SW, Kim TY, Hyun Sh. Effect of surface modification conditions on the synthesis of mesoporous crack-free silica aerogel monoliths from waterglass via ambient-drying. Micropor Mesopor Mat 2010;130:295–302.

[37] Wong JCH, Kaymak H, Brunner S, Koebel MM. Mechanical properties of monolithic silica aerogels made from Polyethoxydisiloxanes. Micropor Mesopor Mat 2014;183:23–29.

[38] Ramezania M, Vaezia MR, Kazemzadeh A. Preparation of silane-functionalized silica films via two-step dipcoating sol–gel and evaluation of their superhydrophobic properties. Appl Surf Sci 2014;317:147–153.

[39] Wörmeyer k, Smirnova I. Adsorption of CO_2, moisture and ethanol at low partial pressure using aminofunctionalised silica aerogels. Chem Eng J 2013;225:350–357.

[40] Linneen NN, Pfeffer R, Lin YS. CO_2 adsorption performance for amine grafted particulate silica aerogels. Chem Eng J 2014;254:190–197.

[41] Lermontov SA, Sipyagina NA, Malkova, Yarkov AV, Baranchikov AE, Kozikc VV, Ivanov VK. Functionalization of aerogels by the use of pre-constructed monomers: the case of trifluoroacetylated (3-aminopropyl)triethoxysilane. RSC Adv. 2014;4:52423.

[42] Duan Y, Jana SC, Lama B, Espe MP. Hydrophobic silica aerogels by silylation. J Non-Cryst Solids 2016;437:26–33.

[43] Smirnova I, Suttiruengwong S, Arlt W. Feasibility study of hydrophilic and hydrophobic silica aerogels as drug delivery systems. J Non-Cryst Solids 2004;350:54–60.

[44] Gorle BSK, Smirnova I, McHugh MA. Adsorption and thermal release of highly volatile compounds in silica aerogels. J Supercrit Fluid 2009;48:85–92.

[45] Oh JK, Perez K, Kohli N, Kara V, Li J, Min Y, Castillo A, Taylor M, Jayaraman A, Cisneros-Zevallos L, Akbulut M. Hydrophobically-modified silica aerogels: Novel food-contact surfaces with bacterial anti-adhesion properties. Food Control 2015;52:132-141.

[46] Kartal AM, Erkey C. Surface modification of silica aerogels by hexamethyldisilazane–carbon dioxide mixtures and their phase behavior. J Supercrit Fluid 2010;53:115–120.

[47] García-González CA, Fraile J, López-Periago A, Saurina J, Domingo C. Mea-surements and correlation of octyltriethoxysilane solubility in supercritical CO_2 and assembly of functional silane monolayers on the surface of nanometricparticles. Ind Eng Chem Res 2009;48:9952–9960.

[48] Builes S, López-Aranguren P, Fraile J, Vega LF, Domingo C. Alkylsilane-functionalized microporous and mesoporous materials: molecular simulationand experimental analysis of gas adsorption. J Phys Chem C 2012;116(18:10150–10161.

[49] Alnaief M, Smirnova I. Effect of surface functionalization of silica aerogel on their adsorptive and release properties. J Non-Cryst Solids 2010;356:1644–1649.

[50] Cui S, Liu Y, Fan M, Cooper AT, Lin B, Liu X, Han G, Shen X. Temperature dependent microstructure of MTES modified hydrophobicsilica aerogels. J Mater Sci Lett 2011;65:606–609.

[51] Venkateswara Rao A , Kulkarni MM , Amalnerkar DP , Seth T . Surface chemical modification of silica aerogels using various alkyl–alkoxy/chloro silanes. Appl Surf Sci 2003;206(1-4):262–70.

[52] Maleki H, Durães L, Portugal A. An overview on silica aerogels synthesis and different mechanical reinforcing strategies. J Non-Cryst Solids 2014;385:55–74.

[53] Martínez S, Vallribera A, Cotet CL, Popovici M, Martín L, Roig A, Moreno-Mañasa M, Molinsd E. Nanosized metallic particles embedded in silica and carbon aerogels as catalysts in the Mizoroki–Heck coupling reaction. New J Chem 2005;29:1342–1345.

[54] Wang CT, Ro SH. Nanocluster iron oxide-silica aerogel catalysts for methanol partial oxidation. Applied Catalysis A: General 2005;285:196–204.

[55] Anderson K, Fernández SC, Hardacre K, Marr PC. Preparation of nanoparticulate metal catalysts in porous supports using an ionic liquid route; hydrogenation and C–C coupling. Inorg Chem Commun 2004;7:73–76.

[56] Navarrete A, Muñoz S, Sanz-Moral LM, Brandner JJ, Pfeifer P, Martín Á, Dittmeyer R, Cocero MJ. Novel windows for “solar commodities”: a device for CO_2 reduction using plasmonic catalyst activation. Faraday Discuss. 2015;183:249-59.

[57] Sorensen L, Strouse JF, Stiegman AE. Fabrication of Stable Low-Density Silica Aerogels Containing Luminescent ZnS Capped CdSe Quantum Dots. Adv. Mater. 2006;18:1965–1967.

[58] Moner-Girona1M, Martínez E, Esteve J, Roig A, Solanas R, Molins E. Micromechanical properties of carbon–silica aerogel composites. Appl. Phys. A 2002;74: 119–122.

[59] Bullita S,Casu A, Casula MF, Concas G, Congiu F, Corrias A, Falqui A, Lochea D, Marrasa C. $ZnFe_2O_4$ nanoparticles dispersed in a highly porous silica aerogel matrix: a magnetic study. Phys.Chem.Chem.Phys., 2014;16:4843.

[60] Martínez S, Vallribera A, Cotet CL, Popovici M, Martín L, Roig A, Moreno-Mañasa M, Molinsd E. Nanosized metallic particles embedded in silica and carbon aerogels as catalysts in the Mizoroki–Heck coupling reaction. New J Chem 2005;29:1342–1345.

[61] Hund JF, Bertino MF, Zhang G, Sotiriou-Leventis C, Leventis N, Tokuhiro AT, Farmer J. Formation and Entrapment of Noble Metal Clusters in Silica Aerogel Monoliths by ɣ -Radiolysis. J. Phys. Chem. *B* 2003;107:465-469.

[62] Dunna BC, Colea P, Covingtona D, Webstera MC, Pugmirea RJ, Ernsta RD, Eyringa EM, Shahb N, Huffman GP. Silica aerogel supported catalysts for Fischer–Tropsch synthesis. Applied Catalysis A: General 2005;278:233–238.

[63] Morley KS , Licence P , Patricia CM , Hyde JR , Brown PD , Mokaya R , Xia Y , How- dle SM . Supercritical fluids: A route to palladium-aerogel nanocomposites. J Mater Chem 2004;14:1212–17.

[64] Yoda S , Hasegawa A , Suda H , Uchimaru Y , Haraya K , Tsuji T , Otake K . Preparation of a platinum and palladium/polyimide nanocomposite film as a precursor of metal-doped carbon molecular sieve membrane via supercritical impregna- tion. Chem Mater 2004;16:2363–8.

[65] Heinrichs B, Noville F, Pirard JP. Pd/SiO2-Cogelled Aerogel Catalysts and Impregnated Aerogel and Xerogel Catalysts: Synthesis and Characterization. J Non-Cryst Solids 2006;352:737–746

[66] Choi K, Shin CB, Suh DJ. Co-promoted Pt catalysts supported on silica aerogel for preferential oxidation of CO. Catalysis Communications 2008;9:880–885.

[67] Casas1 Ll, Roig A, Molins1 E, Grenèche JM, Asenjo J, Tejada J. Iron oxide nanoparticles hosted in silica aerogels. Appl. Phys. A 2002;74:591–597.

[68] Zaluska A, Zaluski L, Ström–Olsen JO. Nanocrystalline magnesium for hydrogen storage. J. Alloys Compd. 1999;288:217–225.

[69] Rueda M, Sanz-Moral LM, Nieto-Márquez A, Longone P, Mattea F, Martín Á. Production of silica aerogel microparticles loaded with ammoniaborane by batch and semicontinuous supercritical drying techniques. J Supercrit Fluid 2014;92:299–310.

Objectives

Many solid state hydrogen storage materials have been proposed that can offer high amounts of hydrogen in their composition but whose performance is hurdled by high decomposition temperature, formation of gas by-products or slow kinetics. Different strategies have been proposed to eliminate these problems, with various degrees of success. Of these, a particularly relevant method that is considered in this thesis is the nanoconfinement of the solid storage material within a micro/mesoporous support material.

As described in the introduction, this approach is limited by two important factors: the amount of hydride that can be effectively confined into the support, and the slow rate of mass and energy transfer within the support. The objective of this thesis is to obtain the knowledge needed to develop a new support material based on aerogels that can overcome these two limitations.

With this general objective, the specific objectives of this thesis are:

1. Development of a light porous complex which stabilizes a hydride inside its pores
   1.1 In situ study of the supercritical drying process of aerogels with carbon dioxide in order to understand the phenomena which takes place during this process.
   1.2 Control of the chemistry of the surface of the synthesized aerogels.
2. Improvement of the heat transfer of nonoconfined hydrides.
   2.1 Synthesis of hybrid aerogels which keeps enough pore volume for the hydride confinement and improve the global heat transfer.
3. Process and energy intensification of the heating system which decomposes the confined hydride.
   3.1 Synthesis of a hybrid aerogels which tunes the dielectric properties of the complex.
   4.2 Design of a system which allows to heat up the confined hydrides by applying microwaves.
4. Explore the creation of novel catalyst by using aerogel as support.
   4.1 Study the influence of the techniques and solvents used for the metal impregnation on the final properties of the catalyst.
5. Design of a business model and evaluation of the viability of a company created around the technology developed during the thesis.

Chapter 1

View cell investigation of silica aerogels during supercritical drying: Analysis of size variation and mass transfer mechanisms

View cell investigation of silica aerogels during supercritical drying: Analysis of size variation and mass transfer mechanisms

Abstract

We report the synthesis and supercritical drying of silica aerogels made via a sol–gel process. Tetramethylortosilicate has been used as precursor. Hydrolysis and poly-condensation steps were followed by carbon dioxide supercritical drying (T=45°C; P = 10.5 MPa). The complete supercritical drying step was video recorded in order to study the evolution of the size of the gels, concluding that a noticeable shrinkage only takes place during the decompression of CO_2 at the end of the drying process, being the total shrinkage of 3–4 %. The mass transfer mechanisms during drying have also been studied through analysis of the evolution transparency of the aerogels along the supercritical drying process. The mass transfer processing during drying was observed to be dominated by convection in the earliest stages, where a direct relationship between drying rate and CO_2 flow were found. In the later stages, diffusion of the remaining organic solvent through the alcogel determined the mass transfer process.

Keywords: Silica aerogel, Supercritical carbon dioxide, Advection, Shrinkage, Drying front.

1. Introduction

Aerogels are micro-mesoporous materials with typical pore sizes of 10–100 nm, high surface areas (400–1500 m^2/g), low densities (typically 0.25–0.5 g/cm^3, although densities as low as 0.003 g/cm^3 can be achieved) and high porosities (92–98 %) [1]. This unique combination of characteristics, that confers very interesting properties to aerogels like a low thermal conductivity, ultralow dielectric constant or low index of refraction, has given rise to a wide range of practical applications. The most developed application of aerogels, already in a commercial stage, is as high performance thermal insulating materials, which is favored by the low thermal conductivity of the material as well as by its low cost, low weight and high transparency to visible light [2]. Aerogels are also widely used as carrier materials, as their very high pore volumes (up to 4 cm^3/g) allow for loading capacities significantly above those of alternative porous materials, while their pore size characteristics provide favorable mass transfer conditions, with gas diffusion coefficients of the order of 0.1 cm^2/s, a similar order of magnitude as bulk gas diffusion coefficients [3]. Active compounds successfully loaded into aerogels include pharmaceuticals [4] and inorganic compounds [5]. The high thermal stability of silica aerogels, with melting temperatures above 1200°C, makes them suitable for applications

as catalyst supports in reactions performed at high temperatures, as for example hydrogenation reactions using palladium catalysts supported in aerogels [6]. Their surface activity, inferred by the abundance of hydroxyl groups, that can be used as active sites for the incorporation of different functionalization agents [7], makes them useful as filters for volatile organics or for other applications in which an active surface is needed [8]. Aerogels are obtained through a two-step process: a sol–gel intertwining reaction, yielding a solid gel structure immersed in an alcohol solvent medium known as alcogel, and the removal of this solvent from the pores of this gel to produce a dry aerogel. The key process step that infers the unique textural properties of aerogels (high surface area, pore volume, pore size distribution. . .) is the solvent removal. This step can be difficult due to the surface tension of the liquid contained in the gel nanopores that infers a capillary pressure gradient during the formation of aerogels by drying of gels. Several techniques have been used in order to dry the aerogels like atmospheric drying and freeze drying [9], but the most successful results have been obtained employing a supercritical drying technique [1,10], either with supercritical carbon dioxide or supercritical alcohol, that allows removing the solvent without formation of gas–liquid interfaces thus reducing the possible collapse of the pore structure of the aerogel during drying. Even employing supercritical drying methods, certain shrinkage of aerogels due to a partial collapse of their pore structure or other morphological variations is frequently observed after drying. This makes it difficult to obtain dry aerogels of a controlled, specified size. The effects of the aging and drying conditions on the properties of silica aerogels using supercritical alcohol drying have been studied by L. Kocon et al. [11] and Juncal Estella et al. [12] concluding that these conditions strongly influence the porous structure of silica gels, and that shrinkage during supercritical alcohol drying is mainly due to the restructuring of clusters. Using supercritical carbon dioxide for the drying, the impact of depressurizing rate on the porosity of resorcinol-formaldehyde gels has been investigated by G. Amaral-Labat et al. [13] and Orsolya Czakkel et al.[14], concluding that shrinkage always increased with increasing depressurizing rates. The results show that during the pressurization stage, the overall structure of the network remains unaffected by the rate of increase of pressure; on the other hand, depressurizing rate of the autoclave after drying has a significant influence on the final shrinkage, and hence on the resultant bulk density, surface area and pore volumes. Another point to consider is that if the diffusion time is not long enough, residual contents of solvent inside the aerogel could form a liquid phase during depressurization. Indeed, Zoran Novak et al. [15] claimed that cracks are caused by entering the two phase region during the depressurization of the autoclave. On the other hand, the precise characterization of the mass transfer mechanisms of aerogel drying is important for the evaluation of the minimum drying time required to achieve the desired solvent residual content, which strongly influences

the textural properties of the aerogel as concluded by García-González et al.[16]. Most modeling studies of aerogel drying assume that drying is governed by the diffusion of organic solvent through aerogel pores. García-González et al. [16] and P. Wawrzyniak et al. [17] studied the kinetic profile of the extraction curves of ethanol from silica aerogel, and correlated the results using the Fick's law in cylindrical coordinates. Novak et al. [15] concluded that the diffusion coefficient was uniform throughout cylindrical aerogel samples. These authors observed significant discrepancies between model and experimental results during the first stages of drying, while a good agreement was attained in the latter stages. Based on these results, García-González et al. [16] hypothesized that the process is governed by a mass transfer mechanism based on a combination of convection and diffusion, with an initial preponderance of convection and an increased contribution of diffusion to the process as drying time progresses and less solvent remains in the gels. In this work, tetramethylortosilicate (TMOS) has been used as precursor of a sol–gel reaction forming gel monoliths of different sizes in methanol solvent media, and solvent from these alcogels has been removed by extraction with supercritical carbon dioxide thus producing dry aerogel monoliths. The drying process has been carried out in a high pressure view cell. It has been video recorded in order to follow the evolution of the aerogels during the drying with supercritical carbon dioxide, paying special attention to the size variation and the advective transport during the first stages of the drying. With this, direct information regarding the mass transfer mechanisms and the drying steps in which variations of the dimensions of the aerogel occur has been obtained.

2. Experimental methods

2.1. Reagents

Tetramethoxysilane (98 % purity), and NH_4OH (28.0–30.0 %) were purchased from Sigma–Aldrich (Spain). Methanol (99.8 %purity) was obtained from Panreac (Spain). CO_2 (>99.95 purity) was supplied by Carburos Metálicos S.A. (Spain) Deionized water was used in all experiments.

2.2 Processing

2.2.1 Preparation of silica gel cylindrical monoliths

Hydrophilic silica alcogels were produced following the sol–gel process used by other authors such as Suzana Standekeret al. [18] or Carlos Folgar et al. [19], following the molar ratio:

TMOS:CH_3OH:H_2O:NH_4OH, 1:3:4:5 × 10^{-3}. Methanol and TMOS were mixed together and the solution of ammonium hydroxide–water was added to the mixture drop by drop. After a few seconds the stirrer was stopped and the mixture was poured into cylindrical molds of different diameters (∼8.9 mm and ∼14.2 mm) for gelation. Straightaway, gels were immersed in methanol for aging during a period of at least 7 days. During this time methanol was renewed twice in order to completely remove water from the solution before initiating the supercritical CO_2 drying of the gels.

2.2.2 Supercritical drying of gels

The equipment schematized in figure 1 was used for supercritical drying of alcogels. The main components were a 1 L CO_2 buffer, a 25 mL extractor (view chamber) and a recirculation gear pump whose frequency of rotation could be modified thus varying the CO_2 flowrate through the view cell. The entire equipment was placed inside a hot air circulating oven that kept the temperature constant during drying. After the aging period described in Section 2.2.1, alcogels were placed on a metallic tray in the extractor. Straightaway, the rest of the container was filled up with methanol in order to avoid the formation of cracks in the alcogel while the supercritical conditions were reached. Then the complete equipment was heated and CO_2 was pumped into the circuit. Once the operation conditions were reached (10.5 MPa, 45°C), the recirculation pump was activated and extraction of methanol began. In order to increase the efficiency of drying, CO_2 in the closed circuit was renewed several times during each experiment. During CO_2 renewal, the extractor was isolated from the rest of the circuit by closing the valves in the inlet and outlet of the extractor, which allowed to renew the CO_2 of the rest of the circuit without decompressing the view chamber, thus minimizing the damage in the aerogel structure due to pressure variations during CO_2 renewal. Three loads of fresh CO_2 were required in order to remove methanol from the alcogels. These loads were renewed after extraction times of 30 min in the first cycle, 45 min in the second cycle, and 45 additional minutes in the third cycle. Adding the time spent between the cycles (when reloads took place), the total drying time was about 3 h, in good agreement with the times proposed by different authors including M.J. van Bommel et al. [20]. Finally the equipment was slowly depressurized in order to avoid formation of cracks in aerogels. Different decompression rates of the order of ∼0.3 bar/min were tested. The entire process was recorded using a DMK 31BU03.H camcorder from Imaginsource connected to a computer using the IC Capture2.1 software.

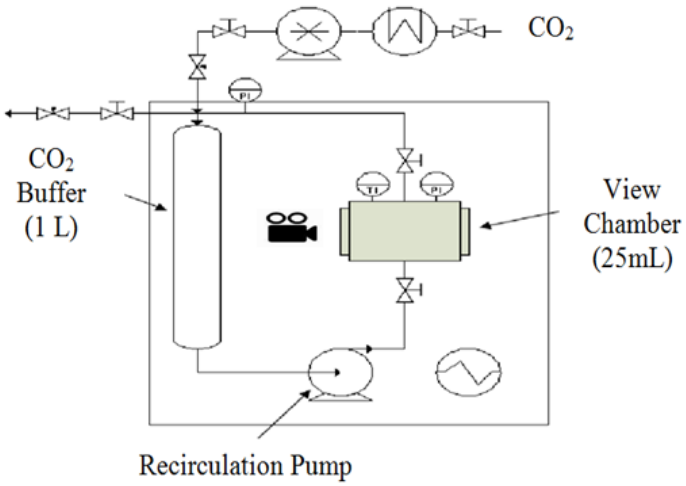

Figure 1. Equipment used for de supercritical drying of the alcogels.

2.3 Image analysis

The size of the gels was followed analyzing video captures using a Leica Application Suite image analysis software. In order to rule out optical effects due to the possible influence of the variation of refractive indexes of the supercritical fluid in the chamber, associated to variations in pressure and fluid density, a metallic rod of known dimensions was also introduced in the view cell near the aerogel, and its size, determined using the same image analysis software, was used as a reference for the calculation of the size of the aerogels. Additionally, captures taken from the videos during different instants of the process were transformed into a matrix of gray scale light intensity values using the Image Processing Toolbox™ of Matlab (r) R2012a. These matrixes were processed using the improfile function of the Image Processing Toolbox™ in order to obtain radial profiles of light intensity in the aerogel.

2.4 Characterization of textural properties

The physical characterization of surface area and pore volume was done using a Quantasorb Sorption System (QuantachromeInstruments) with N_2 (at −196°C) as sorbate. Prior to analysis, samples were degassed overnight at 180°C. Total specific surfaceareas were determined by the multipoint BET method at nitrogen partial pressure/saturated vapor pressure at −196°C $P/P_0 \leq 0.3$,and total specific pore volumes were evaluated from N_2 uptake at $P/P_0 = 0.99$.

3. Results and discussion

3.1 Monitoring of the size evolution of the hydrophilic aerogels during the supercritical drying

Aerogels obtained by supercritical CO_2 drying in this work presented specific areas of ~500 m^2/g and pore volumes of 1.15 cm^3/g which agrees with typical values of these properties for aerogels obtained by other authors such as Rami Al-Oweini et al. [21], thus indicating that the formation of the aerogels by supercritical drying was successful. The size of gels was followed studying captures taken from the attached video 1 provided as supplementary material, and examining the dimensions of the radius of gels as shown in figure 2. Supplementary video 1 related to this article can be found, in the online version, at http://dx.doi.org/10.1016/j.supflu.2014.05.004. In figure 3, the evolution of the dimension of the radius of the cylindrical silica monoliths whose initial dimensions were ~8.9 mm and~14.2 mm diameter, and ~15 mm height, is represented. A small increase in the radius of the alcogels was noticed between the load and the pressurization of the view-chamber. That must be induced by the expansion of the methanol when the CO_2 is dissolved (30 min) and by the pressure exerted by the expanded methanol when leaving the pores. After it and during all the supercritical washing (till 180 min), the dimension almost stayed unaltered. Finally, a considerable drop in the radius was observed during the depressurization coinciding with the observations of G. Amaral-Labat et al. [13] and Orsolya Czakkel et al. [14] on the importance of this last stage on the shrinkage of the aerogels. The total shrinkage for the ~8.9 mm and ~14.2 mm diameter aerogels was about 3 % and 4 % (with respect to the initial aerogel radius) respectively. These values of shrinkage agree with those obtained by H. Yokogawa et al.[22].

It was also checked that under the same drying conditions (i.e.: same drying time with the same CO_2 flowrate, temperature and pressure conditions and aerogel dimensions), that can be expected to lead to the same residual methanol concentration in the final aerogels, there is a critical depressurization velocity above which cracks appear in the aerogel, being the aerogels of bigger diameter the more sensitive ones to this phenomena. This result suggests that damages to aerogels during depressurization are caused by mechanical stresses caused by the expansion of CO_2 inside the aerogel pores, rather than to the appearance of liquid methanol if the aerogel is not dry enough. Mechanical stresses can become more severe if the depressurization is faster, and there not enough time is given to let the expanding CO_2 leave the pores of the aerogel. The same conclusion was also reported by George W. Scherer [23].

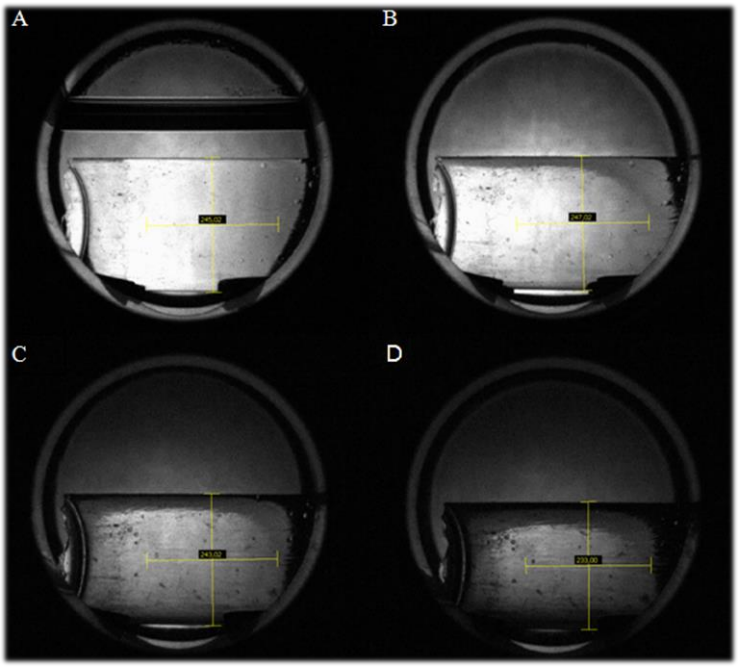

Figure 2. Evolution of the aerogel dimensions during the supercritical drying (longitudinal view): A.Before pressurizing (immersed in methanol) B.After pressurizing C.After the supercritical washing D.After depressurizing.

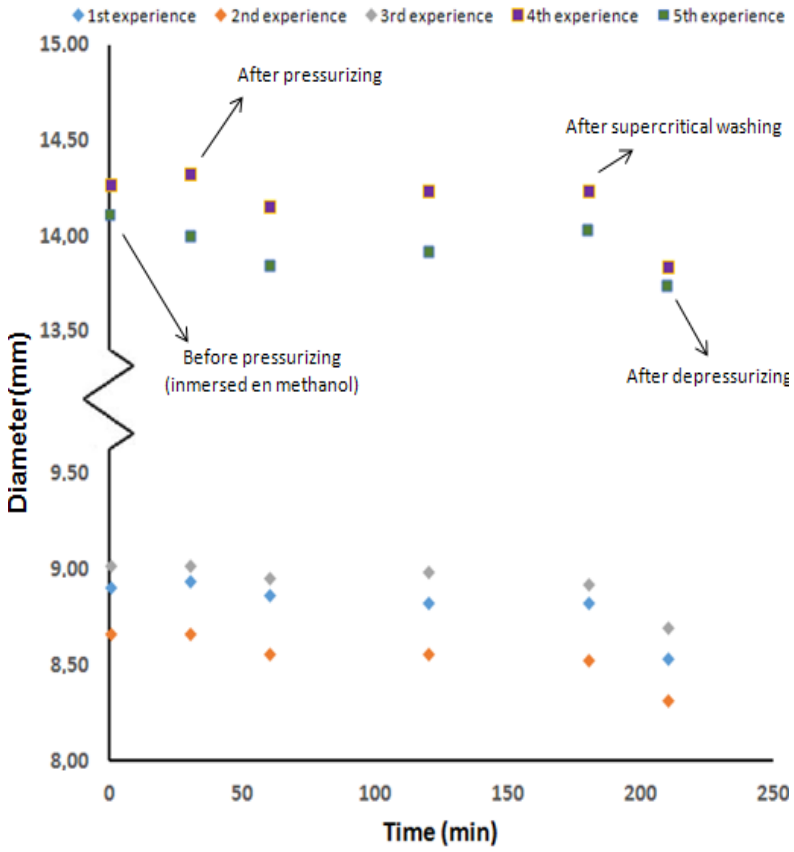

Figure 3. Evolution of the monoliths radius dimensions during the supercritical drying.

3.2 Observations of mass transfer mechanisms during the drying period

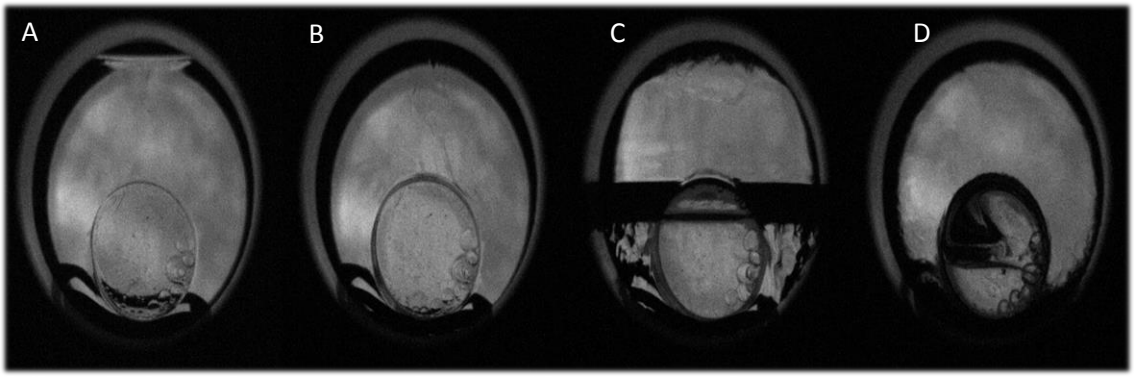

Figure 4. Captures of a ~ 8,90 mm diameter monolith during the first stages of the drying (axial view): A.Before pressurizing (immersed in methanol); B.After pressurizing; C.During the supercritical washing (2 min after the recirculation started); D.Just after the interphase left the view chamber.

The drying took place at ∼45 ± 1°C and ∼10.5 ± 0.5 MPa. According to Ah-Dong et al. [24], these conditions are above the critical point of the methanol–carbon dioxide mixture (Tc= 45°C; Pc∼ 9 MPa). Nevertheless, in figure 4, captures of the first stages of the drying of a ∼8.9 mm diameter monolith, taken from the attached video 2, show an interface between methanol and carbon dioxide: capture A shows the alcogel immersed in methanol before being compressed; capture B shows the same chamber once being compressed; capture C shows the appearance of an interface when the CO_2 recirculation was connected and methanol started to be drained out of the view cell; and capture D shows the aerogel just after the interface left the view chamber when the recirculation started. In this last capture, it can be noticed that a crack has appeared due to the capillary forces caused by the interface. The appearance of the methanol-CO_2 interface is attributed to the fact that the diffusion surface between methanol and carbon dioxide is very small (when the level of the methanol is dragged out of the view chamber by CO_2, the interface is just the cross section of the outlet tube of the view cell), and a long period is required in order to reach the equilibrium, thus giving rise to a dynamic interfacial tension between methanol and CO_2. However, if the change of the phases in the chamber is slow enough, drying of crack-free aerogels were performed with the presence of this interface. Supplementary video 2 related to this article can be found, in the online version, at http://dx.doi.org/10.1016/j.supflu.2014.05.004. What is more, the movement velocity of this interface across the chamber is related to the recirculation flows during the drying, and the structure of the ∼8.9 mm samples withstood without damages higher flows (up to 150 mL/min) than the ∼14.2 mm samples (which presented cracks with flowrates above 110 mL/min). Therefore, as it could be expected, bigger aerogels are damaged more easily when the CO_2

flowrate is increased. This could be due to the creation of stronger mechanical tensions in the structure of bigger aerogels. The explanation to the phenomena of drying without breaking the aerogels even in the presence of this interface could be explained by the fact that capillary forces are related to the difference between the densities of the phases, being the one of the carbon dioxide and the one of the methanol very similar under these conditions, and to the steepness of the composition and density gradient at the interface, which is reduced due to the complete miscibility between the two fluids. A parallelism can be drawn between the drying process with a transient interface between methanol and CO_2 at supercritical conditions, and the approach presented by Guoyou Wu et al. [25] to produce aerogels by ambient drying, that was based on reducing capillary forces during the evaporation of solvent by employing a n-hexane rich atmosphere for drying. Figure 5 shows several captures of a ∼14.2 mm diameter monolith, taken from the video 3 included as supplementary material, made during different stages of the drying. Capture A shows the alcogel immersed in methanol before being compressed. Capture B shows the same chamber once being compressed. During the pressurization, CO_2 is gradually dissolved in the methanol, expanding its volume and moving the interface between methanol and CO_2 to the top. Capture C has allowed to detect a crown formation along the perimeter of the gel during the early stages of the drying (can be differentiated for about the first 45 min of drying). The appearance of this crown was attributed to the previously mentioned interface, inside the gel matrix. It grows toward the center of the monolith and we have denominated this structure as drying front. Capture D shows the crown once it has moved toward the center of the gel. Capture E shows the gel when the drying is finished but the chamber is still pressurized. Capture F shows the chamber once it has been depressurized. Supplementary video 3 related to this article can be found, in the online version, at http://dx.doi.org/10.1016/j.supflu.2014.05.004. By converting the video captures presented in figure 5 into numerical grayscale light intensity matrixes, and obtaining an intensity profile correspond to a horizontal line of the porthole (Ø = 18 mm) which passes through the center of the ∼14.2 mm diameter monolith, the results presented in figure 6 are obtained. The plateaus or dips (depending on the drying time) delimit the monolith diameter. The elevation of them change over the drying time; at the beginning, the alcogel is immersed in methanol and its brightness is kept after the pressurization and even inside the crown which is formed during the first stages of the drying. That supports the existence of two phases in the pressurized system. After it, the brightness of the aerogel undergoes a gradual reduction, which directly relates the brightness with the methanol concentration in the pores of the gel. Finally, after the depressurization, the density and diffraction dropped drastically even for the area of the porthole which is free of aerogel. Another

high-light is the form of the curve of the capture taken at a time of 60 min, period during which a crown was formed. That crown is reflected in the two dips that appear in the outline of the monolith. Following the movement of this crown, it has been possible to calculate the velocity of movement of the drying front inside the gel. Figure 7 shows the drying front velocity during the first stages of the drying. It can be noticed that at the very beginning of the process, higher recirculation flows resulted in higher drying front velocity, indicating that mass transfer is controlled by advection. By contrast, after a while, the velocity of the lower recirculation flows surpasses the one of the higher flows (∼7 min in the case of Ø = 8.90 mm and ∼22 min in the case of Ø = 14.20). This is attributed to the fact that the higher is the velocity at the very beginning, the deeper is the situation of the drying front after a while, taking diffusivity a more important role over the contribution of the advective transport. What is more, the velocity at the very beginning is higher in the case of the monoliths with smaller diameter, but comes to similar values after some minutes (∼22 min). That supports that the influence of the diffusion is an important transport mechanism from the very beginning (smaller diameters reduce the diffusion distances, favoring the mass transfer through this mechanism) coming to a point in which diffusivity totally controls drying. As a support to these conclusions, figure 8 shows the drying front velocity (mm/min) vs. the position of the crown in the radius of the monolith measured from the perimeter of the gel. It can be observed that initially, higher drying front velocities are observed at higher flow rates, but once the drying front has penetrated 2–2.5 mm inside the aerogel, nearly equal drying velocities are obtained independently of the CO_2 flowrate and the total size of the aerogel. This behavior confirms how diffusivity influence increases till it dominates completely the process. Figure 9 presents the evolution of the brightness at the center of an aerogel monolith during the drying process. A fast decrease of brightness is observed after the connection of the CO_2 recirculation pump that can be associated with a fast removal of solvent by advective transport. Later on, a nearly linear reduction of brightness is observed as drying progresses by diffusion of organic solvent out of the pores of the aerogel. Although at the moment we cannot propose a quantitative relationship between organic solvent residual content and brightness, because the concentration of residual solvent inside the aerogel along the drying process could not be measured, the results presented in figure 9 show that the evolution of brightness can be a useful monitoring parameter for the aerogel drying process. These results obtained by analysis of the captures can be related to the different steps proposed by García-González et al. [16], in which the expansion and solvent spillage is described during the pressurization step till the supercritical conditions are reached. After it the convection reduces its influence, the amount of methanol in the gel decreases and the role of diffusion mass transport resistance in the solid substrate becomes predominant until the gel is fully dried.

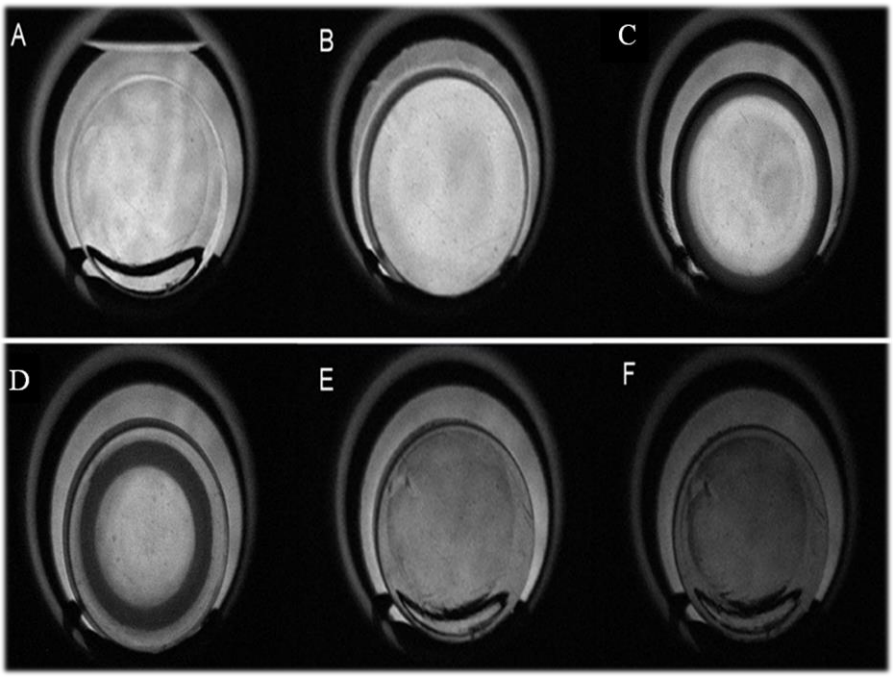

Figure 5. Captures of the aerogels during the supercritical drying (axial view): A.Before pressurizing (immersed in methanol); B.After pressurizing; C.After power the recirculation pump; D.During the supercritical washing (crown formation); E.After the supercritical drying; F.After depressurizing.

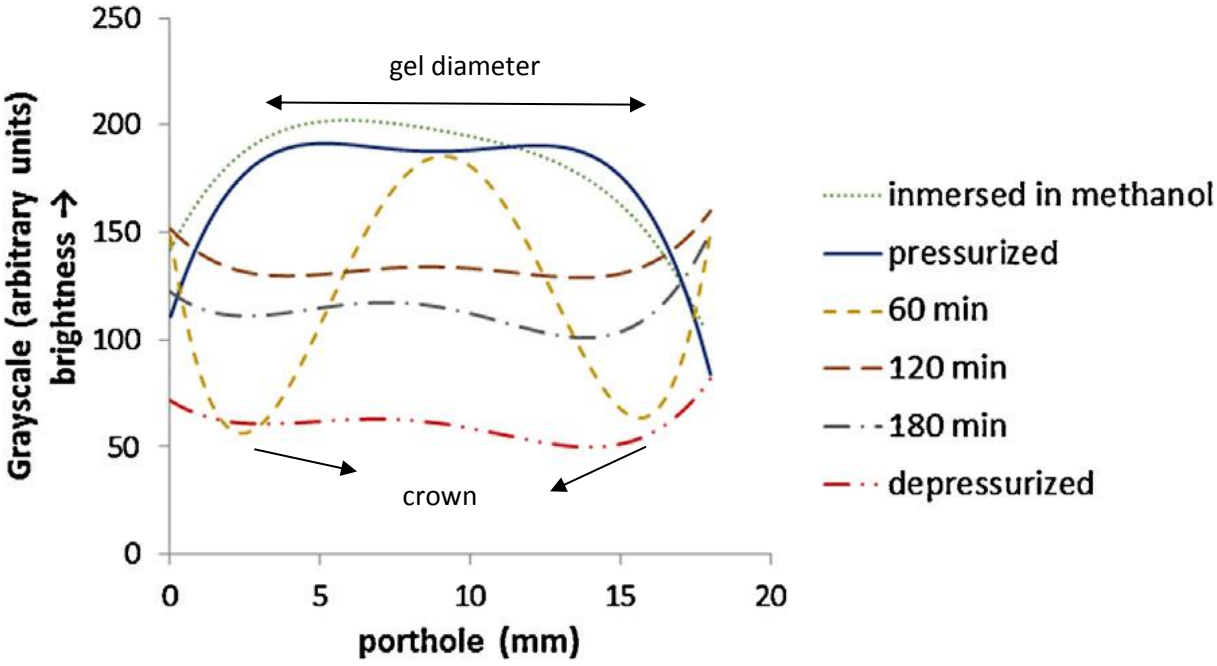

Figure 6. Grayscale intensities along an horizontal line of the window (Ø = 18 mm) which passes through the center of the ~14.2 mm diameter aerogel monolith.

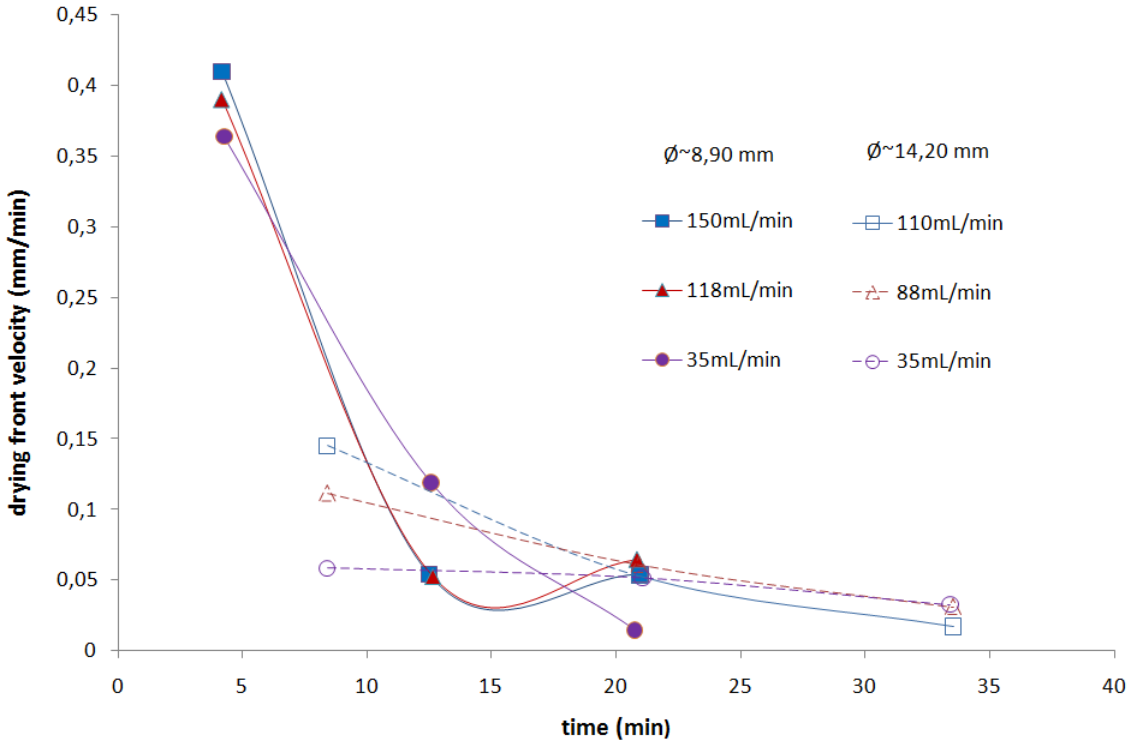

Figure 7. Drying front velocity (mm/min) vs time (min).

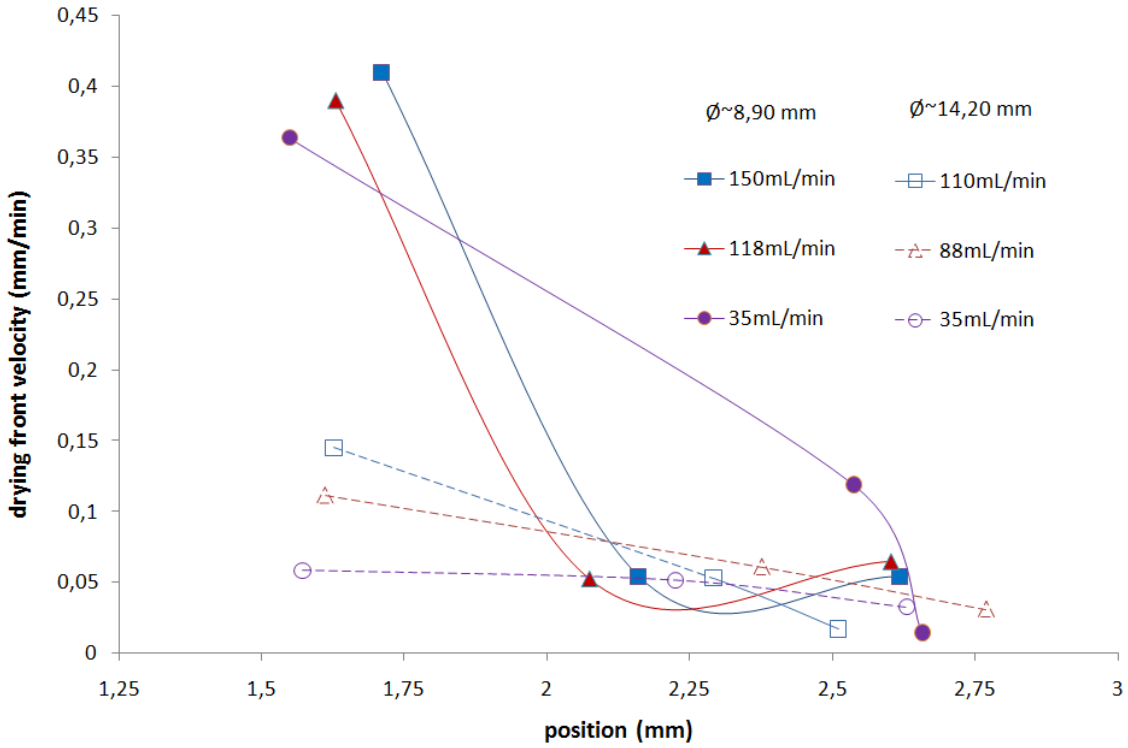

Figure 8. Drying front velocity (mm/min) vs position (mm).

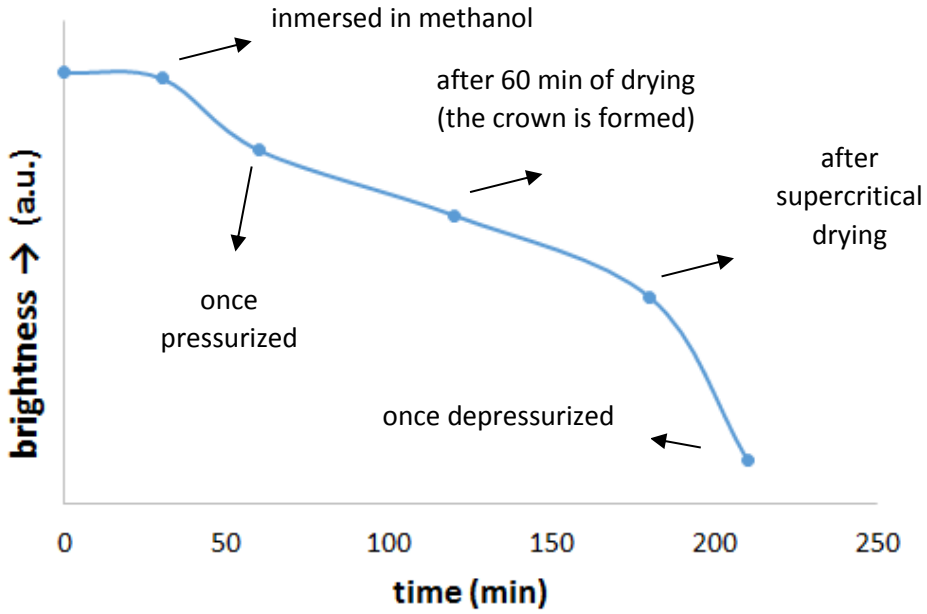

Figure 9. Brightness of the center of a of the ~ 14,2 mm diameter monolith during the supercritical drying.

4. Conclusions

Supercritical CO_2 aerogel drying experiments in a high pressure view cell have been followed by image analysis of video captures. This has allowed to optimize the drying conditions, reducing the time required for drying by maximizing the carbon dioxide flow and hence making the maximum advantage of the advective transfer mechanism during the first stages of the drying, and showing that after a period this flow can be reduced without affecting the drying velocity, since the process comes to a period when diffusion completely governs drying. Size variations of gels have been followed studying the video captures. It has been observed that a noticeable aerogel shrinkage only takes place during CO_2 decompression at the end of drying process. Damages to aerogels during this decompression step seem to be governed by the mechanical stresses caused by CO_2 expansion. Further studies seeking a quantitative relationship between the diffusion rate of CO_2 out of the pores of the aerogel, the decompression rate and the extent of aerogel shrinkage would be useful to confirm this hypothesis. Furthermore, although at the operating conditions considered in this work methanol and carbon dioxide are completely miscible, a transient interface at the beginning of the drying process has been observed both between bulk CO_2 and methanol phases and inside the alcogel. The formation of this interface does not appear to have a detrimental effect on the integrity of the aerogel. This result can be due to the similarity between the densities of methanol and CO_2 at the operating conditions,

and the reduced composition gradients at the interface due to the miscibility between the two phases, that contribute to reduce capillary forces.

References

[1] J. Fricke, Aerogels, Springer-Verlag, Berlin, 1986.

[2] J. Fricke, A. Emmerling, Aerogels – recent progress in production techniques and novel applications, J. of Sol–Gel Science and Technology 13 (1999)299–303.

[3] C. Stumpf, K. Gässler, G. Reichenauer, J. Fricke, Dynamic gas flow measurements on aerogels, J. of Non-Crystalline Solids 145 (1992) 180–184.

[4] I. Smirnova, J. Mamic, W. Arlt, Adsorption of drugs on silica aerogels, Langmuir19 (2003) 8521–8525.

[5] T.J. Goodwin, V.J. Leppert, C.A. Smith, S.H. Risbud, M. Nuemeyer, P.P. Power,H.W.H. Lee, L.W. Hrubesch, Synthesis of nanocrystalline gallium nitride in silica aerogels, Applied Physics Letters 69 (21) (1996) 3230–3232.

[6] H.T. Jespersen, S. Standeker, Z. Novak, K. Schaumburg, J. Madsen, Z. Knez, Supercritical fluids applied to the sol–gel process for preparation of AERO-MOSILS/palladium particle nanocomposite catalyst, J. Supercritical Fluids 46(2008) 178–184.

[7] L.M. Sanz, M. Rueda, A. Nieto, Z. Novak, Z. Knez, Á. Martín, Gradual hydrophobic surface functionalization of dry silica aerogels by reaction with silane precursors dissolved in supercritical carbon dioxide, J. Supercritical Fluids 84 (2013)74–79.

[8] S. Yoda, K. Ohtake, Y. Takebayashi, T. Sugeta, T. Sako, T. Sato, Preparation oftitania-impregnated silica aerogels and their application to removal of benzene in air, J. Materials Chemistry 10 (2000) 2151–2156.

[9] S. Smitha, P. Shajesh, P.R. Aravind, S. Rajesh Kumar, P. Krishna Pillai, K.G.K. Warrier, Effect of aging time and concentration of aging solution on the porosity characteristics of subcritically dried silica aerogels, Microporous and Mesoporous Materials 91 (2006) 286–292.

[10] C. Pierre Alain, M. Pajonk Gérard, Chemistry of aerogels and their applications, Chemical Reviews 102 (2002) 4243–4265.

[11] L. Kocon, F. Despetis, J. Phalippou, Ultralow density silica aerogels by alcohol supercritical drying, J. Non-Crystalline Solids 225 (1998) 96–100.

[12] E. Juncal, J.C. Echeverría, M. Laguna, J.J. Garrido, Effects of aging and drying conditions on the structural and textural properties of silica gels, Microporous and Mesoporous Materials 102 (2007) 274–282.

[13] G. Amaral-Labat, A. Szczurek, V. Fierro, E. Masson, A. Pizzi, A. Celzard, Impact of depressurizing rate on the porosity of aerogels, Microporous and Mesoporous Materials 152 (2012) 240–245.

[14] O. Czakkel, B. Nagy, E. Geissler, K. László, In situ SAXZ investigation of structural changes in soft resorcinol-formaldehyde polymer gels during CO2-drying, J.Supercritical Fluids 75 (2013) 112–119.

[15] Z. Novak, Z. Knez, Diffusion of methanol-liquid CO2and methanol-supercriticalCO2in silica aerogels, J. Non-Crystalline Solids 221 (1997) 163–169.

[16] C.A. García-González, M.C. Camino-Rey, M. Alnaief, C. Zetzl, I. Smirnova, Super-critical drying of aerogels using CO2: effect of extraction time on the end material textural properties, J. Supercritical Fluids 66 (2012) 297–306.

[17] P. Wawrzyniak, G. Rogacki, J. Pruba, Z. Bartczak, Effective diffusion coefficient in the low temperature process of silica aerogel production, J. Non-Crystalline Solids 285 (2001) 50–56.

[18] S.Standeker, Z. Novak, Z. Knez, Adsorption of toxic organic compounds from water with hydrophobic silica aerogels, J. Colloid and Interface Science 301(2007) 362–368.

[19] C. Folgar, D. Folz, C. Suchicital, D. Clark, Microstructural evolution in silica aerogel, J. Non-Crystalline Solids 353 (2007) 1483–1490.

[20] M.J. van Bommel, A.B. de Haan, Drying of silica gels with supercritical carbon dioxide, Journal of Materials Science 29 (1994) 943–948.

[21] R. Al-Oweini, H. El-Rassy, Surface characterization by nitrogen adsorption of silica aerogels synthesized from various Si(OR)4 and R__Si(OR_)3 precursors, Applied Surface Science 257 (2010) 276–281.

[22] H. Yokogawa, M. Yokoyama, Hydrophobic silica aerogels, J. Non-Crystalline Solids 186 (1995) 23–29.

[23] G.W. Scherer, Stress in aerogel during depressurization of autoclave: I. Theory, J. Sol–Gel Science and Technology 3 (1994) 127–139.

[24] C. Ah-Dong, Y.K. Samuel, D.B. Robinson, The equilibrium phase properties of (carbon dioxide + methanol), J. Chemical Thermodynamics 23 (1991) 979–985.

[25] G. Wu, Y. Yu, X. Cheng, Y. Zhang, Preparation and surface modification mechanism of silica aerogels via ambient pressure drying, Journal of Materials Chemistry and Physics 129 (2011) 308–314.

Chapter 2

Gradual hydrophobic surface functionalization of dry silica aerogels by reaction with silane precursors dissolved in supercritical carbon dioxide

Gradual hydrophobic surface functionalization of dry silica aerogels by reaction with silane precursors dissolved in supercritical carbon dioxide

Abstract

We report the synthesis and the surface modification of hydrophilic and hydrophobic silica, aerogels obtained via a sol–gel process. Tetramethylorthosilicate or a mix of the first one with, trimethylethoxysilane have been used as precursors. The hydrolysis and poly-condensation steps were, followed by carbon dioxide supercritical drying (T = 45°C; P = 10.5 MPa). The resulting dry hydrophilic, aerogels were subjected to a hydrophobic surface functionalization using supercritical carbon dioxide, as the solvent for different silane functionalization reactants: trimethylethoxysilane, octyltrimethoxysilane and chlorotrimethylsilane. Effects of the working pressure and reagent concentration on the functionalization were analyzed using FT-IR spectroscopy and exposing the treated aerogels to saturated moisture conditions in order to study the mass increment during the humidification. Nitrogen adsorption measurements show a considerable drop on the specific areas (13–17 %) and on the pore volumes which were reduced by 50 %. By modification of the operating pressure and variation of the functionalization agent employed, the degree of functionalization could be gradually increased up to the values of the aerogels synthesized as hydrophobic in the sol–gel phase.

Keywords: Aerogel; hydrophilic; hydrophobic; surface functionalization; silanization, supercritical carbon dioxide.

1. Introduction

Aerogels are a class of materials with extraordinary properties like high porosity, low density, high thermal insulation value, ultra-low dieletric constant or low index of diffraction [1]. That makes them suitable materials for different interesting applications [2]. On the other hand, silica aerogels are very brittle structures, and they are highly susceptible to fracture or collapse of their pore structure during the drying step of their production due to the surface tension of the liquid contained in the gel nanopores, that infers a capillary pressure gradient. Several techniques have been used in order to dry the aerogels, including atmospheric drying and freeze drying, but supercritical drying, where the alcohol is solved in supercritical carbon dioxide, is one of the better established and more frequently used methods to dry aerogels overcoming the collapse of their structure [3].

Common silica aerogels synthesized from precursors such as tetramethoxysilane or tetraethoxysilane are highly hydrophilic due to the abundance of hydroxyl surface groups in

these aerogels. A collapse of the structure of such hydrophilic silica aerogels can be induced even by absorption of ambient humidity. In order to avoid this problem, or in cases in which a highly hydrophilic surface is not desirable, several surface modifications have been proposed. In general, the surface modification of silica alcogels occurs predominantly according to the following reaction:

$$xRE(OR')_n + yE(OR')_m + zH_2O \rightarrow R_qEO_p + wR'OH \quad (1)$$

Varying the functional groups (R) or the metal oxide (E) or the ratio between them can result in a number of interesting hybrid materials [4]. The main route for incorporation of these surface groups consists of adding different silica precursors as methyltrimethoxysilane or trimethylethoxysilane in the standard sol–gel synthesis. This enables synthesizing highly hydrophobic aerogels with high efficiency [5]. Another option is adding functionalizing agents in the liquid phase in which the sol–gel reaction takes place before drying [6]. Using this method, alcogels were functionalized by immersing them in chlorotrimethylsilane/ethanol/n-hexane solutions by Zhang et al. [7].

In some applications, it may be advantageous to switch from a hydrophilic to a hydrophobic surface functionalization of a finished, dry aerogel in different stages of the application. An example could be the deposition of an active compound inside the pores of the aerogel, which can be facilitated by the active surface hydroxyl groups of hydrophilic aerogel, followed by a use of this material in which the enhanced stability of a hydrophobic surface functionalization is required. Thus the development of methods for reversibly changing the surface functionalization of dry aerogels is of interest. Some methods for a reversible hydrophobic surface modification of dry aerogels have been proposed. A possibility is boiling and vaporizing the functionalization agent, and putting this vapor into contact with the aerogel [8]. A limitation of this method is the possible damage to the aerogel by condensation of the functionalization agent inside its pores. Another possibility is putting into contact the aerogel with a solution of the functionalization agent in supercritical carbon dioxide. This facilitates the penetration of the functionalization agent into the pores of the aerogel thanks to the favorable transport properties in the supercritical fluid, and reduces the risk of damages to pore structure by condensation. Using this method, the surfaces of monolithic silica aerogels were rendered hydrophobic using hexamethyldisilazane (HDMS) as surface modification agent and sc-CO_2 as solvent by Kartal and Erkey [9]. Highly hydrophobic aerogels, with no modification of their optical properties, were obtained, and it was observed that the concentration of HDMS and the reaction time did not have a significant influence on the functionalization. Similarly, Concepción

Domingo et al. measured the solubility of octyltriethoxysilane (OTES) in sc-CO_2 [10] and studied the functionalization of different porous materials by treatment with a solution of this precursor in the supercritical fluid [11]. Finally, the silane coating can be easily removed by heating the materials [12].

In applications of surface functionalization of preformed dry silica aerogels, it is important to achieve a good preservation of the properties of the aerogel after the functionalization treatment, and particularly of essential physical properties such as the available surface area and pore volume. Moreover, the possibilities to control the process in order to achieve different degrees of hydrophobicity tailored for specific applications are also relevant. In order to address these questions, in this work silica aerogel surfaces were functionalized using supercritical carbon dioxide as solution media for different functionalizing agents including trimethylethoxysilane (TMES), octyltriethoxysilane (OTES) and clorotrimethylsilane (CTMS). Several experiments were developed with different concentrations of functionalization agent, varying the pressure which allows to control the solubility of the chemicals in the supercritical fluid. The presence of the different functionalizing groups was detected using FT-IR. The degree of hydrophobicity of the materials was analyzed by studying the variation of the areas of the SiOH groups in the infrared spectrums and by the weight variation between the surface modified aerogels before and after been exposed to controlled humidity conditions. The influence of the treatment on the physical properties was also characterized measuring nitrogen adsorption isotherms.

2. Experimental methods

2.1 Reagents

Tetramethoxysilane (TMOS, 98 % purity), trimethylethoxysilane (98 % purity), octyltriethoxysilane (97.5 % purity), clorotrimethylsilane (97 % purity) and ammonium hydroxide (28–30 %) were purchased from Sigma–Aldrich. Methanol (99.8%) was obtained from Panreac. CO_2 (>99.95 mol % purity) was supplied by Carburos Metálicos S.A. Deionized water was used in all experiments.

2.2 Processing

2.2.1 Preparation of alcogels

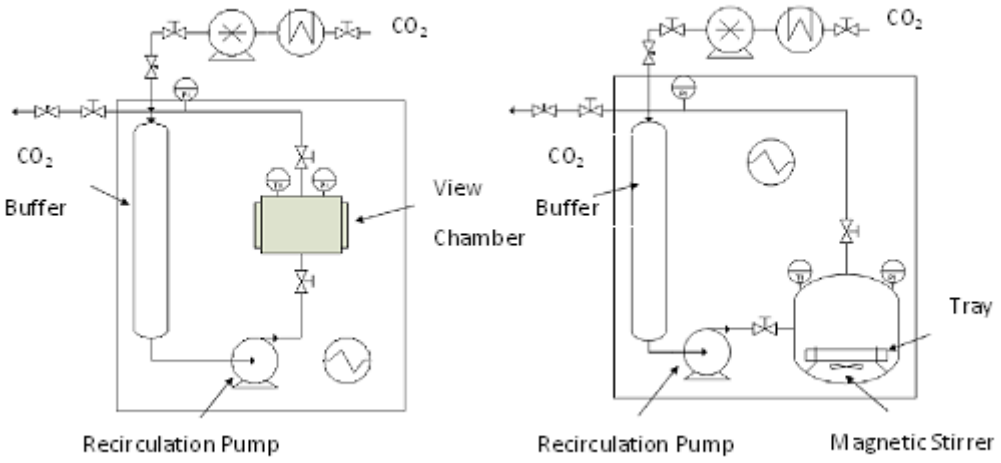

Figure 1. flow diagrams of equipment used for supercritical drying of alcogels (on the left), and equipment used for functionalization (on the right)

Hydrophilic silica alcogels were produced following the two step sol–gel process [13,14]. Using a fixed molar ratio of reagents (TMOS:methanol:H_2O:ammonium hydroxide, mol ratio1:3:4:5×10^{-3}), methanol and TMOS were mixed together and the solution of ammonium hydroxide–water was added to this mixture drop by drop under stirring. After a few minutes the stirrer was stopped and the mixture was poured into cylindrical molds for gelation. Straightaway, the gels were immersed in methanol for an aging period of at least 7 days. During this time the methanol was renewed 3 times in order to remove the water content of the solution. The hydrophobic gels were developed in the same way but using also TMES as precursor (in a mol ratio TMOS:TMES:methanol:H_2O:ammonium hydroxide,1:1:9:5:0.01).

2.2.2. Supercritical drying of alcogels

Silica aerogels were produced by supercritical drying of alcogels with CO_2. The batch equipment showed on figure 1 was used for drying. The main components were the 1 L CO_2 buffer vessel, the recirculation gear pump and the view chamber which had a capacity of 25 mL. The entire equipment was placed into a hot air circulating oven that kept the temperature constant during the drying. After the aging period, the alcogels were placed in the view chamber; straightaway, the rest of the container was filled up with methanol in order to avoid the cracking of the alcogel till the supercritical conditions were reached. In each drying experiment, 10–12 silica monoliths, amounting to a total mass of approximately 2 g, were dried. Then the complete equipment was heated and CO_2 was pumped into the circuit, increasing pressure at an approximate rate of 3 bar/min. Once the operation conditions were reached (10.5 MPa, 45°C), the recirculation pump was activated (CO_2 flow rate ∼60 mL/min, corresponding to a CO_2 mass rate of ∼34 g/min in the

selected drying conditions) and the extraction of methanol from the extractor began. After a drying period, CO_2 in the circuit was renewed in order to remove the methanol dissolved in this fluid and improve drying. Three loads of new CO_2 after recirculation times of 30, 45 and 45 min were required in order to remove all methanol and produce dry aerogels, thus amounting for total CO_2 consumption of about 2000 g in the entire drying process. The extractor can be isolated from the rest of the circuit closing valves at its inlet and outlet, which allowed to renew the CO_2 of the circuit without decompressing the aerogel inside the view chamber and thus limiting the possible damages to the aerogel in pressurization–depressurization processes. Finally, after completing all three drying cycles, the equipment was slowly depressurized in order to avoid damage to aerogels, at a rate of 3 bar/min.

2.2.3 Aerogels functionalization

The equipment used for the functionalization of the aerogels (figure 1) consisted of a 100 mL buffer vessel, a recirculation pump and a ∼83 mL vessel with magnetic stirring. The entire equipment was placed into a hot air circulating oven that kept the temperature constant during the functionalization. The chemicals used for the functionalization (OTES, TMES or CTMS) were poured at the bottom of the vessel. The aerogels were put on a tray, being suspended in the vessel above the functionalization agents in order to avoid direct contact with the functionalization reagents. Then the equipment was heated to 45°C and CO_2 was pumped into the circuit increasing pressure at a rate 3 bar/min. The operating pressure was adjusted at 9, 11 or 13 MPa, depending on the experiment. Once the operational conditions were reached, the vessel was isolated from the rest of the circuit and the chemicals were stirred for 45 min. After that, the recirculation pump was activated and a flow of neat CO_2 from the buffer vessel crossed the vessel in order to remove the excess of the chemicals used for the functionalization. Finally the equipment was slowly depressurized in order to avoid damage to aerogels (3 bar/min).The influence of pressure on the functionalization of aerogels by treatment with sc-CO_2 solutions of OTES or TMES was analyzed carrying out experiments at pressures of 9, 11 and 13 MPa. In order to eliminate the possible influence of small variations on conditions during the sol–gel synthesis and drying of aerogels, batches of several monoliths were produced pouring the same sol–gel solution on several molds, as described in Section 2.2.1, and simultaneously drying all the alcogels as described in Section 2.2.2. Monoliths coming from the same batch were used in all experiments with each functionalization agent, thus ensuring equivalent initial conditions of the aerogel in each series of experiments.

2.3 Characterization

With the objective of evaluating the behavior of the treated aerogels against water and moisture, the aerogels were dried under vacuum at 60°C during 8 h in order to remove adsorbed humidity without damaging the structure or surface functionalization of the aerogel. After that, they were either directly exposed to water droplets, or to air saturated with moisture at 30°C, depending on their degree of hydrophobicity. The mass increase during the humidification was used to compare the degree of hydrophobic functionalization under the different selected conditions. Each measurement was carried out in triplicate and experimental errors were estimated by calculation of 95 % confidence intervals with standard statistical methods. The aerogel structure was studied by Fourier transform infrared spectra (FT-IR model TENSOR from BRUKER, Spain). The physical characterization of surface area and pore volume was done by determination of BET isotherms (surface area analyzer Quantasorb Sorption System from Quantachrome Instruments, UK) with N_2 (at −196°C) as sorbate. Prior to analysis, the samples were degassed overnight at 180°C. Total specific surface areas were determined by the multipoint BET method at $P/P_0 \leq 0.3$, and total specific pore volumes were evaluated from N_2 uptake at $P/P_0 = 0.99.3$

3. Results and discussion

3.1 Infrared spectra (IR) of untreated hydrophilic aerogels and treated hydrophobic aerogels

The FT-IR spectra of hydrophilic aerogels (figure 2) are relatively simple and shows different bands assigned to various vibrations in the solid network. According to literature [15,16], the intense silicon–oxygen covalent bonds vibrations appear mainly in the 1200–1000 cm^{-1} range revealing the existence of a dense silica network, where oxygen atoms play the role of bridges between each two silicon sites. The very intense and broad band appearing at 1050 cm^{-1} and the shoulder at around 1200 cm^{-1} are respectively assigned to the transversal optical and longitudinal optical modes of the Si-O-Si asymmetric stretching vibrations. On the hand, the symmetric stretching vibrations of Si-O-Si appear at 800 cm^{-1}. Weak points were noticed at 1460, 2854 and 2956 cm^{-1}.They were assigned to the C-H antisymetric and symetric CH_2-CH_3 groups. These latter groups are expected to correspond to residual non-hydrolyzed alkoxy groups on the surface of the silica aerogels. The broad band centered at around 3100–3600 cm^{-1} corresponds to the overlapping of the O-H stretching bands of hydrogen-bonded water molecules (H-O-H···H) and Si-OH stretching of surface silanols hydrogen-bonded to molecular water (SiO-H···H_2O). Furthermore, the Si-O in-plane stretching vibrations of the silanol Si-OH groups appear at around

960 cm^{-1} and the absorption bands corresponding to the adsorbed water molecules deformation vibrations appear at 1630 cm^{-1}.

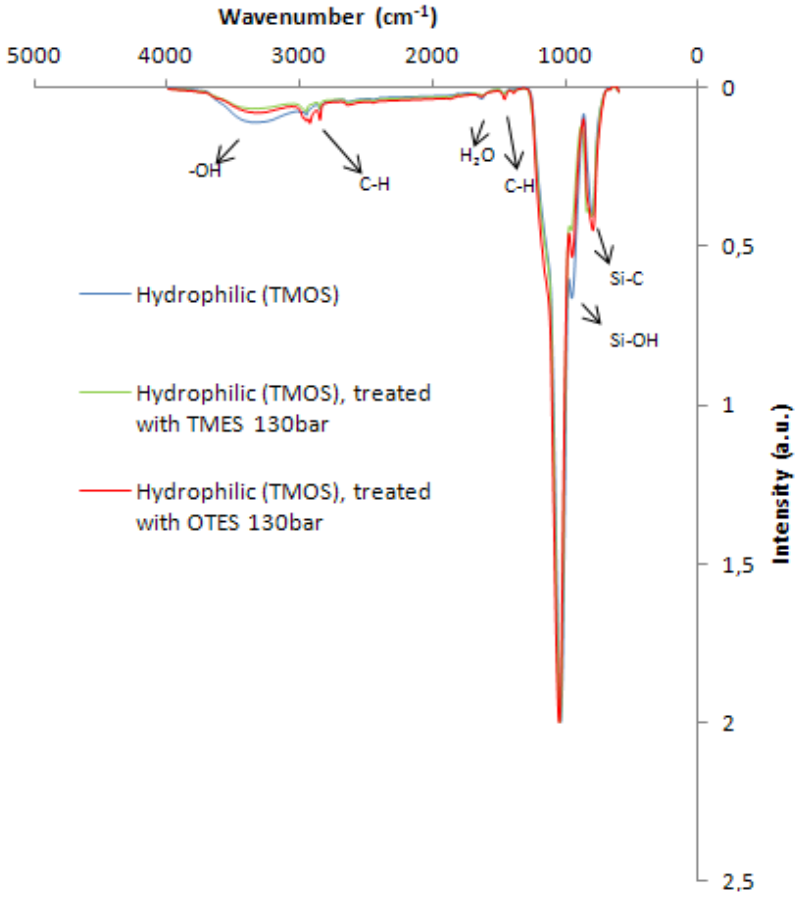

Figure 2. FTIR spectra from the hydrophilic silica aerogel (TMOS), in comparison with hydrophilic silica aerogel treated with OTES at 13 MPa and treated with TMES at 13 MPa.

In the case of hydrophobic aerogels synthesized with a mixture of TMOS/TMES in the sol–gel step, FT-IR spectrum of these aerogels, presented in figure 3, shows two peaks at 1273 cm^{-1} and 766 cm^{-1} which correspond to the CH_3 group. In contrast, comparing with the FT-IR spectra of hydrophilic aerogels, the bands corresponding to the O-H and Si-OH do not exist. That indicates a high degree of surface functionalization and confirms the high hydrophibicity of the material. By treatment of hydrophilic silica aerogels with supercritical solutions of functionalizing agents, the peak of the adsorbed water disappeared and the broad band centered at around 3100–3600 cm^{-1} was reduced. This can be noticed in the spectra of aerogels functionalized with OTES and TMES presented in figure 2. Focusing on the TMES-treated aerogels, a peak appears at 841 cm^{-1} due to the Si-C stretching vibration which confirms the replacement of some hydroxyl groups by alkyl groups. Respecting the ones treated with OTES, a peak appears at 2928 cm^{-1} due to the

symmetric and antysimmetric C-H bonds of the CH_2 group in the octyl substituent. A peak also appeared at 1392 cm^{-1} with indicates antisymmetric deformation vibration of C-H which shows a slight substitution of the octyl groups in place of the -OH. Additionally, a cylindrical monolith with a diameter of 22 mm was functionalized with OTES at 11 MPa, and 2 samples of the center and of the surface of the monolith were analyzed showing the similar spectra. That demonstrates that the functionalization is homogeneous in the entire aerogel regardless of the thickness. Finally, as shown in figure 3, the spectrum of the aerogels treated with CTMS dissolved in sc-CO_2 shows an important reduction on the O-H stretching bands and on the Si-OH peak. In contrast, the peaks at 757 cm^{-1} and 843 cm^{-1} confirm the presence of the Si-CH_3 group. Both results indicate a high hydrophobicity of the material. As a drawback of the treatment with this precursor, the formation of hydrochloric acid as a byproduct of the functionalization reaction caused some corrosion damage to the reaction vessel.

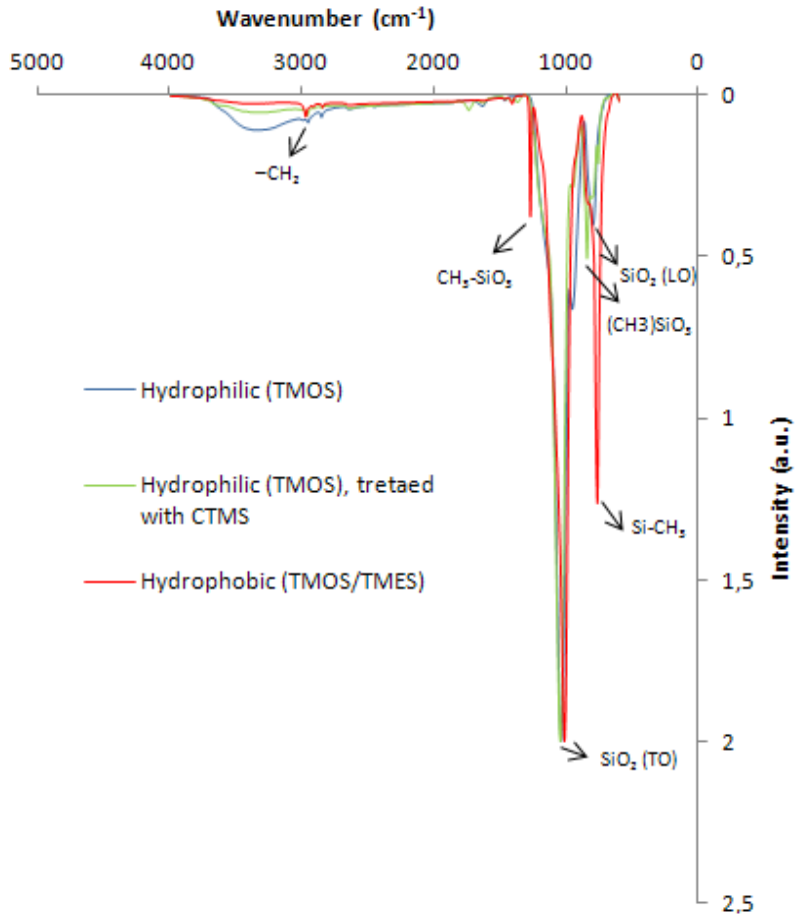

Figure 3. FTIR spectra from the hydrophilic silica aerogel (TMOS), in comparison with hydrophilic silica aerogel treated with CTMS at 10.5 MPa and hydrophobic silica aerogel (TMOS/MTMS).

3.2 Variation of the degree of functionalization by modification of process conditions

The aerogels synthesized with TMOS/TMES in the sol–gel and the ones treated with sc-CO_2 solutions of CTMS floated on water for several days, and presented a high contact angle with water droplets as shown in figure 4, indicating that they were highly hydrophobic, as shown in the results of FT-IR analyses of these aerogels. On the contrary, aerogels treated with sc-CO_2 solutions of OTES or TMES immediately sank when they were immersed in water, indicating a certain degree of hydrophilicity.

In order to assess whether it is possible to modify the degree of functionalization by variation of the operating pressure, experiments at three different pressures (9, 11 and 13 MPa) were carried out, as described in Section 2.2.3. Increasing pressures were chosen as the main process parameter because the solubility of the functionalization agents increases at increasing pressures [10], thus allowing to perform experiments with higher concentrations of functionalization agent at higher pressure. The main operating conditions employed in experiments are reported in table 1.

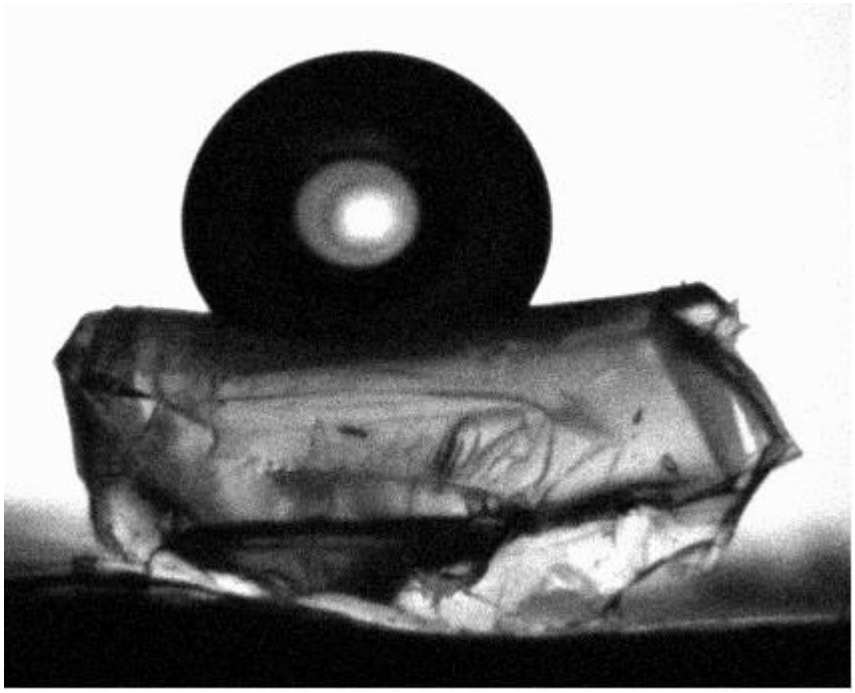

Figure 4. Photograph of a water droplet deposited at ambient conditions over a hydrophobic aerogel synthesized using TMES and TMOS (in molar proportion 1:1) precursors. Photograph obtained with a Imaging Source DMK 31BU03 monochrome camera.

In order to quantify the degree of hydrophobic functionalization of these aerogels, two types of measurements were carried out: firstly, the reduction in FT-IR spectra in the area of the peak corresponding to Si-OH bonds was calculated, as these superficial hydroxyl bonds are directly responsible for the hydrophilic nature of the aerogels. Secondly, dry aerogels were exposed to

controlled humidity conditions, and the increase in their weight due to the absorption of water was measured, as described in Section 2.3.

Results of these measurements are presented in figure 5, which shows the percentage of mass increment during the humidification of the samples on the primary axis, and the variation of the area under the Si-OH peak in the infrared spectra on the secondary one. Treatments with both functionalization agents showed a gradual hydrophobic functionalization as pressure was increased. Indeed, in both cases the amount of humidity absorbed and the area of the Si-OH peak of FT-IR assays decreased as pressure was increased.

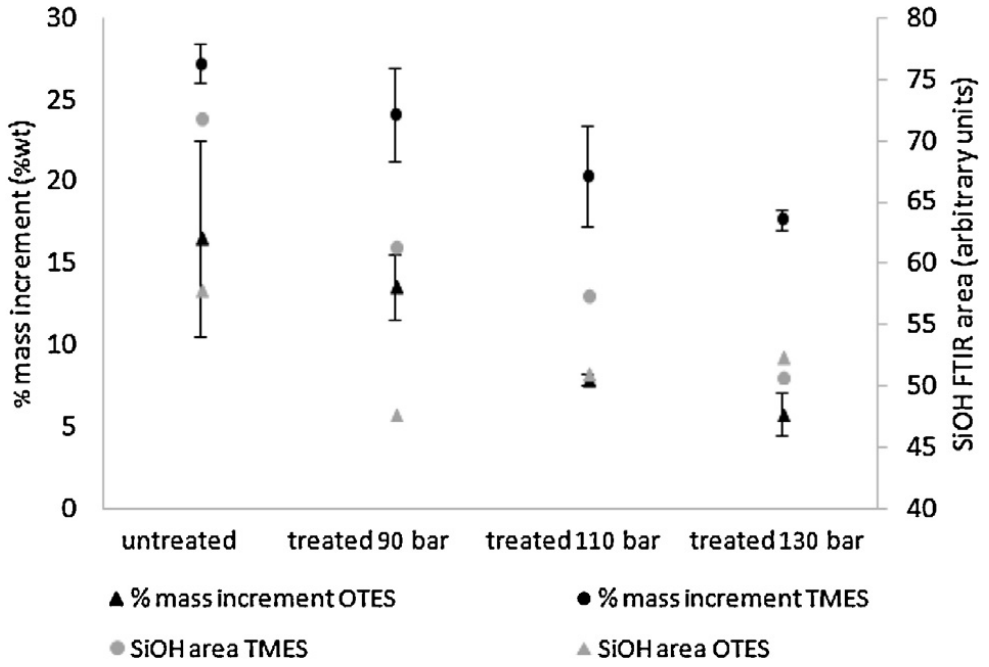

Figure 5. Percentage of mass incremented during the humidification process and SiOH area of the FT-IR spectra of untreated aerogels and aerogels functionalized with OTES or TMES at different pressures.

Focusing on the samples treated with TMES, the percentage of mass increment due to the adsorbed water was reduced from 27.2 % to 17.6 % as pressure was increased up to 13 MPa. On the ones treated with OTES, the reduction went from 16.6 % for the untreated ones to 5.8 % to the ones treated at 13 MPa. In both cases, the SiOH area in the FTIR spectra decreased inversely to the operating pressure, corroborating the relationship between the affinity for water and the value of the area of this peak. Comparing with an amount of 5.6 % of water absorbed by hydrophobic aerogels prepared with TMOS:TMES in mol proportion 1:1, it can be observed that the treatment with OTES not only enabled producing more hydrophilic aerogels at lower operating pressures than the treatment with TMES, but also allowed obtaining aerogels with equivalent hydrophobic characteristics as those functionalized in the sol–gel phase.

In figure 5, it can also be noticed that the amount of humidity absorbed by untreated aerogels varied between different batches of untreated aerogels (from 27.7 % to 16.6 %). This can be due to small variations in a number of factors during the aging and the supercritical drying that have an influence on the final result [2,17]. In any case, the influence of this variation on results was eliminated by using aerogels produced in the same batch on all experiments with each functionalization agent.

3.3 Variation of the physical properties of aerogels

Table 1. Properties and results of the aerogels before and after the silanization step

Sample	% mass increment exposed to humidity	SiOH area (a. u.)	Specific Area (m^2/g)	Pore Volume (cm^3/g)
Untreated silica aerogel	20.7	72	485	1.25
OTES (90bar)	13.6	48	-	-
OTES (110bar)	8.4	51	402	0.53
OTES (130bar)	5.8	52	-	-
TMES (90bar)	17.7	61	-	-
TMES (110bar)	16.0	57	418	0.50
TMES (130bar)	16.2	51	-	-
OTES (110 bar), after calcination	-	-	1010	0.94

In aerogels treated either with TMOS or OTES functionalization agents, no variations of the morphology or transparency of silica monoliths were apparent. As an example, figure 6 presents photographs of an untreated aerogel and an aerogel treated with OTES.

Results of the specific surface and pore volume derived from the nitrogen adsorption measurements are shown on table 1. After functionalization, a small reduction of specific area and a large reduction of pore volumes is evident. These variations are attributed to the filling or blocking of small pores and the volume occupied by the silane coating. This conclusion is drawn from the results obtained from the analysis of a sample functionalized with OTES and then calcinated in order to remove the silane coating, that are reported in table 1. As shown in this table, after calcination at 300°C, the sample recovered most of its initial pore volume, and also

showed an increase in its specific area. FT-IR spectrum of these aerogels, presented in figure 7, confirms the disappearance of the peak at 2928 cm^{-1} due to the symmetric and antisymmetric C-H bonds of the CH_2 group in the octyl substituent. Additionally, the SiOH area has increased.

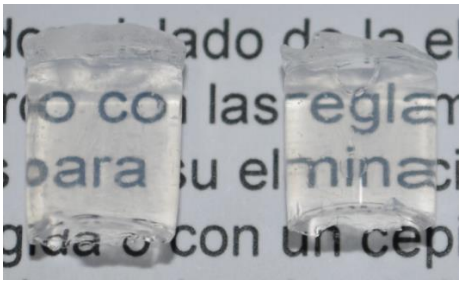

Figure 6. Untreated hydrophilic silica aerogel (on the left), hydrophilic aerogel treated with OTES solved in sc-CO_2 (on the right)

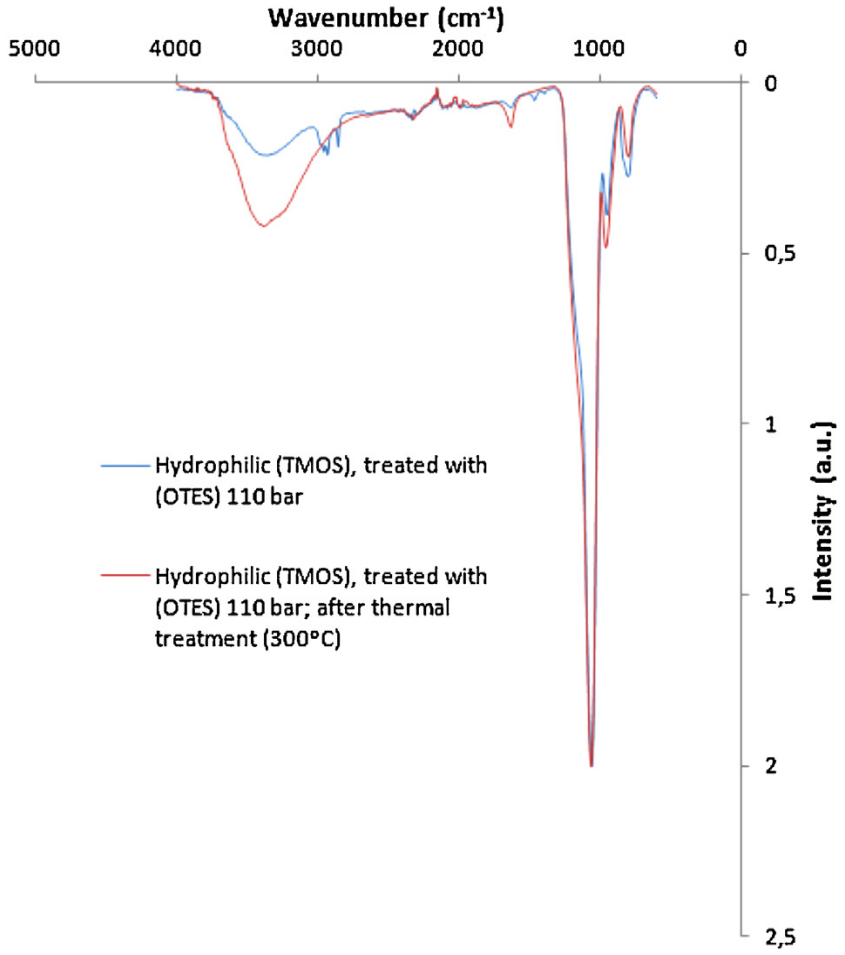

Figure 7. FTIR spectra from the hydrophilic silica aerogel (TMOS) treated with OTES at 13 MP, in comparison with hydrophilic silica aerogel (TMOS) treated with OTES at 13 MPa and treated at 300°C.

4. Conclusions

Results obtained in this work show that the treatment of dry aerogels with solutions of different precursors in supercritical carbon dioxide enables a successful surface functionalization of the aerogels. Varying the operating pressure or the functionalization reagent, it is possible to control the degree of funcionalization, allowing to achieve a gradual variation of the hydrophobicity of the aerogel in a wide range that is extended from highly hydrophilic aerogels, to hydrophobic aerogels with an equivalent behavior as those synthesized using hydrophobic precursors in the sol–gel step. The treatment with supercritical solutions of functionalization agents does not cause apparent morphological variations of the monoliths, and allows a highly homogeneous functionalization of aerogel monoliths. However, after the functionalization, significant reductions of the specific surface area, and particularly of the pore volume, are observed. This is probably due to a partial filling or blocking of pores by the silane coating.

References

[1] K. Kanamori, Organic–inorganic hybrid aerogels with high mechanical proper-ties via organotrialkoxysilane-derived sol–gel process, Journal of the Ceramic Society of Japan 119 (1) (2011) 16–22.

[2] S. Smitha, P. Shajesh, P.R. Aravind, S. Rajesh Kumar, P. Krishna Pillai, K.G.K.Warrier, Effect of aging time and concentration of aging solution on the porosity characteristics of subcritically dried silica aerogels, Journal of Microporous and Mesoporous Materials 91 (2006) 286–292.

[3] A.C. Pierre, G.M. Pajonk, Chemistry of aerogels and their applications, Chemistry Reviews 102 (2002) 4243–4265.

[4] U. Schubert, N. Husing, A. Lorenz, Hybrid inorganic–organic materials by sol-gel processing of organofunctional metal alkoxides, Chemistry of Materials 7(1995) 2010–2027.

[5] S.Standeker, Z. Novak,Z. Knez, Adsorption of toxic organic compounds from water with hydrophobic silica aerogels, Journal of Colloid and Interface Science310 (2007) 362–368.

[6] H. Yokogawa, M. Yokoyama, Hydrophobic silica aerogels, Journal of Non-Crystalline Solids 186 (1995) 23–29.

[7] G. Wua, Y. Yu, X. Cheng, Y. Zhang, Preparation and surface modification mechanism of silica aerogels via ambient pressure drying, Materials Chemistry and Physics 129 (2011) 308–314.

[8] B.S.K. Gorle, I. Smirnova, M.A. McHugh, Adsorption and thermal release of highly volatile compounds in silica aerogels, Journal of Supercritical Fluids 48(2009) 85–92.

[9] A.M. Kartal, C. Erkey, Surface modification of silica aerogels by hexamethyldisilazane–carbon dioxide mixtures and their phase behavior, Journal of Supercritical Fluids 53 (2010) 115–120.

[10] C.A. García-González, J. Fraile, A. López-Periago, J. Saurina, C. Domingo, Measurements and correlation of octyltriethoxysilane solubility in supercritical CO_2 and assembly of functional silane

monolayers on the surface of nanometric particles, Industrial & Engineering Chemistry Research 48 (2009) 9952–9960.

[11] S. Builes, P. López-Aranguren, J. Fraile, L.F. Vega, C. Domingo, Alkylsilane-functionalized microporous and mesoporous materials: molecular simulation and experimental analysis of gas adsorption, Journal of Physical Chemistry C116 (18) (2012) 10150–10161.

[12] S. Cui, Y. Liu, M.-H. Fan, T. Adrienne, Cooper, B.-L. Lin, X.-Y. Liu, G.-F. Han, X.-D.Shen, Temperature dependent microstructure of MTES modified hydrophobic silica aerogels, Journal of Materials Letters 65 (2011) 606–609.

[13] Z. Novak,Z. Knez, Diffusion of methanol–liquid CO_2 and methanol–supercriticalCO_2 in silica aerogels, Journal of Non-Crystalline Solids 221 (1997) 163–169.

[14] C. Folgar, D. Folz, C. Suchicital, D. Clark, Microstructural evolution in silica aerogel, Journal of Non-Crystalline Solids 353 (2007) 1483–1490.

[15] R. Al-Oweini, H. El-Rassy, Synthesis and characterization by FTIR spectroscopy of silica aerogels prepared using several $Si(OR)_4$ and $R00Si(OR0)_3$ precursors, Journal of Molecular Structure 919 (2009) 140–145.

[16] S. Cui, Y. Liu, M. Fan, A.T. Cooper, B. Lin, X. Liu, G. Han, X.Shen., Temperature dependent microstructure of MTES modified hydrophobic silica aerogels, Journal of Materials Letters 65 (2011) 606–609.

[17] Y. Ru, L. Guoqiang, L. Min, Analysis of the effect of drying conditions on the structural and surface heterogeneity of silica aerogels and xerogel by using cryogenic nitrogen adsorption characterization, Microporous and Mesoporous Materials 129 (2010) 1–10.

Chapter 3

Tuned Pd/SiO_2 aerogel catalyst prepared by different synthesis techniques

Tuned Pd/SiO_2 aerogel catalyst prepared by different synthesis techniques

Abstract

Pd nanoparticles have been embedded on silica aerogel by using three different techniques. In each of them the metal was loaded in the matrix at different steps of the production: the direct synthesis, the wet impregnation and the supercritical impregnation of the previously dried aerogels. The resultant materials have been characterized to analyze the differences depending on the applied technique for its impregnation. Atomic absorption, nitrogen physisorption, X-ray diffraction, infrared spectroscopy *and* transmission electron microscopy where performed. In all the techniques the concentration of metal has been varied (from 0.13 to 1.61 wt%) by modifying the concentration of the suspension (Pd-polyvinylpyrrolidone nanoparticles used in the direct synthesis) or of the solution of the metallic precursor (palladium acetylacetonate), both in the organic solvent and the supercritical media. The characterization had generally shown a good distribution of the metallic particles in the matrix, and the negligible effect of the metal on the textural properties. Finally, considerable variations where observed on the silanol groups on the surface of the catalysts. These materials were tested in D-glucose hydrogenation, observing significant differences on the performance of the catalyst depending on the synthesis technique employed.

Keywords: aerogel; silanol; tuned selectivity; palladium catalyst; nanoparticles; supercritical CO_2

1. Introduction

Effective routes to obtain more valuable products require the design of efficient catalysts. Novel catalytic structures are therefore needed to overcome the present challenges. These novel structures require the integration of support active sites in a way that preserves their advantages and capabilities. Therefore the development of novel catalytic structures achieved by the integration of metallic nanoparticles evenly distributed in a mesoporous and high-surface aerogel appears as a promising alternative.

Silica aerogels present remarkable properties which make them suitable materials to overcome these new challenges: high pore volumes, favorable transport properties, stability and surface activity. What is more, their properties can be easily tuned: their textural properties can be tailored by changing the ratios of precursor [1]; the chemistry of their surface can be controlled by using different alkyl-alkoxy/chloro silanes allowing to govern their grade of hydrophobicity [2]; in addition, the option of creating hybrid aerogels make almost all properties requirements achievable [3].

By constrast, due to its breakability special techniques must be applied for the metal impregnation before or after the drying in order to avoid the capillarity forces which could damage the structure of the matrix. Cogelled aerogel and impregnated aerogel catalysts were already produced [4], concluding that the cogelled ones showed better resistance to sintering. Also Ni and Pd nanoparticles were embedded on aerogels by impregnation of the gels followed by supercritical drying [5]. Ionic liquids have also been considered as a possible route [6]. Finally supercritical CO_2 has been used as impregnation media and 1,1,1,5,5,5-Hexafluoro-2,4-pentanedione-palladium (2:1) as metal precursor [7]. Furthermore, the solubility of Palladium(II) acetylacetonate in supercritical CO_2 has been already studied, providing another Pd precursor which could be used in the supercritical impregnation (SCI) technique[8].

Therefore, different preparation techniques have been proposed for incorporating Pd catalytic nanoparticles in a silica matrix, showing different results depending on the technique employed. But to our knowledge, a systematic study of the variation of the final properties of the materials depending on the techniques and solvents used for the metal impregnation has not been done. What is more, this variation of properties could be translated into differences on the functionality of the final catalysts.

Catalytic hydrogenation of D-glucose into sorbitol seems to be a simple reaction, but in fact D-glucose can follow different reaction pathways instead of being converted into sorbitol. In essence, D-glucose can isomerize into D-fructose by Lobry de Bruyn Alberda – Van Ekenstein reaction [9] and its subsequent hydrogenation allows to obtain mannitol / sorbitol mixture[10]. In addition, byproducts such as glycolaldehyde and glyceraldehyde could appear as a result of retro aldol condensation reaction [11], which are hydrogenated into smaller sugar alcohols like ethylene glycol and glycerol respectively. Ru-based catalysts demonstrated to be the most effective for catalytic hydrogenation into sorbitol. However, metals such as Ni, Pt, Pd and Rh have been used for similar purposes due to their lower price in comparison with Ru [12]. Bizhanov et al. reported that the combination of Pd and Ni in the hydrogenation of D-glucose was very effective in comparison with other bimetallic catalysts [13].

In this work, Pd nanoparticles have been embedded on silica aerogel by using three different techniques. In each of them the metal was loaded in the matrix at different steps of the production: the direct synthesis (DS), the wet impregnation (WI), and the SCI of the previously dried aerogels. Kinetic tests of D-glucose hydrogenation into sugar alcohols were carried out in order to check the catalytic behavior of the catalysts. The influence of the preparation technique in the activity of each catalyst was reported.

2. Experimental

2.1 Reagents

Tetramethoxysilane (TMOS, 98 %), Palladium(II) acetylacetonate ($Pd(acac)_2$, 99 %), Polyvinylpyrrolidone (PVP) average mol wt 10,000, Borane-ammonia complex (97 %) and D-(+)-glucose (≥99.5 %) were purchased from Sigma–Aldrich. Methanol (99.8 %) and ammonium hydroxide (25 %) were obtained from Panreac. CO_2 (>99.95 mol %) and technical H_2 were supplied by Carburos Metálicos S.A. Deionized water was used in all experiments.

2.2 Aerogels synthesis

Hydrophilic silica alcogels were produced following the single step sol–gel process [14]. The molar ratio was TMOS:CH_3OH:H_2O:NH_4OH, 1:2.3:3.8:1.2 × 10^{-2}.Then the alcogels were dried by using supercritical CO_2. The drying took place in a closed circuit where the CO_2 at 10.5 MPa and 45°C was recirculated till the solvent was completely removed. Three loads of fresh CO_2 where needed. A detailed description of the setup can be found elsewhere [15].

2.2.1 Palladium impregnation

Three different techniques were used to impregnate Pd into the silica matrix by using the same metal precursor.

The first one was the traditional WI method, which consisted on adding $Pd(acac)_2$ into the aging solvent. That was followed by the supercritical drying with CO_2. Two solvents were used: methanol and acetone. Acetone one was chosen because of the higher solubility of the precursor. The solutions were saturated at 20, 40 and 50°C.

The second one was the SCI. It is based on the dissolution-precipitation principle. After the supercritical drying of aerogels, the supercritical CO_2 was also used as solvent media for the $Pd(acac)_2$. The precursor was placed in excess in a batch reactor where the samples stayed at 25 MPa and 60°C for a long time to secure the solubilization till saturation conditions and diffusion of the metal precursor. Then the solubility of the precursor was decreased to force its precipitation into the aerogels pores by reducing temperature till room temperature. Finally the system was decompressed at a rate of 0.3 MPa/min.

The third one, the DS, was made by suspending metallic Pd nanoparticles in the methanol of the alcogels synthesis. These nanoparticles were produced by taking as reference the methodology described by other authors, which reduces the metal precursor with ammonia borane in a methanol solution [16]. Then the samples were calcinated at 400°C during 3 hours in order to eliminate the surfactant.

Finally, in all the cases, the aerogels were milled during 60 minutes at 100 rpm with a Planetary Ball Mill PM 100 (Retsch) and the powder was treated with a flow of 2 Nl/min of pure H_2 at 150°C during 30 minutes to activate the catalyst.

2.2.2 D-glucose hydrogenation:

The reaction was performed in batch in an experimental set-up with a commercial stainless steel high pressure reactor (Berghof BR-25) with an internal volume of 25 cm^3, agitated with a magnetic stirring bar 1400 rpm and fitted up with a proportional–integral–derivative system for temperature control. The hydrogenation reaction was performed by pumping 5 mL of glucose solution (10g/L) and charging 150 mg of the hydrophilic aerogels with different loads of Pd. All the catalytic tests were performed at 120°C and 2.5 MPa of pure hydrogen during 360 min. A more detailed description of the set-up can be found elsewhere [17]. Activity of the different catalyst (A, $mol_{converted\ glucose} \cdot mol_{metal}^{-1} \cdot min^{-1}$) and selectivities to the products (S, %) were calculated using Eq. (1) and Eq. (2).

$$A = \frac{n_{glucose\ 0} - n_{glucose\ f}}{n_{metal} \cdot min} \qquad (1)$$

$$S(\%) = \frac{n_{product}}{n_{glucose\ o} - n_{glucose\ f}} \cdot 100 \qquad (2)$$

2.3 Characterization

The aerogel structure was studied by Fourier transform infrared spectra (FT-IR model TENSOR fromBRUKER, Spain)

Metal loading was determined by atomic absorption (AA) using a VARIAN SPECTRA 220FS analyzer. Digestion of the samples was performed with HCl, H_2O_2 and HF using microwave at 250 °C.

The crystallinity of the impregnated Pd particles were analyzed by X-ray diffraction (Discover D8-Bruker)

A JEOL field emission microscope, model JEM-FS2200 HRP, operating at 200 kV was used for HR TEM (High Resolution Transmission Electron Microscopy) and EDX (Energy-Dispersive X-ray spectroscopy).

The textural properties of the catalysts were determined by nitrogen isothermal adsorption-desorption. A Surface Area and Porosity Analyzer (ASAP2020-Micrimetrics) was used. The specific surface area was calculated by the BET (Brunauer–Emmett–Teller) method. The specific

pore volume is determined by the single point adsorption method. The shown average pore diameter is based on the desorption isotherm of the Barrett-Joynes-Halenda (BJH) method. Hydrogenation products were analyzed by liquid chromatography (HPLC). The HPLC column used was SUGAR SC-1011 from Shodex at 80 °C and a flow of 0.8 $cm^3 \cdot min^{-1}$ using water Milli-Q as the mobile phase. A Waters IR detector 2414 was used to identify sugars, polyols and their derivatives.

3. Results

3.1 Infrared spectra studies

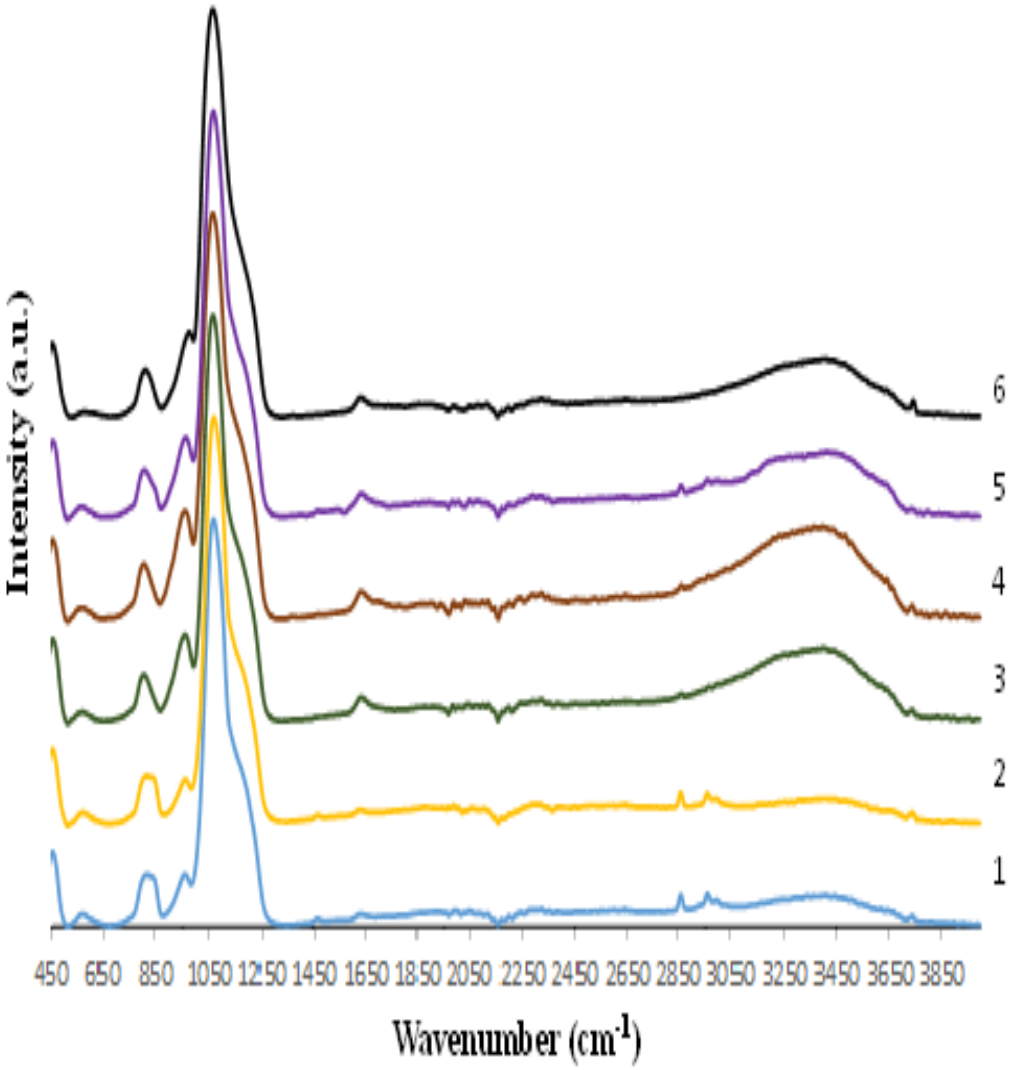

Figure 1. Infrared spectra of the raw aerogel (1), reduced aerogel (2), reduced WI with acetone at 20°C (3), reduced WI with acetone at 50°C (4), reduced SCI (5) and reduced DS (6).

Figure 1 shows the infrared spectra of the silica aerogel and the different synthesized catalysts. The untreated support shows some methyl groups on the surface (815, 2862, 2936 and 2974cm^{-1}); these groups are expected to correspond to residual non-hydrolyzed alkoxy groups on the surface of the silica aerogels [18]. The free metal support was also reduced under the same conditions which were used to reduce the catalysts and not important fluctuations where noticed on the spectra. By contrast a significant decrease on the methyl groups followed by an increment of the silanol peak (960 cm^{-1}) was noticed in the samples produced by WI. What is more, comparing the sample prepared at 20°C and the one at 50°C, the hydroxylation seems to be related with the temperature of the impregnation. A similar but slighter effect is observed on the sample prepared by SCI. Although the temperature of SCI is 60°C, the reduction in the methyl groups and the increment at 960cm^{-1} is less pronounced in supercritical CO_2 than in acetone. A different phenomena is observed in the catalyst made by direct synthesis which has completely lost these methyl groups but does not show the higher intensity on the silanol region. This could be explained by the temperatures reached during the calcination of the PVP which allows the loose of the methyl groups but also the initialization of the dihydroxylation [19].
Concerning the OH stretching region, three different bands can be distinguished. The one at 3735cm^{-1} corresponds to the free silanol groups on the silica surface. The broad band at ~3502cm^{-1} belongs to the stretching vibrations of the hydroxyl groups of water physically adsorbed on SiO_2 surface and the surface silanol groups entering into a hydrogen bond. The band at ~3660cm^{-1} can be assigned to the hydroxyls that have formed weak hydrogen bonds [20]. The different catalysts show different intensities in these peaks, which is translated into different chemical properties of the surfaces of the materials.

3.2 Nitrogen physisorption studies

The N_2-adsorption experiment with the raw aerogel and the activated catalyst led to the isotherms illustrated in figure 2. The isotherms belongs to “type IV” which is typical for mesoporous materials. The hysteresis loop is wide, and the desorption curve is more precipitous than the adsorption curve. This situation is classified as H2 type loops and usually occurs when the distributions of pore size radius are wide [21]. Like the raw aerogel, all the catalyst present a unimodal pore size distribution except the DS one, whose distribution is bimodal.

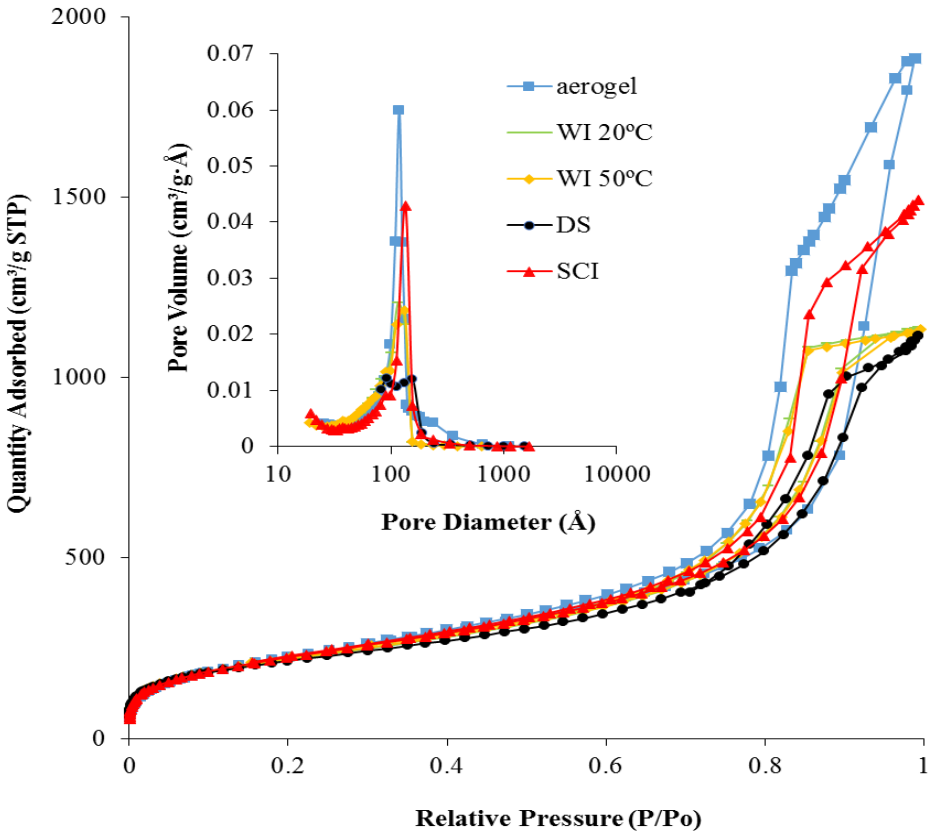

Figure 2. Nitrogen adsorption isotherms and pore size distribution of the raw aerogel, the WI with acetone at 20°C, the WI with acetone at 50°C, the SCI and the DS.

Table 1. BET surface area, pore volume and pore diameter of raw aerogel and activated catalysts.

	BET Surface Area (m^2/g)	Pore Volume (cm^3/g)	Pore diameter (Ø) (nm)
raw aerogel	845	2.91	11.66
WI 20°C	788	1.76	10.37
WI 50°C	799	1.71	8.86
SCI	825	2.31	11.13
DS	766	1.72	13.67

As shown in table 1 the impregnated sample which keeps its final properties closer to the ones of the raw aerogel is the one prepared by SCI. Apparently this technique has allowed to block

less of the pores than the WI technique because the size of the biggest particles of metal produced by SCI is smaller than the biggest particles produced by WI. Concerning this WI catalyst, the possibility of increasing the Pd loading by increasing the temperature at which the solvent is saturated with the Pd precursor does not seem to increase the number of obstructions because there is not an important effect on the textural properties. With respect to the catalyst prepared with suspended Pd nanoparticles during the sol-gel process, the drop in surface and pore volume is bigger than in the other samples and its pore diameter is the biggest. As said above, this sample is the only one with a bimodal pore size distribution. But in this case, the changes on the properties could be attributed to the thermal treatment of the sample during the calcination in order to remove the surfactant which requires temperatures of 400°C [22].

3.3 Powder X-ray diffraction studies

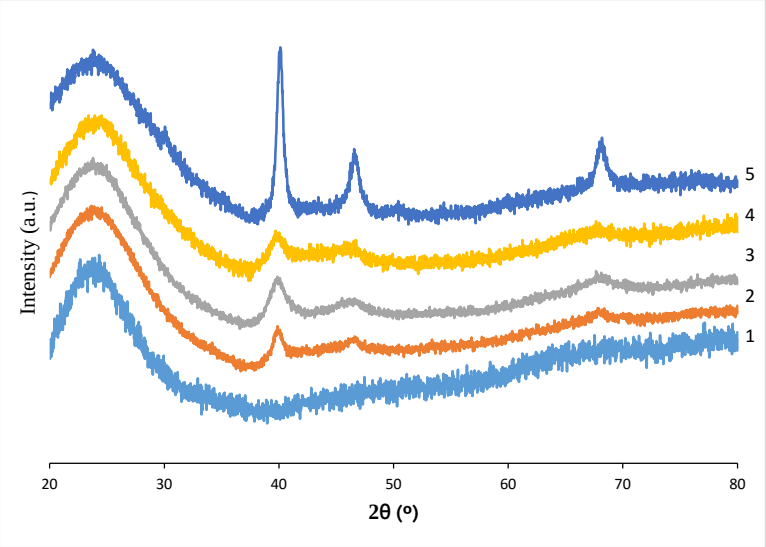

Figure 3. X-ray diffraction patterns of silica aerogel (1) and palladium containing aerogels; WI with acetone at 20 (2) and 55°C (3), SCI (4) and DS (5) samples.

X-ray diffraction patterns for bare silica aerogel and Pd-based catalysts are shown in figure 3. Three characteristic diffraction peaks were detected at 2θ=40°, 46° and 68° (JCPDS 46-1043)) corresponding to the presence of (111), (200) and (220) planes [23]. This information suggested the presence of Face-Centered Cubic (FCC) Pd^0 nanoparticles [24]. The broader base of the peaks in the cases of the WI and SCI indicate a better distribution of the metal inside the matrix[25]. No PdO peaks were observed which means that the samples were completely reduced under pure H_2. By applying the Scherrer equation to the samples prepared by WI with acetone at 20

and 50°C, SCI sample and the ones prepared by DS, the calculated crystal size are 4.4 nm, 3.72 nm, 5.01 nm and 7.14 nm respectively.

3.5 Transmision electron microscopy studies

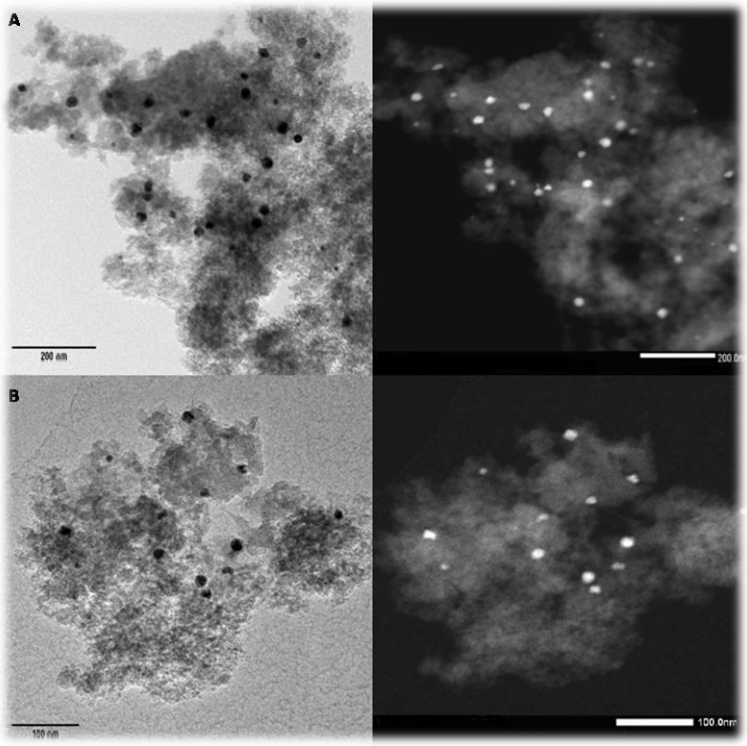

Figure 4. HR TEM and dark field images of cataltalyst prepared by WI (A) and SCI (B)

Figure 4 shows the HR TEM and dark field of the catalyst prepared by WI and SCI. Both of them present a homogeneous and well distributed particles, which is in good relation with the small and wide peaks in the X-ray spectra. Nevertheless an important variation on the size of the particles is seem; in the case of the WI, the size varies from 4 to 30 nm and in the case of the SCI, from 3 to 20 nm. This variation in the size of the biggest particles could be important; it is similar to the expected pore size of the matrix, which indicates that particles with sizes in this range probably are blocking some of the pores of the aerogel scaffold.

By contrast the images showed on figure 5 demonstrate the agglomeration of the metallic particles in the catalyst prepared by DS. This bad distribution is also checked by comparing region 1 and 2 in the dark field. Their corresponding EDX show the presence of palladium just in region 1, without presence of palladium in the rest of the scaffold. The agglomerates present a size above 100 nm. This result is in good agreement with the highest reduction on the pore volume observed in the BET analysis. This result could be due to the incorrect suspension of the

Pd-PVP nanoparticles in the solvent during the sol-gel reaction. Indeed, a correct dispersion of the particles in the gel during ageing is difficult due to the high viscosity of this medium. The use of ultrasounds could be useful to overcome this defect. Another reason could be the formation of PdO during the calcination of PVP, which could promote the sintering due to the weaker interactions of the metallic particles with the support.

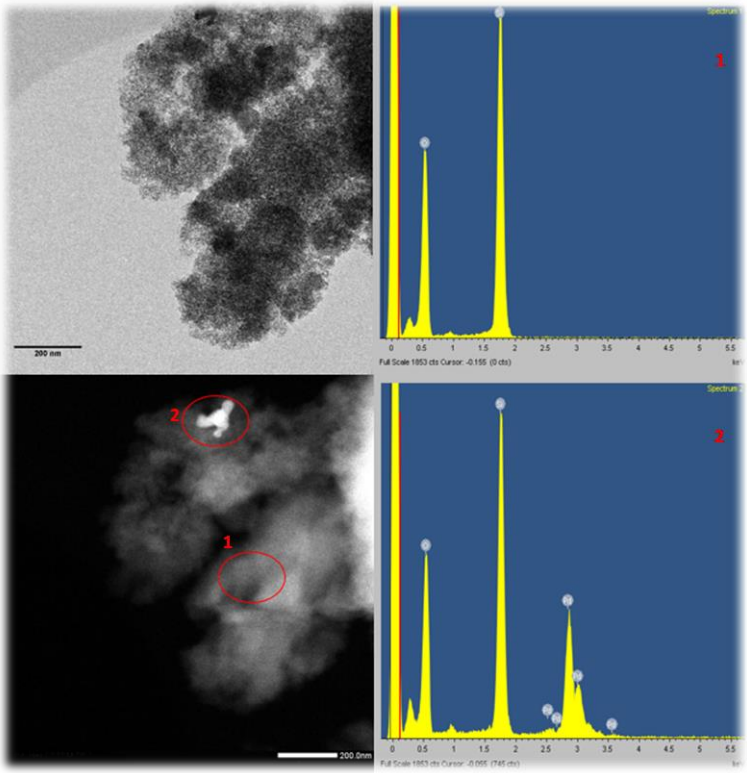

Figure 5.HR TEM, dark field images and EDX of direct synthesis catalyst.

3.6 Atomic absorption studies

As can be seem in table 2, the catalyst with less metal content was the on impregnated with methanol (0.13 %). By contrast, the ones impregnated with acetone present higher concentrations from 0.54 to 1.03 %. On the one hand, this gradient was achievable by increments of the impregnation solution temperature and concentration. On the other hand the low ebullition temperature of the acetone limits the maximum operating temperature, and therefore the maximum concentration of $Pd(acac)_2$ in the solution. It can be concluded that two effects govern the final metal content: the solubility of the precursor and the interactions between the silanol groups on the surface and the solvent. Further studies could also be done in order to check the SCI results when using other pressure and temperature conditions,

resulting in other solubilities. Finally the amount of Pd on the sample prepared with suspended Pd PVP particles can be controlled by adding more or less metal in the suspension used for the synthesis of the gels. The amount of metal added to the suspension and the final one is in good agreement.

Table 2. Metallic content on the activated catalysts

	WI				SCI	DS
P (MPa)					25	
solvent	MeOH		Acetone		Supercritical CO_2	
T (°C)	20	20	40	50	60	
Pd wt %	0.13	0.54	0.65	1.03	0.84	1.61
Particle size (nm)				4-30	3-20	> 100

3.7 Catalytic activity studies

The results of the hydrogenations of D-glucose are summarized in table 3 in terms of activity and selectivity. On the one hand, the materials have shown different catalytic behaviors depending on the preparation method. The catalysts prepared by WI method (WI 20°C and WI 50°C) showed the highest activity during the hydrogenation experiments and the material synthesized by DS presented the lowest one. This fact can be attributed to the different crystallite size calculated from XRD patterns and Scherrer equation, where WI 20°C and WI 50°C obtained crystallite sizes around 4 nm while DS achieved 7 nm. In addition the crystals are not just the biggest but also forms agglomerates as shown in HR TEM images (figure 5). Small differences in terms of activity were observed comparing both WI 20°C and WI 50°C. The higher concentration of the metal in the matrix has not been turned into a higher activity. This could be explained by the size of the particles in the matrix, which is probably bigger in the case of the catalyst with more metal content, reducing the exposed active surface of the metal. Another point to contrast is that the textural properties of the SCI sample are the best, but its activity is lower than those obtained by WI. Therefore, other factors should be taken into account. First of all, the different concentration and nature of the hydroxyl groups on the surface seem to be

playing a role. Secondly, the formation of different types of carbide on the surface due to the direct reduction under hydrogen atmosphere [26] cannot be ignored.

On the other hand, selectivity to sorbitol results presented in table 3 demonstrated the influence of the preparation method and metal loading in the composition of the final product. Comparing the selectivities of the WI 20°C and the WI 50°C to sorbitol, it was observed that an increase in Pd loading from 0.54 to 1.03 % enhanced selectivity to sorbitol from 54 to 76 %. Low amounts of fructose were detected suggesting retro aldol condensation reaction to produce glyceraldehyde that is subsequently hydrogenated into glycerol which is the main byproduct in both cases. In addition, glycerol was the main compound in the liquid product when hydrogenation of D-glucose was carried out over the catalyst prepared by SCI achieving a selectivity to glycerol around 89 %. In the case of SCI sorbitol was not detected in the final product. As it was explained above, hydroxyl groups and carbide on the surface of the support could decrease the activity of the catalyst and favor glycerol production. Finally, D-glucose is hydrogenated with a selectivity around 47 % to sorbitol over the catalyst prepared by DS and no other products could be identified by HPLC in this case.

Table 3. Catalytic activity, (moles of converted glucose per moles of metal and per minute) and selectivity to sorbitol of the synthesized catalysts at 120 °C, 2.5 MPa H_2 and 360 min

	WI 20°C	WI 50°C	SCI	DS
Activity	$1.42 \cdot 10^{-2}$	$1.07 \cdot 10^{-2}$	$4.45 \cdot 10^{-3}$	$2.27 \cdot 10^{-3}$
$S_{SORBITOL}$ (%)	54.23	75.85	0	47.26
$S_{GLYCEROL}$ (%)	34.71	22.43	88.45	0

Conclusions

Three different routes have been used to impregnate silica aerogels with Pd. The load of the metal could be tuned by controlling the concentration of Pd in the different impregnation media but at the same time the achievable concentration is limited by the solubility of the precursor. Well distributed particles were obtained with WI and SCI but agglomeration was observed on the DS catalyst. The test of the catalysts in the hydrogenation of D-glucose have proved that the influence of the concentration of metal and the size of the metallic particles are important. In addition, the chemistry of the support, which is modified depending on the way in which the support is impregnated, and the presence of carbides, seem to play an important role on activity and selectivity.

References

[1] Rao AV, Pajonk GM, Parvathy NN. Influence of Molar Ratios of Precursor, Catalyst, Solvent and Water on Monolithicity and Physical Properties of TMOS Silica Aerogels. J. Sol-Gel Sci. Technol. 1994;3:205-217.

[2] Venkateswara Rao A, Kulkarni MM, Amalnerkar DP, Seth T. Surface chemical modification of silica aerogels using various alkyl-alkoxy/chloro silanes. Appl. Surf. Sci. 2003;206(1-4);262-270.

[3] Maleki H, Durães L, Portugal A. An overview on silica aerogels synthesis and different mechanical reinforcing strategies. J. Non-Cryst. Solids 2014;385:55-74.

[4]Heinrichs B, Noville F, Pirard JP. Pd/SiO2-Cogelled Aerogel Catalysts and Impregnated Aerogel and Xerogel Catalysts: Synthesis and Characterization. J. Catal. 1997;170:366-376.

[5] Martínez S, Vallribera A, Cotet CL, Popovici M, Martín L, Roig A, Moreno-Mañas M, Molins E. Nanosized metallic particles embedded in silica and carbon aerogels as catalysts in the Mizoroki–Heck coupling reaction. New J. Chem. 2005;29:1342-1345.

[6] Anderson K, Cortiñas Fernández S, Hardacre K, Marr PC. Preparation of nanoparticulate metal catalysts in porous supports using an ionic liquid route; hydrogenation and C–C coupling. Inorg. Chem. Commun. 2004;7;73–76.

[7] Morley KS, Licence P, Patricia CM, Hyde JR, Brown PD, Mokaya R, Xia Y, Howdle SM. Supercritical fluids: A route to palladium-aerogel nanocomposites. J. Mater. Chem. 2004;14;1212-1217.

[8] Yoda S, Hasegawa A, Suda H, Uchimaru Y, Haraya K, Tsuji T, Otake K. Preparation of a Platinum and Palladium/Polyimide Nanocomposite Film as a Precursor of Metal-Doped Carbon Molecular Sieve Membrane via Supercritical Impregnation. Chem. Mater. 2004;16:2363-2368.

[9] Mishra DK, Dabbawala AA, Park JJ, Jhung JP, Sung SH, Hwang JS. Selective hydrogenation of d-glucose to d-sorbitol over HY zeolite supported ruthenium nanoparticles catalysts. Catal. Today. 2014;232:99-107.

[10] Heinen AW, Peters JA, van Bekkum H. Hydrogenation of fructose on Ru/C catalysts. Carbohydr. Res. 2000;328:449-457.

[11] Cantero DA, Sánchez Tapia Á, Bermejo MD, Cocero MJ. Pressure and temperature effect on cellulose hydrolysis in pressurized water.Chem. Eng. J. 2015; 276;145-154.

[12] Lazaridis A, Karakoulia S, Delimitis A, Coman SM, Parvulescu VI, Triantafyllidis KS. d-glucose hydrogenation/hydrogenolysis reactions on noble metal (Ru, Pt)/activated carbon supported catalysts. Catal. Today. 2015;257:281-290.

[13] Bizhanov FB, Sokol'ssskii DV, Popov NI, Malkina NYa, Khisametdinov AM. kinetica I kataliz, 1967; 8: 620.

[14] Novak Z, Knez Z. Diffusion of methanol–liquid CO_2 and methanol–supercritical CO_2 in silica aerogels J. Non-Cryst. Solids. 1997;221:163–169.

[15] Sanz-Moral LM, Rueda M, Mato R, Martín Á. View cell investigation of silica aerogels during supercritical drying: Analysis of size variation and mass transfer mechanisms . J. Supercrit. Fluids 2014;92:24–30.

[16] Erdogan H, Metin Ö, Özkar . I*n situ*-generated PVP-stabilized palladium(0) nanocluster catalyst in hydrogen generation from the methanolysis of ammonia–borane Phys. Chem. Chem. Phys. 2009;11:10519-10525.

[17] Romero A, Alonso E, Sastre A, Nieto-Márquez A. Conversion of biomass into sorbitol: Cellulose hydrolysis on MCM-48 and D-glucose hydrogenation on Ru/MCM-48. Microporous Mesoporous Mater. 2016;224:1-8.

[18] Sanz-Moral LM, Rueda M, Nieto A, Novak Z, Knez Z, Martín Á. Gradual hydrophobic surface functionalization of dry silica aerogels by reaction with silane precursors dissolved in supercritical CO_2. J. of Supercritical Fluids.2013;84:74–79.

[19] Cui S, Liu Y, Fan M, Cooper AT, Lin B, Liu X, Han G, Shen X. Temperature dependent microstructure of MTES modified hydrophobic silica aerogel. Mater. Lett. 2011;65:606–609.

[20] Yi-hua Xie, Bing Li, Wei-Zheng Weng, Yan-Ping Zheng, Kong-Tao Zhu, Nuo-Wei Zhang, Chuan-Jing Huang, Hui-Lin Wan. Mechanistic aspects of formation of sintering-resistant palladiumnanoparticles over SiO2prepared using Pd(acac)2as precursor Appl. Catal. 2015;504:179–186.

[21] Wang W, Liu P, Zhang M, Hu J, Xing F. The Pore Structure of Phosphoaluminate Cement. Open Journal of Composite Materials. 2012;2:104-112.

[22] Wagh PB, Pajonk GM, Haranath D, Rao AV. Influence of temperature on the physical properties of citric acid catalyze TEOS silica aerogels. Mater. Chem. Phys. 1997;50:76–81.

[23] Habibi B, Mohammadyari S. Palladium nanoparticles/nanostructured carbon black composite on carbon–ceramic electrode as an electrocatalyst for formic acid fuel cells. J. Taiwan Inst. Chem. Eng. 2016;58:245-251

[24] Teranishi T, Miyake M. Size Control of Palladium Nanoparticles and Their Crystal Structures. Chem. Mater. 1998;10:594-600.

[25] Kibombo HS, Balasanthiran V,Wu CM, Peng R, Koodali RT. Exploration of room temperature synthesis of palladium containing cubic MCM-48 mesoporous materials. Microporous Mesoporous Mater. 2014;198:1-8.

[26] Daniell W, Landes H, Fouad NE, Knözinger H. Influence of pretreatment atmosphere on the nature of silica-supported Pd generated via decomposition of $Pd(acac)_2$: an FTIR spectroscopic study of adsorbed CO. J. Mol. Catal. A: Chem. 2002;178: 211–218

Chapter 4

Release of hydrogen from nanoconfined hydrides by application of microwaves

Release of hydrogen from nanoconfined hydrides by application of microwaves

Abstract

The release of hydrogen from solid hydrides by thermolysis can be improved by nanoconfinement in a suitable micro/mesoporous support, but the slow heat transfer by conduction through the support can be a limitation. In this work, a C/SiO_2 mesoporous material has been synthesized and employed as matrix for nanoconfinement of hydrogen-storing hydrides. The matrix shows high surface area and pore volume (386 m^2/g and 1.41 cm^3/g), which enables the confinement of high concentrations of hydride. Furthermore, by modification of the proportion between C and SiO_2, the dielectric properties of the complex can be modified, making it susceptible to microwave heating. As with this heating method the entire sample is heated simultaneously, the heat transfer resistances associated to conduction can be eliminated. To validate this possibility, ethane 1,2-diaminoborane (EDAB) was embedded on the C/SiO_2 matrix at concentrations ranging from 11 to 31 wt% using a wet impregnation method, and a device appropriate for hydrogen release from this material by application of microwaves was designed with the aid of a numerical simulation. Hydrogen liberation tests by conventional heating and microwaves were compared, showing that by microwave heating hydrogen release can be initiated and stopped in shorter times.

Keywords: hydrogen storage, hydrides microwave heating, aerogel, supercritical CO_2.

1. Introduction

The increasing share of solar and wind in the energetic mix and the COP21 agreement pave the way for a new family of technologies based on renewable energy. Since these renewable energy forms are by its nature fluctuating, it is necessary to develop technologies for storage of energy in periods of excess supply, to use it during the periods of excess demand. Direct use of these energy forms on onboard applications is also not possible, and requires an intermediate form of energy storage.

Storage of this energy in form of hydrogen is one of the most explored methods. The challenge is being addressed using storage systems based on compressed, liquefied and materials-bounded hydrogen [1]. Compared to gas and liquid storage tanks, solid hydrides can store high amounts of hydrogen in small volumes, which are liberated by a reversible chemical reaction by thermolysis. However, currently investigated hydrides are limited by slow hydrogen release kinetics or by high thermodynamic stabilities which make it necessary to apply high

temperatures to decompose them [2]. Therefore, one of the technological challenges which restrain the development of hydrides for H_2 storage is the heat transfer inside the storage tanks [3]. Great efforts have been made in order to overcome this problem. However, this issue can be circumvented if heating energy is delivered directly to the material, and not by heat transfer through the storage tank. Application of microwaves offers this possibility.

The decomposition of several metal hydrides under microwave irradiation was studied by Yuko Nakamori et al. [4]. They concluded that the conductive lost and the particle size were the two most important parameters controlling the H_2 release. Ivaldete da Silva Dupim et al. [5] showed that by particle size reduction a more effective heating of the particles was achieved by approximating the size of the particles to the penetration depth of the electromagnetic field in metallic powders. They obtained this size reduction by applying cold rolling. Another alternative is modifying the general dielectric properties of the complex by mixing with a hydride which actuates as a microwave absorber ($LiBH_4$) [6]. Huajun Zhang et al. [7] propose the use of a honeycomb ceramic monolith coated with 0.54 wt% Ni (corresponding to 0.2 micron Ni thin layer) to hold the hydrides and allowed the rapid heating of the complex.

An alternative to improve the kinetic decomposition of hydrides is using a catalyst [8]. But catalyst add weight to the complex and sometimes require the use of expensive metals. Another alternative is the nanoconfinement of the hydride [9, 10]. By confining the hydride inside the porous host, hydride particle size is restrained to the pore size, and particle agglomeration and growth process, which could have an adverse effect on the kinetic decomposition, are avoided. Moreover, some porous hosts, like carbon or silica mesoporous materials, chemically interact with different hydrides and destabilize it, further improving the decomposition kinetics. By combination of these effects, the decomposition temperature and release kinetics have been significantly improved by nanoconfinement [11]. On the negative side, the support materials usually employed, such as mesoporous carbon or silica, have very low thermal conductivities that slow down the kinetics of hydrogen release if conventional heating by conduction is applied. However, the mesoporous host can be functionalized to provide additional properties to the material [12]. In particular, it can be functionalized to enhance the absorption of microwave energy, and thus combine the main advantages of the two approaches: nanoconfinement and microwave heating. Indeed, a porous material with a high dielectric lost could confine the hydride and change the global dielectric properties of the complex. A material that fulfills this requirement is carbon, which can be manufactured as mesoporous carbon or as carbon aerogel. Some researchers have already confined hydrides into carbon scaffolds like $NaAlH_4$, $LiBH_4$ [13] or $Mg(BH_4)_2$ [14]. But these carbon structures present a limitation which is its low pore volume that restricts the space available for the confinement of hydride inside the support. Due to this

limitation, the maximum hydride loadings achieved in carbon matrixes are between 15 and 30 wt%, which limits the hydrogen storage capacity below the requirements for practical applications. An alternative could be a hybrid material with leaves more pore space for the confinement of a hydride and tunes the global dielectric properties of the complex, making it susceptible of microwave heating. Silica aerogel was already suggested as a very promising material for hydrides confinement due to its remarkable surface properties, and in particular to its high pore volumes that allow confining as much as a 60 wt% of hydride [15]. Carbon/silica hybrid aerogels can combine favorable dielectric properties with high pore volumes. Carbon/silica porous materials can easily made by the carbonization of resorcinol–formaldehyde/silica aerogels, as describe by Y. Kong et al. [16], keeping favorable textural properties for encapsulation.

In this work, a C/SiO_2 porous material susceptible to be heated up by microwaves has been synthesized and impregnated with a hydride. Ethane 1,2-diaminoborane (EDAB) has been chosen as hydride because of its promising properties for H_2 storage: high H_2 content (~10 wt%) and the absence of undesirable volatile impurities in the released gas [17]. Material characterization and H_2 liberation tests by conventional heating and microwaves have been performed in order to evaluate the possible advantages of application of microwave heating in nanoconfined materials. In addition a numerical simulation of the device under microwaves has been performed to reach better understanding of the process.

2. Materials and methods

2.1 Materials

Resorcinol (R, ≥99 % purity from Digma-Aldrich), formaldehyde(F, 36.5-38 % in H_2O from Digma-Aldrich), 3-(aminopropyl)triethoxysilane (APTES, 99 % purity from Digma-Aldrich), ethanol (EtOH, 99.5 % from Panreac) and technical carbon dioxide (from Carburos Metálicos) were used for the aerogels synthesis and technical nitrogen (from Carburos Metálicos) was used for the aerogels pyrolysis. Chlorotrimethylsilane (CTMS, ≥98 % from Sigma-Aldrich) and methanol (MeOH, 99.8 % from Panreac) was used to functionalice the C/SiO_2 particles. EDAB (96 %, from Sigma-Aldrich) and MeOH were used for the wet impregnation of samples.

2.2 Complex synthesis:

The resorcinol-formaldehyde aerogels were synthesized following the methodology of Y. Kong et al. [16]. Cylindrical monoliths were made by using R:F:APTES:EtOH, in a molar ratio of 1:2:1:60. After gelation the alcogels were dried by using supercritical CO_2 in order to avoid the capillary stresses which could damage de aerogel structure. The drying took place in a closed circuit. The alcogels were placed in a chamber which can be isolated from the rest of the circuit. Then CO_2 was pumped till 10.5 MPa and heated till 40°C. After it the CO_2 was recirculated till the solvent was completely removed. Three loads of fresh CO_2 where needed. A detailed description of the setup can be found elsewhere [18]. Subsequently the RF/SiO_2 aerogels were pyrolysed in a homemade tubular oven. The samples were heated till 800°C were the T was held for 3 hours. All this process was made under inert atmosphere (~10 $NmLN_2/h$). The pyrolysed monoliths were then mill in a planetary ball mill (PM100 from *Retsch*) 100 rpm during 3 h. The resultant powder was immersed in a CTMS MeOH mixture overnight, in order to minimize the hydroxyl and carboxyl of the matrix surface which could destabilize the hydride impregnated. The rest of the functionalization agent was washed with excess of MeOH.

Finally the powders were loaded with EDAB by wet impregnation, using MeOH as solvent for the hydride (28mg/mL).

2.3 Material Characterization

The chemical structure of the complex was studied by Fourier transform infrared spectroscopy (FT IR model TENSOR from BRUKER).

The crystallinity of the impregnated EDAB was analyzed by X-ray diffraction (Discover D8-Bruker) Differential scan calorimetry (DSC) assays were performed with a (Mettler-Toledo 822e). The heating rate was 5°C/min from 30 to 250°C under a N_2 constant flow of 60 mL/min.

The textural properties of the complex were determined by nitrogen isothermal adsorption-desorption. A Surface Area and Porosity Analyzer (ASAP2020 from Micrimetrics) was used. The specific surface area was calculated by the BET (Brunauer–Emmett–Teller) method. The specific pore volume was determined by the single point adsorption method. The shown average pore diameter is based on the desorption isotherm of the Barrett-Joynes-Halenda (BJH) method.

The determination of the complex dielectric properties was carried out by means of a cavity perturbation method described by V. Ramopoulos et al. [19]. Namely, the powdered sample was introduced in a quartz tube (inner diameter 7.8 mm) without compaction. 0.49 cm^3 of material were tested for samples with ~11 wt% EDAB. Then, the sample was introduced at the center of a TE-111 mode cavity with a resonance frequency close to 2.45GHz.

Numerical simulations. Design of hydrogen liberation cell.

The design of the cell used in hydrogen liberation experiments by application of microwaves was supported on a numerical simulation. For this, the process of microwave heating and release of the hydrogen from the material is represented in this work by three basic stages [20, 21]:

1) Generation of the microwaves in the magnetron.

2) Propagation of the electromagnetic waves.

3) Heat generation and transfer in the material.

The model combines all relevant physics. It simulates the electromagnetic interactions in the microwave circuit, including the forward and backward interaction between the applicator section of the circuit and the magnetron microwave source. This was done via microwave network analysis.

The time harmonic stationary microwave field is simulated over the applicator section of the microwave circuit including the load, while the characteristics of the microwave source are represented by an idealized lumped magnetron model. The model characteristics are described in more detail in [20].

Moreover, the model also includes conductive heat transfer. Using the interaction between electromagnetic waves and the material information, the temperature and heat generation were predicted. All the simulations have been carried out using Comsol Multiphysics® 3.5 [22].

The medium parameters relevant in the electromagnetics model are the relative permittivities of the materials present in the microwave circuit. The dielectric properties of the composite measured as described earlier, were introduced in the model.

Hydrogen liberation experiments.

To decompose the hydride and liberate hydrogen, the sample was heated by two different methods:

By conventional heat transfer, introducing the vessel in a gas chromatography oven (Agilent 7890).

With a microwave oven (CEM Discover), by placing the vessel vertically, centered and at a high of 3cm from the bottom of the cavity.

The H_2 flow generated by the thermolysis was measured by a volumetric method by using a fully open mass flow controllers (EL-Flow F-200 from Bronkhorst) with ranges from 0.02 to 1 ml min^{-1}. It was considered that all the released gas was hydrogen. Temperature was followed by placing a fiber-optic temperature sensor TS2 (OPTOCOM) inside the internal capillary of the glass vessel.

3. Results

3.1 Nitrogen isothermal adsorption-desorption isotherms

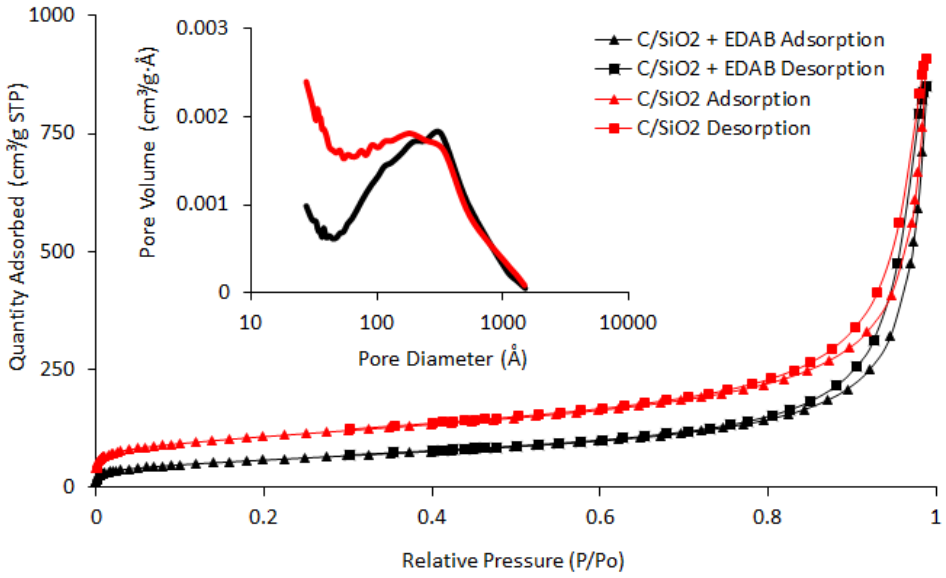

Figure 1. Nitrogen adsorption isotherms and pore size distribution of the raw aerogel and the impregnated one.

Table 1 shows the main textural properties of the non-impregnated aerogel and the impregnated ones. Carbon aerogels obtained from the pyrolysis of resorcinol formaldehyde are microporous materials with pore volume under 1 cm^3/g [23]. By contrast silica aerogels are mesoporous materials with high pore volume (above 2.5 cm^3/g) [11]. By mixing silica and carbon it is intended to maintain the high the pore volume of silica aerogels, which is important in order to have enough pore space to confine the hydride. Results presented in table 1 demonstrate that the materials obtained have pore volumes above 1 cm^3/g. In the pore diameter distribution, presented in figure 1, two separate regions of microporous and mesoporous attributed to the carbon and silica regions are distinguished, with a broad mesoporous size distribution.

Table 1.Textural properties of the samples.

	BET Surface Area (m^2/g)	t-Plot Micropore Area (m^2/g)	t-Plot External Surface Area (m^2/g)	Pore Volume (cm^3/g)	Pore diameter (Ø) (nm)
C/SiO_2	386	108	277	1.40	21.9
C/SiO_2 + EDAB 11 wt%	216	15	202	1.31	19.4

As could be expected, by impregnating hydride a significant decrease of the surface area and the pore volume is observed, filling and blocking the smaller pores at this concentration of hydride (~11 wt%). Concerning the isotherms showed on figure 1, the scaffolds present type IV isotherms, typical of mesoporous materials. In addition, adsorption and desorption branches are almost vertical and nearly parallel over an appreciable range of gas uptake, corresponding to a behavior classified as hysteresis loop H1. This kind of porous material consists of well-aligned, spheres and briquettes [24].

3.2 XRD

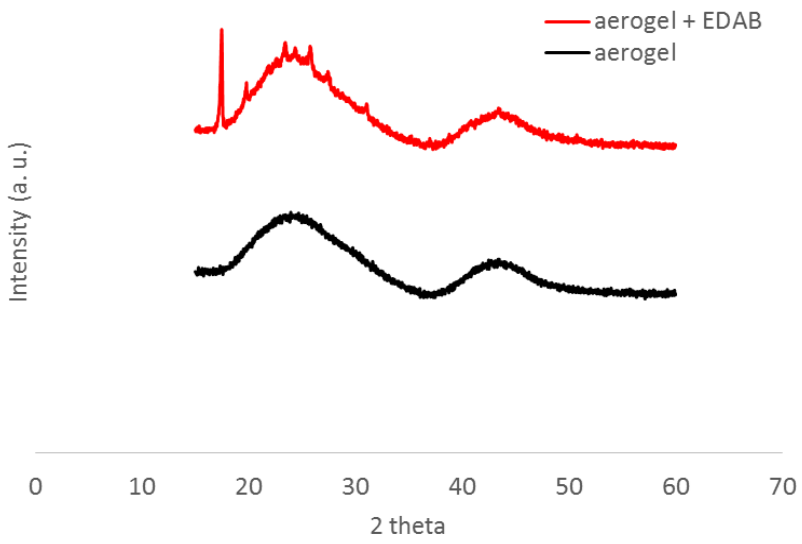

Figure 2. X-ray diffraction patterns of the raw aerogel and the impregnated one.

As shown in figure 2, the XRD pattern exhibited two broad peaks centered at 2θ = 24° and 43°, which corresponded to the 002 and 100 reflection planes of graphite [25]. The diffraction peak around 22° [26], associated with amorphous silica, seems to be overlapped with the graphite. Concerning the EDAB peaks, they fit with the raw EDAB pattern reported by Doinita Neiner et al. [27]. Therefore no transition phases where observed because of the confinement, and it can be concluded that the hydride is stabilized inside the scaffold without variation of its crystalline structure.

3.3 DSC

The DSC analysis of the pure EDAB and the complex impregnated with different EDAB loads are shown in figure 3. Liberation of H_2 on the impregnated samples starts at lower temperatures

than in the case of the pure compound. However, the peak of the decomposition takes place at temperatures near 140°C, corresponding to the decomposition temperature of pure EDAB. The samples with the lowest concentration show also a reduction or even disappearance of the right shoulder of the second decomposition step of the EDAB. Both phenomena could be explained by the nanoconfinement effect. This conclusion is supported by the behavior of the complex when the concentration of EDAB is increased; the higher is the concentration, the more similar to the pure compound is the decomposition, indicating that some of the EDAB remains outside of the pores. Some endothermic peaks are observed around 80°C and 100°C, probably due to some residual solvent content or moisture in the sample.

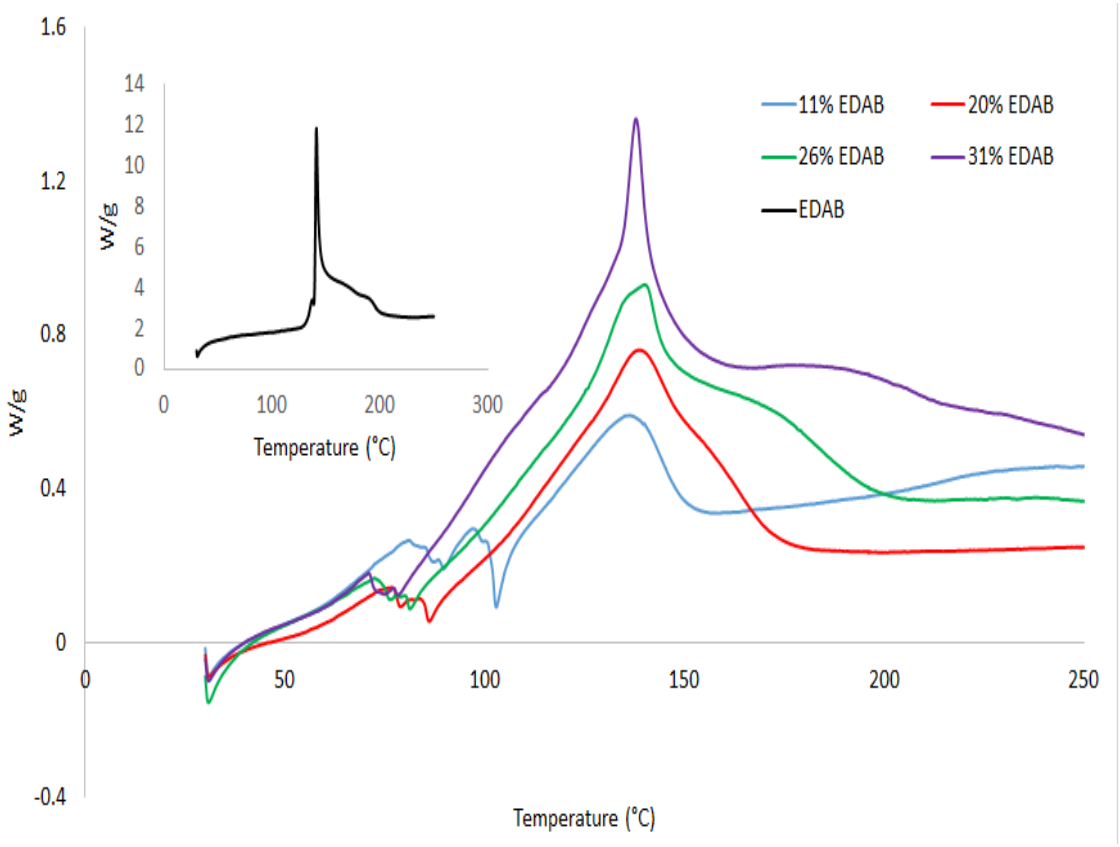

Figure 3. DSC profile of EDAB and the impregnated complex before and after the H_2 released.

3.4 Numerical Simulation and vessel design

Table 2 shows the results of the dielectric properties measurements. Taking into account the pore volume of the sample 1.31cm^3/g and that it is full of air it is logic that the global dielectric properties are not very different from the air (~1). By contrast the presence of carbon in the matrix has confer a significant dielectric loss.

Table 2. of the matrix before and after the impregnation of the EDAB.

Sample	Sample density [g/cm3]	ε'	ε ' accuracy [%]	ε ''	ε '' accuracy [%]
C/SiO_2 + EDAB					
11 wt%	0.143	1.24	1	0.26	2

Figure 4 shows the simulation results. The 3D electromagnetics model revealed that despite the relatively non-uniform electromagnetic dissipation, the temperature distribution homogenizes well due to internal heat conduction. The temperature measured in the center of the bed can be considered representative for the majority of the bed volume.

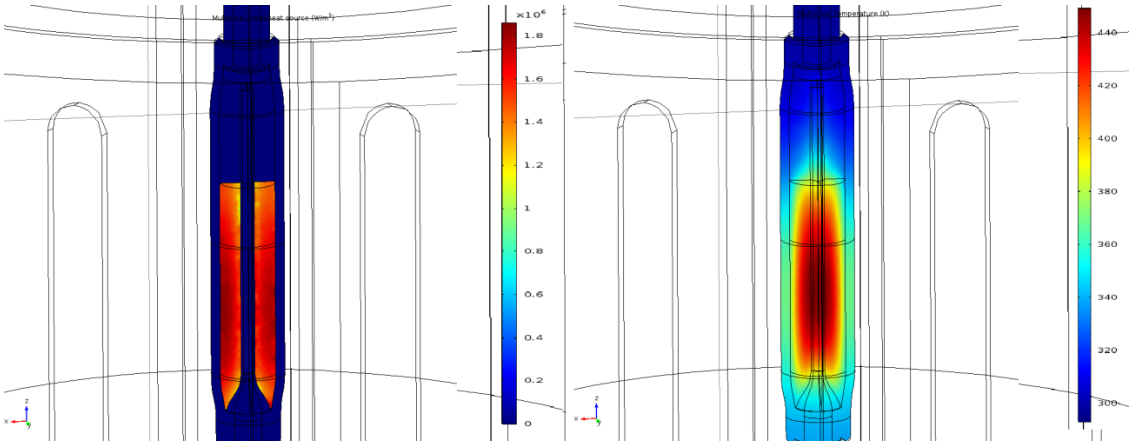

Figure 4. On the left, heat source (W/m^3); on the right, T (K).

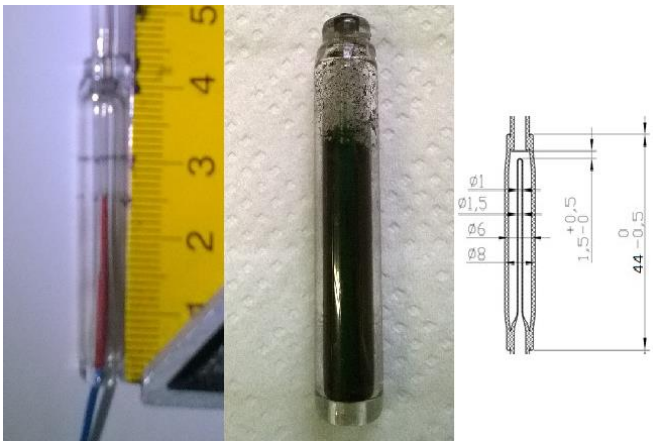

Figure 5. On the left, empty vessel with optic fiber inside the capillary. At the center, vessel filled with the complex. On the right, dimensions of the vessel in mm.

Once the simulations were completed, the glass vessel showed in figure 5 was custom-made by Euroglass Instruments. It was used for the hydrogen liberations. The sample filled the vessel till a high of 2.5cm and with a density of 0.143g/cm^3).

3.5 Liberation test

Figure 6 shows the temperature profiles of the sample along the time, obtained by conventional heating in an oven and by microwave heating. The complex used during these tests was the one with ~11 wt% content of EDAB. The temperature sensor was placed inside the central capillary of the glass vessel. On one hand, in all the cases, even with the lower powers, the heating rate by application microwaves is higher than the one of the one achieved with the oven. The reason is that in the case of the microwaves, the temperature is increased within all the sample, while the oven heats from outside to the center of the sample which is traduced in a delay. On the other hand the temperature profile of the sample heated in the oven is much more stable than the ones heated by microwaves. The temperature gradients along the samples and the expansions of the sample during the heating tests are behind this fluctuations.

Figure 7 shows the H_2 flows during the test. Analyzing the thermolysis tests with pure EDAB and nanoconfined EDAB by conventional heating in the oven at 140°C, it can be clearly observed that the nanocofinemnt has an important effect: First, with the nanoconfined sample, hydrogen release starts 85 s after heating is started, while in the case of the pure compound no hydrogen release is observed during the first 200 s. Second, at 140°C the total H_2 released for the complex is much higher than the one of the pure EDAB (91 % vs 43 %). This phenomena is in good agreement with the DSC profiles, supporting the reduction of the decomposition temperature of the second decomposition step of the EDAB.

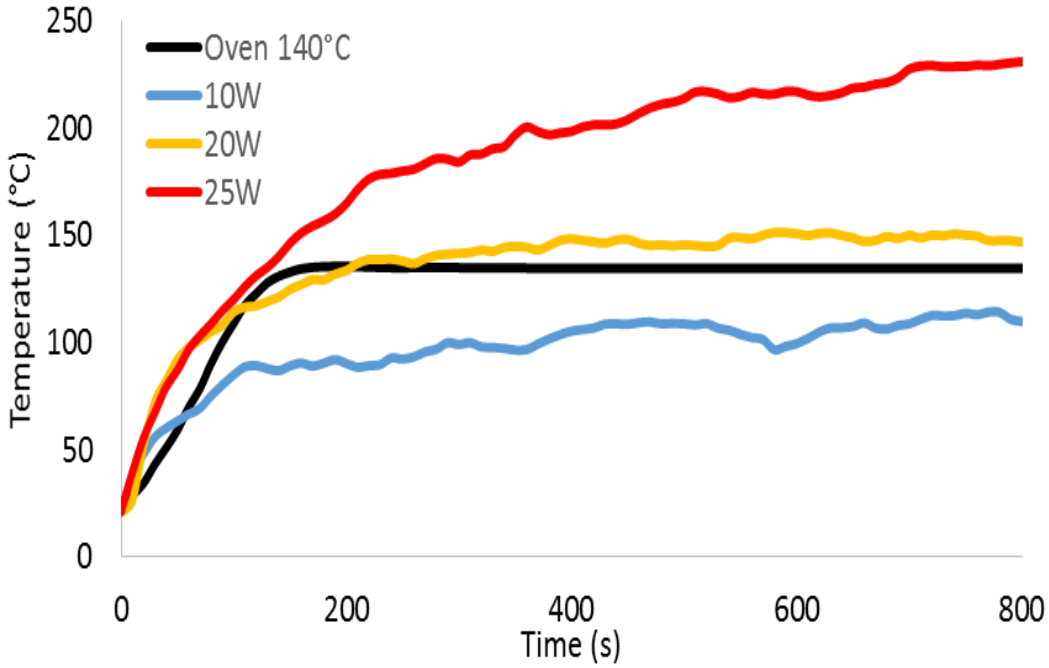

Figure 6. Temperature profile of the liberation tests.

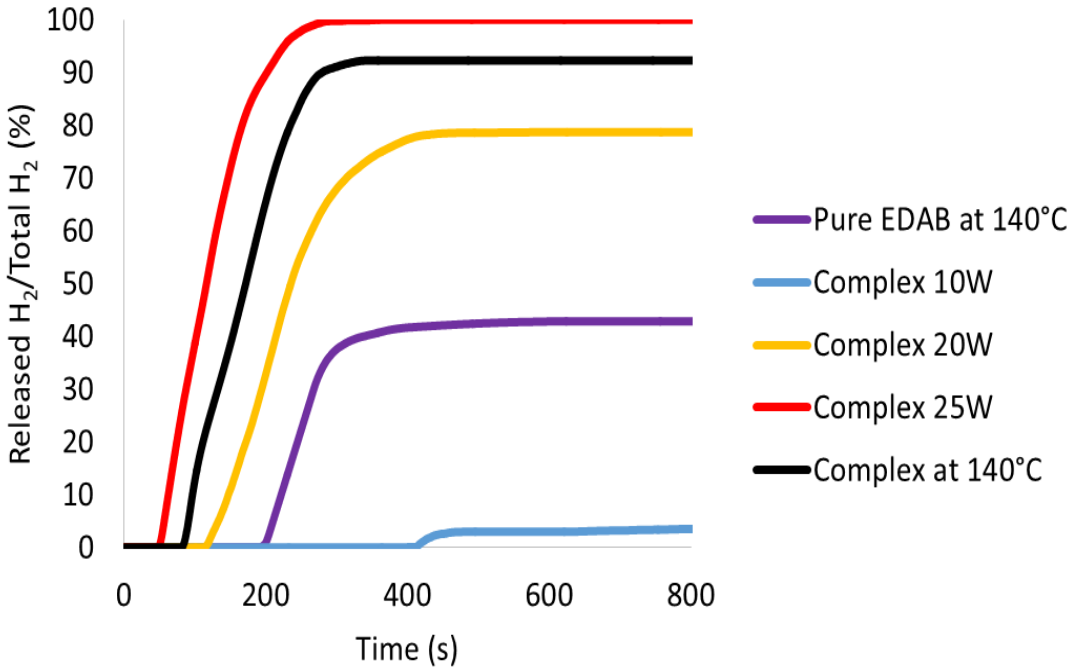

Figure 7. H_2 flow during the liberation tests.

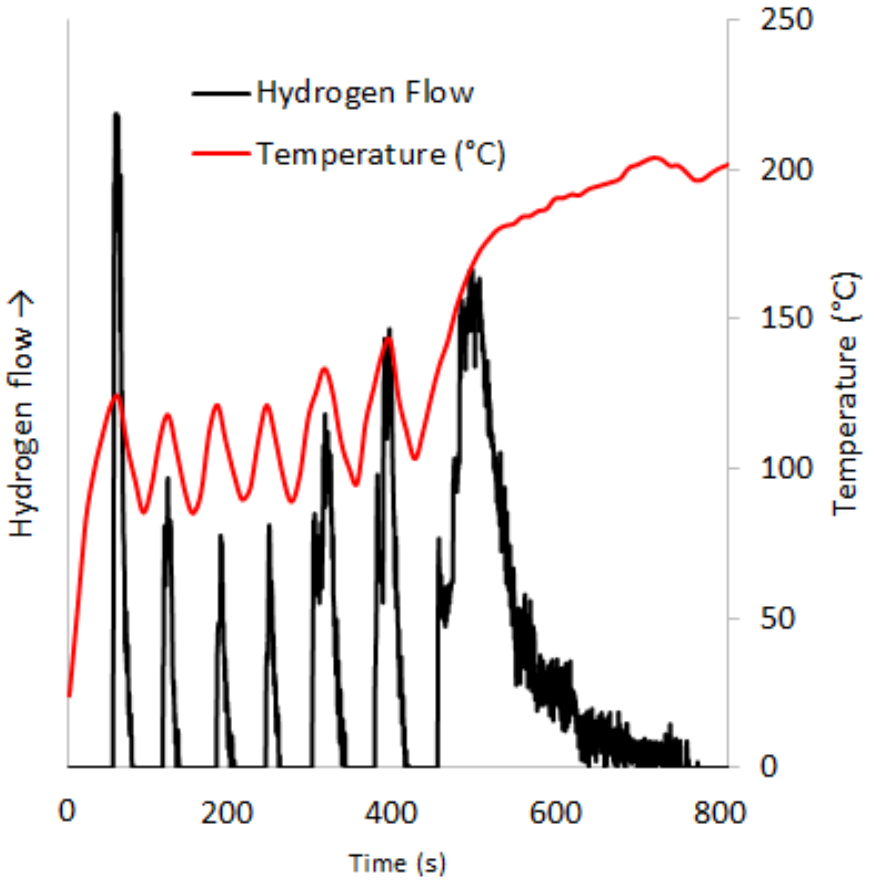

Figure 8. H_2 flow and sample temperature during a liberation test with pulses of 25W.

In the case of the liberations performed with the microwave, the one that is reaching the 100 % liberation of its H_2 content is the test performed at 25W which clearly pass the decomposition temperature of the EDAB. For the test performed with 20W, the total H_2 liberation was of almost 80 %, even though the reached temperature was above 140°C, temperature that in the case of the oven was enough to release above 91 % of the H_2 content in the sample. The temperature gradients along the sample could explain that some areas have not reached the decomposition temperature, therefore the H_2 could not be totally released. Finally the test performed at 10W which reaches ~100°C, has released just a small H_2 flow. This is in good agreement with the IR spectra of the sample after this test which kept the BH and NH bonds, and supports the stability of this complex at medium temperatures.

Additionally a liberation test was performed by using pulses of 25W along time, simulating the fluctuating energy demand of a real system. Again the liberation did not take place until the decomposition temperature was reached but this flow could easily controlled by stopping the power source and reactivating it. Additionally, as the microwave system just heats up the sample, and not the container, the thermal inertia is reduced in comparison with traditional heating, and the temperature started to drop as soon as the microwave was stopped. At the end

of the test the power was hold till the hydrogen contained in the sample was exhausted. The results of this test are shown in figure 8.

3.6 Infrared Spectra

Figure 9 shows the IR spectra of the complex before and after H_2 release tests. The pyrolysed aerogel shows intense silicon–oxygen covalent bonds vibrations appear mainly in the 1200–1000 cm^{-1}. The very intense and broad band appearing at 1050 cm^{-1} and the shoulder at around 1200 cm^{-1} are respectively assigned to the transversal optical and longitudinal optical modes of the Si-O-Si asymmetric stretching vibrations. On the hand, the symmetric stretching vibrations of Si-O-Si appear at 800 cm^{-1} [28]. The strong band at 1569 cm^{-1} stems from the aromatic C=C stretching vibrations of the carbons [29]. The broad band centered at around 3100–3600 cm^{-1} corresponds to the overlapping of the O-H stretching bands of surface silanols and carboxylic groups.

Furthermore, the Si-O in-plane stretching vibrations of the silanol Si-OH groups appear at around 960 cm^{-1}. The surface functionalization with CTMS has reduced the intensity of the two OH areas. In addition the band at 1705 cm^{-1} of the untreated carbons related to the carbonyl and the one at 1359cm^{-1} (OCO) [30] have disappeared because of the treatment with CTMS. Instead, CH peak appears at 740 cm^{-1}, 1249 cm^{-1} and 2965 cm^{-1} (CH_3) and the Si-C stretching vibration at 841 cm^{-1}. These two peaks confirms the replacement of some hydroxyl groups by alkyl groups. This functionalization is traduced in a decrease of the oxygen groups on the support surface, avoiding the chemical interactions between EDAB and the support which could produce the EDAB destabilization.

The spectra of the impregnated aerogel shows the typical peaks of EDAB: 702 cm^{-1} of the BN bond; 1039 cm^{-1} of CN bond; 1162 cm^{-1} and 1189 cm^{-1} of BH bond and 1357 cm^{-1}, 1581 cm^{-1},3221 cm^{-1} and 3257 of NH bond. After decomposition, BH and NH peaks disappear, and two new bands at 1326 cm^{-1} and 1362 cm^{-1} grow stronger. These bands are characteristic of B=N stretching, thus evidencing the formation of double bonds between B and N [31]. The only sample which keeps the BH and NH signals after the heating is the one performed at 10W in the microwave. As was said above, this power was not high enough to reach the decomposition temperature, proving at the same time the stability of the composite till the decomposition temperature.

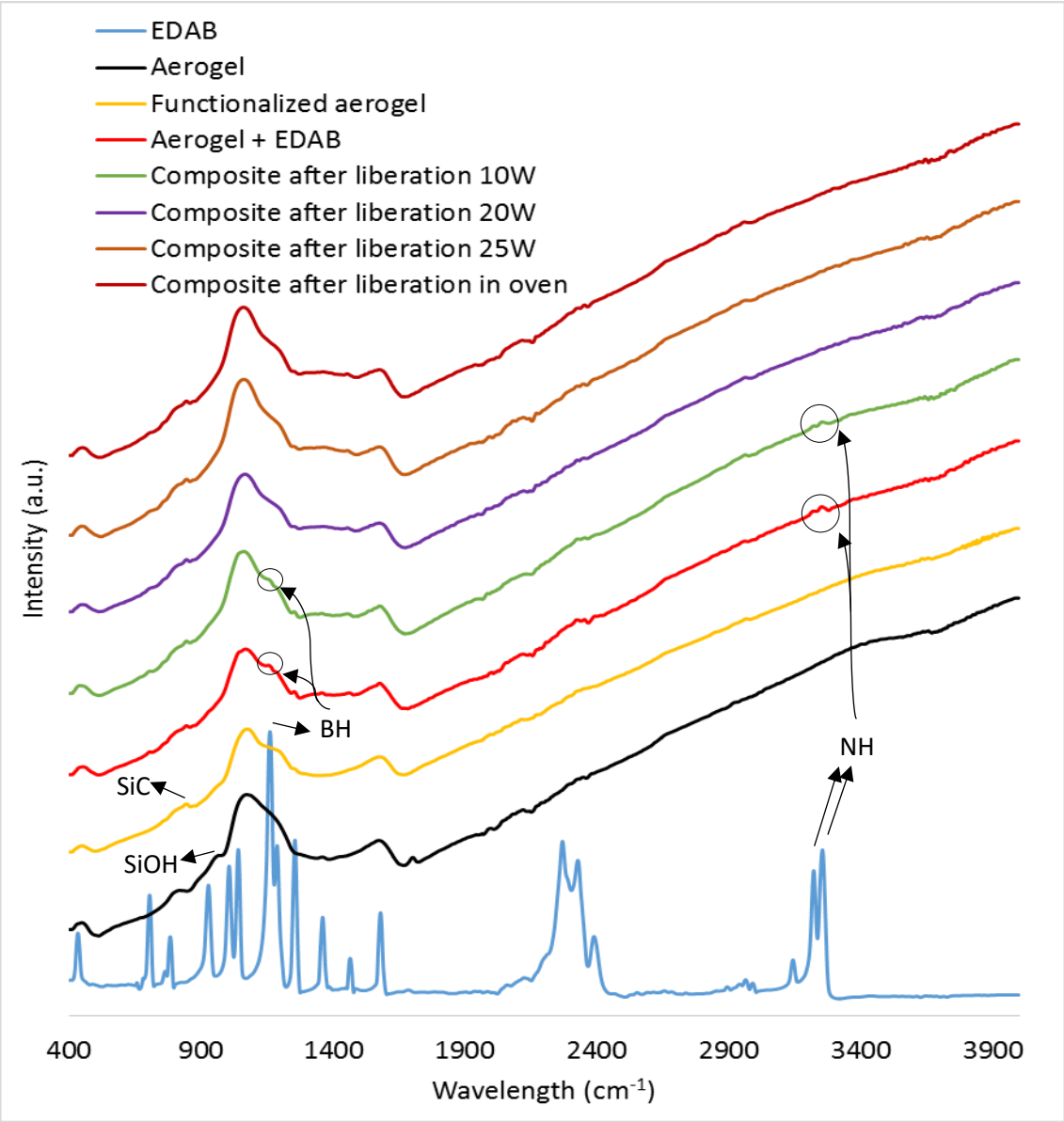

Figure 9. Infrared spectra of EDAB and the impregnated complex before and after the H_2 released.

4. Conclusions

A hybrid C/SiO_2 aerogel has been synthesized and functionalized keeping high pore volume in order to hold EDAB inside its pores. The confinement of the hydride has allowed reducing the response time during the decomposition and has minimized the second decomposition step characteristic of pure EDAB.

The addition of carbon to the matrix has modified the dielectric properties of the matrix and has allowed heating up the system by using microwaves, improving the heating rate. In addition this heating rate could be easily controlled by tuning the power of the electromagnetic field. What is more, the system just heat up the sample, not the container. Therefore the thermal inertia is

reduced in comparison with traditional heating, and the temperature started to drop as soon as the microwave was stopped, allowing controlling the produced hydrogen flow.

References

[1] Zhou L, Progress and problems in hydrogen storage methods. Renewable and Sustainable Energy Reviews 2005;9:395–408.

[2] Rusman NAA, Dahari M. A review on the current progress of metal hydrides material for solid-state hydrogen storage applications. Int J Hydrogen Energ 2016;41:12108-12126.

[3] Mazzucco A, Dornheim M, Sloth M, Jensen TR, Jensen JO, Rokni M. Bed geometries, fueling strategies and optimization of heat exchanger designs in metal hydride storage systems for automotive applications: A review. Int J Hydrogen Energ 2014;39:17054-7074.

[4] Nakamoria Y, Orimo S, TsutaokaT. Dehydriding reaction of metal hydrides and alkali borohydrides enhanced by microwave irradiation. Appl PhysLett 2006;88:112104.

[5] da Silva Dupim I, Ferreira Santos S, Huot J. Effect of Cold Rolling on the Hydrogen Desorption Behavior of Binary Metal Hydride Powders under Microwave Irradiation. Metals 2015;5:2021-2033.

[6] Leng HY, Wei J, Li Q, Chou KC. Effect of microwave irradiation on the hydrogen desorption properties of MgH2/LiBH4 composite. J Alloy Compd 2014;597:136–141.

[7] Zhang H, Geerlings H, Lin J, Chin WA. Rapid microwave hydrogen release from MgH2 and other hydrides. Int J Hydrogen Energ 2011;36:7580-7586.

[8] Mooij LPA, Baldi A, Boelsma C, Shen K, Wagemaker M, Pivak Y, Schreuders H, Griessen R, Dam B. Interface Energy Controlled Thermodynamics of Nanoscale Metal Hydrides. Adv. Energy Mater. 2011;1: 754–758.

[9] Jia Y, Cheng L, Pan N, Zou J, Lu G M, Yao X. Catalytic De/Hydrogenation in Mg by Co-Doped Ni and VO*x* on Active Carbon: Extremely Fast Kinetics at Low Temperatures and High Hydrogen Capacity. Adv. Energy Mater. 2011;1:387–393.

[10] Nielsen TK, Besenbacherb F, Jensen TR. Nanoconfined hydrides for energy storage. Nanoscale 2011;3:2086–2098.

[11] Sanz-Moral LM , Romero A, Holz F, Rueda M, Navarrete A, Martín A. Tuned Pd/SiO 2 aerogel catalyst prepared by different synthesis techniques. J Taiwan Inst Chem E 2016; 65:515–521.

[12] Gao J, Ngene P, Herrich M, Xia W, Gutfleisch O, Muhler M, de Jong KP, de Jongh PE. Interface effects in NaAlH4ecarbon nanocomposites for hydrogen storage. Int J Hydrogen Energ 2014; 3 9;10175-10183.

[13] Yan Y, Au YS, Rentsch D, Remhof A, de Jongh PE, Züttel A. Reversible hydrogen storage in Mg(BH4)2/carbon nanocomposites. J Mater Chem A 2013;1:11177.

[14] Au YS, Yan Y, de Jong KP, Remhof A, de Jongh PE. Pore Confined Synthesis of Magnesium Boron Hydride Nanoparticles. J Phys Chem C 2014;118:20832–9.

[15] REVERSIBLE HYDROGEN SORPTION IN THE COMPOSITE MADE OF MAGNESIUM BOROHYDRIDE AND SILICA AEROGEL. In press

[16] Kong Y, Zhong Y, Shen X, Cui S, Yang M, Teng K, Zhang J.Facile synthesis of resorcinol–formaldehyde/silica composite aerogels and their transformation to monolithic carbon/silica and carbon/silicon carbide composite aerogel. J. Non-Cryst. Solids 2012;354:3150–3155.

[17] Neiner D, Karkamkar A, Bowden M, Choi YJ, Luedtke A, Holladay A, Fisher A, Szymczak N, Autrey T. Kinetic and thermodynamic investigation of hydrogen release from ethane 1,2-di-amineborane. Energ Environ Sci 2011;**4**:4187-4193.

[18] Sanz-Moral LM, Rueda M, Mato R, Martín Á. View cell investigation of silica aerogels during supercritical drying: Analysis of size variation and mass transfer mechanisms . J. Supercrit. Fluids 2014;92:24–30.

[19] Ramopoulos V, Soldatov S, Link G, Kayser T, Jelonnek J. System for in-situ dielectric and calorimetric measurements during microwave curing of resins. GeMiC 2015:16–18, Nürnberg, Germany.

[20] Sturm GSJ, Verweij MD, van Gerven T, Stankiewicz AI, Stefanidis GD. On the effect of resonant microwave fields on temperature distribution in time and space. Int J Heat Mass Tran 2012;55:3800-3811.

[21] Navarrete A,Mato RB, Cocero MJ. A predictive approach in modeling and simulation of heat and mass transfer during microwave heating. Application to SFME of essential oil of Lavandin Super. Chem Eng Sci 2012;68:192-201.

[22] Comsol Multiphysics 3.5® with RF-module, COMSOL AB Stockholm 2008.

[23] Horikawa T, Hayashi J, Muroyama K. Controllability of pore characteristics of resorcinol–formaldehyde carbon aerogel. Carbon 2004;42:1625–1633.

[24] Wang W , Liu P , Zhang M , Hu J , Xing F . The pore structure of phosphoaluminate cement. Open J Compos Mater 2012;2:104–12 .

[25] Ganeev RA, Naik PA, Chakera JA, Singhal H, Pramanik NC, Abraham PA, Panicker NR, Kumar M, Gupta PD. J. Opt. Soc. Am. B 2011;28:360-364.

[26] Xu W, Du A, Tang J, Yan P, Li X, Zhang Z, Shen J, Zhou B. Template confined synthesis of Cu- or Cu2O-doped SiO2 aerogels from Cu(II)-containing composites by in situ alcohothermal reduction. RSC Adv. 2014;4:49541–49546.

[27] Neiner D, Karkamkar A, Bowden M, Choi YJ, Luedtke A, Holladay J, Fisher A, Szymczak N, Autrey T. Kinetic and thermodynamic investigation of hydrogen release from ethane 1,2-di-amineborane. Energy Environ. Sci. 2011;4:4187.

[28] Sanz-Moral LM, Rueda M, Nieto A, Novak Z, Knez Z, Martín Á. Gradual hydrophobic surface functionalization of dry silica aerogels by reaction with silane precursors dissolved in supercritical carbon dioxide. J. of Supercritical Fluids 2013;84:74–79.

[29] Lin XX, Tan B, Peng L, Wub ZF, Xie ZL. Ionothermal synthesis of microporous and mesoporous carbon aerogels from fructose as electrode materials for supercapacitors. J. Mater. Chem. A 2016;4:4497–4505.

[30] Mattsson nA, Hu S, Hermansson K, Österlund L. Adsorption of formic acid on rutile TiO2 (110) revisited: An Infrared Reflection-Absorption Spectroscopy and Density Functional Theory study. J. Chem. Phys. 2014;140:034705.

[31] Leardini F, Valero-Pedraza MJ, Perez-Mayoral E, Cantelli R, Bañares MA. Thermolytic Decomposition of Ethane 1,2-Diamineborane Investigated by Thermoanalytical Methods and in Situ Vibrational Spectroscopy. J. Phys. Chem. C 2014;118:17221−17230.

Chapter 5

Patente Nacional 201500170

Material y procedimiento para el almacenamiento y regulación de la liberación de hidrógeno en estado sólido

Patente Nacional 201500170

Título de la invención:

Material y procedimiento para el almacenamiento y regulación de la liberación de hidrógeno en estado sólido

Campo técnico de la invención:

La invención se sitúa en el sector energético, en el desarrollo de materiales para la aplicación de hidrógeno como fuente de energía en sistemas móviles con consumos energéticos variables, como vehículos o dispositivos electrónicos.

Antecedentes de la invención y estado del arte:

En la actualidad existe un gran interés en el desarrollo de sistemas basados en células de combustible para aplicaciones móviles, como la automoción o los equipos electrónicos portátiles. Este interés se justifica por las excelentes propiedades del hidrógeno como vector energético: la combustión del hidrógeno es limpia, ya que únicamente produce agua, el calor específico de combustión es muy alto, y el hidrógeno se puede obtener mediante electrólisis de agua con energías renovables. Para aplicar esta tecnología, aún deben resolverse diversas cuestiones técnicas, entre las que se incluye el desarrollo de un sistema eficiente para almacenar el hidrógeno. El almacenamiento como gas comprimido es muy costoso, ya que debido a la baja densidad del hidrógeno, se debe utilizar recipientes a presión de gran volumen y peso. El almacenamiento como líquido tampoco es una buena solución, ya que en este caso se necesitan temperaturas criogénicas, lo que hace que se desperdicie gran cantidad de la energía contenida en el hidrógeno únicamente en los procesos de licuefacción y para mantener el depósito frío. Estos problemas han llevado al estudio de sistemas de almacenamiento de hidrógeno en fase sólida (J. Graetz. Chem. Soc. Rev. 38 (2009) 73-82)

Unos de los tipos de materiales de almacenamiento de hidrógeno más prometedores son los hidruros químicos y metálicos (C. Liu et al., Advanced Energy Materials 22 (2010) 28-62). El uso de estos compuestos como materiales de almacenamiento de hidrógeno es bien conocido y está recogido en varias patentes, como la patente GB1568374, “Hydrogen from a hydride material”, de N. J. Bridger, que describe la liberación de hidrógeno desde hidruros por termólisis. Fruto de

estos estudios, las limitaciones de estos materiales también son bien conocidas, y las mejoras se centran en reducir las condiciones de temperatura necesarias para realizar la termólisis, incrementar la velocidad de liberación de hidrógeno, y estabilizar esta velocidad de liberación durante ciclos repetidos de carga-descarga de hidrógeno (M. U. Niemann et al., Journal of Nanomaterials, Article ID 950967 (2008) 1-9).

Una de las estrategias más exitosas para mejorar la velocidad de liberación de hidrógeno y estabilizar esta velocidad, es confinar nanopartículas del hidruro en el interior de la estructura porosa de un material de soporte (J. J. Vajo. Currrent Opinion in Solid State and Materials Science 15 (2011) 52-61). La utilización de materiales porosos como soporte de compuestos químicos es una técnica bien conocida; ejemplo de ello son las zeolitas, M415, SBA o los aerogeles. Normalmente suelen utilizarse para alojar los metales activos en catálisis heterogénea. En la literatura se describen diferentes técnicas con el fin de impregnar estos soportes con los metales; algunas de ellas son la síntesis directa, intercambio iónico o la infiltración en fase vapor (Krijn P. de Jong et al., Current Opinion in Solid State and Materials Science, 4, 1, (1999) 55–62.) Extendiendo este conocimiento, existen diferentes patentes que describen el uso de diferentes materiales porosos para nanoconfinar hidruros: WO2005014469, “Materials encapsulated in porous matrices for the reversible storage of hydrogen”, que describe el uso de hidruros metálicos encapsulados en matrices porosas de carbón o de sílice; US7303736, “Nanostructured materials for hydrogen storage”, que describe la absorción de hidrógeno en un metal semiconductor con estructura porosa; GB2067983, “Metal hydride/metal matrix compacts”, que describe un método para producir materiales compuestos de hidruro estabilizado en una matriz metálica porosa; US5958098, “Method and composition in which metal hydride particles are embedded in a silica network”, que describe un método para fabricar partículas de hidruro embebidas en una matriz de sílice.

Sin embargo, el uso de estos materiales porosos introduce una nueva limitación importante: debido a su alta porosidad, todos estos soportes son en mayor o menor medida buenos aislantes térmicos. (Hyung-Ho Park et al., Journal of Thin Solid Films 516 (2007) 212–215). Esta propiedad supone una importante limitación para las aplicaciones de almacenamiento de hidrógeno, ya que al ralentizarse la transmisión de calor, se introduce un retardo equivalente en la termólisis del hidruro y la liberación de hidrógeno. Debido a esta limitación, si bien los hidruros nanoconfinados presentan una mayor estabilidad frente a la repetición ciclos de carga-descarga de hidrógeno que los hidruros puros, en general también presentan peores propiedades de cinética de liberación de hidrógeno.

Dado que esta limitación se debe a la lenta cinética de la transferencia de calor a través de la estructura porosa del material, puede eliminarse sustituyendo el aporte de energía térmica para

la termólisis mediante calentamiento por conducción, por un aporte energético alternativo. Una forma particularmente útil para realizar este aporte es mediante el uso de radiación electromagnética, como las microondas.

La patente EP1382566, "Method for inducing hydrogen desorption from a metal hydride", describe el uso de microondas para inducir la termólisis de hidruros. Sin embargo, esta patente no describe ningún método para sensibilizar el hidruro a la aplicación de las microondas, de forma que su aplicación se limita a hidruros que en sí presenten propiedades dieléctricas adecuadas para captar la energía de microondas u otras fuentes de radiación elecromagnética. Esta limitación se incrementa si, además, el hidruro está confinado en un soporte poroso que en general puede no ser sensible a dichas fuentes de energía. Huajun Zhang et al. (International Journal of hydrogen energy 36 (2011) 7580-7586) han descrito un método para sensibilizar a las microondas una estructura con un hidruro depositado en los canales de un soporte cerámico, mediante la deposición de una capa de níquel, pero dicho método sólo es aplicable a soportes con estructura porosa macroscópica (con canales de un diámetro de 1.5 mm en la aplicación descrita por los autores), y no a soportes meso o microporosos (con diámetros de poro por debajo de 100 nm) como los empleados para nanoconfinar hidruros, y requiere cantidades relativamente altas de metal sensibilizador, que incrementan el peso del material y reducen su capacidad de almacenamiento de hidrógeno por unidad de masa.

Por tanto, no se ha descrito la utilización de nanopartículas de un metal u óxido sobre soportes porosos con el fin de mejorar su calentamiento mediante la técnica de microondas, y así permitir una liberación de hidrógeno por termólisis más rápida y controlable.

Breve descripción de la invención:

Se propone la adición de materiales sensibilizadores a la radiación electromagnética a soportes meso o microporosos utilizados para confinar compuestos de almacenamiento de hidrógeno. La adición de estos dopantes, aporta diferentes ventajas a la hora de calentar al soporte y su superficie: el calentamiento es más rápido y eficiente que con los métodos tradicionales por conducción; y el material se calienta de forma homogénea, evitando así los gradientes de temperatura. Estos hechos pueden aplicarse en el campo de almacenamiento de hidrógeno en estado sólido, ya que muchos de los compuestos sólidos que se proponen con este fin, son depositados y nanoconfinados en soportes porosos con el fin de evitar su sinterizado, y requieren de cierta temperatura para descomponerse por termólisis y liberar así el hidrógeno almacenado. Teniendo en cuenta que, a una temperatura constante, la velocidad de liberación

de hidrógeno desde estos compuestos no se mantiene constante, sino que va reduciéndose a medida que se el material se agota, y que además muchas de las aplicaciones de estos materiales (vehículos, electrónica móvil…) necesitan aportes de hidrógeno variables en el tiempo para responder a incrementos súbitos del consumo de energía, resulta necesario disponer de un método que permita regular de forma rápida y sin retardos la velocidad de liberación de hidrógeno desde el material, mediante una variación rápida y homogénea de la temperatura a la que se efectúa la termólisis.

Descripción de las figuras

Figura 1: Diagrama esquemático de la estructura del material.
Matriz de sílice
Poro
Hidruro impregnado
Partícula dopante de las propiedades dieléctricas

Figura 2: Evolución de la temperatura en un monolito poroso mediante aplicación por microondas frente a un calentamiento convencional por conducción.
Mediante radiación electromagnética
Mediante calentamiento tradicional

Figura 3: aerogel de sílice (izquierda), tras impregnación con ferroceno (centro) y tras calcinación de la muestra y formación del óxido de hierro (derecha)

Figura 4: Calentamiento de un aerogel de sílice sensibilizado con óxido hierro mediante aplicación de microondas a diferentes potencias de microondas (línea de puntos), frente a calentamiento del mismo monolito por conducción en un horno a diferentes temperaturas (línea continua).

Figura 5: Curvas de calentamiento de un aerogel de sílice sensibilizado con óxido hierro a diferentes temperaturas mediante microondas.

Figura 6: Propiedades dieléctricas de aerogeles de sílice sin sensibilizar (línea continua), y sensibilizados con óxido de hierro (línea de puntos).

Figura 7: Liberación de hidrógeno desde un aerogel de sílice cargado con hidruro de magnesio mediante aplicación de microondas, sensibilizado con óxido de hierro (línea de puntos) y sin sensibilizar (línea continua).

Descripción detallada de la invención

Muchos materiales porosos presentan una baja constante dieléctrica (ya que contienen mucho aire) y por tanto también una baja conductividad térmica. La presente propuesta consiste en la adición de metales u óxidos en forma de nanopartículas o la adición de carbono a la estructura porosa, con el fin de aumentar la constante dieléctrica media del conjunto del material, consiguiendo así que su calentamiento por radiación electromagnética sea viable y efectivo. La potencia a aplicar puede ser variable en tiempo e intensidad; consiguiéndose cualquier temperatura deseada, limitada únicamente por la resistencia térmica de las sustancias empleadas, y pudiendo regularse así la velocidad de liberación de hidrógeno.

La **Figura 1** muestra un diagrama esquemático del material. La base del material es un material meso o microporoso (con diámetro de poro inferior a 100 nm), como los comúnmente empleados para estabilizar partículas de hidruros mediante confinación de las partículas en los poros del material. Este material se sensibiliza a las microondas mediante deposición de nanopartículas de metales u óxidos o la adición de carbono a la estructura porosa. Con ello, el material se hace sensible al aporte de energía por radiación electromagnética, con independencia de las propiedades del soporte o el hidruro.

Este diseño del material se aprovecha de la homogeneidad inherente a la estructura porosa de los materiales de soporte, ya que mediante dispersión de las nanopartículas del óxido o el metal o la adición de carbono a la estructura porosa en la estructura porosa del material, se puede conseguir una sensibilización homogénea del material a la radiación electromagnética, empleando proporciones bajas del óxido o el metal o carbono en la estructura porosa.

Mediante este tratamiento de sensibilización, el calentamiento se produce de forma homogénea en toda la masa del material, sin los gradientes de temperatura que son inherentes a los procesos de calentamiento por conducción, tal y como se muestra en la **Figura 2**. Además, mediante este diseño del material, al producirse el calentamiento de forma simultánea en toda la masa del material, el calentamiento depende únicamente de la potencia de radiación electromagnética aplicada y se vuelve independiente de las dimensiones o geometría del material.

Descripción de una realización particular de la invención

Se fabricaron aerogeles de sílice sensibilizados a las microondas mediante incorporación de partículas de óxido de hierro. Los alcogeles de sílice se sintetizan utilizando tetrametilortosilicato como precursor y siguiendo el método sol-gel. El secado de los mismos para producción de los aerogeles de sílice fue llevada a cabo utilizando dióxido de carbono en estado supercrítico. A continuación parte de la muestra fue impregnada con ferroceno utilizando el dióxido de carbono como disolvente para el precursor. Por último la parte orgánica del ferroceno fue eliminada mediante calcinación a 200°C antes de despresurizar el CO_2, precipitando el metal. La **Figura 3** muestra fotografías de los aerogeles de sílice obtenidos tras cada una de estas etapas.

Las muestras de igual masa y densidad, fueron a continuación secadas a estufa a 105°C durante 6 horas con el fin de eliminar cualquier resto de humedad que pudiera influenciar en las medidas. Seguidamente fueron expuestas a un campo de microondas. La **Figura 4** muestra las curvas de calentamiento así obtenidas, midiendo la temperatura en el centro del aerogel de sílice, comparadas con las alcanzadas mediante un calentamiento convencional por conducción en un horno. Mediante la aplicación de microondas se aceleró el proceso de calentamiento, y tal y como se muestra en la **Figura 5** se pudo alcanzar de forma simple diversas temperaturas mediante modificación de la potencia de microondas; además, tal y como se muestra en la **Figura 4**, el calentamiento se inició de forma inmediata, sin el retardo característico de los procesos de calentamiento por conducción. Esta propiedad es esencial para conseguir una respuesta rápida del material frente a cambios en la demanda de hidrógeno. Como se muestra en la **Figura 6**, estas posibilidades de calentamiento se deben a la modificación de las propiedades dieléctricas del material debido a la sensibilización con el óxido metálico. Si a continuación el material se impregna con hidruro de magnesio, mediante el calentamiento por microondas se consigue la liberación de hidrógeno por termólisis, como se muestra en la **Figura 7**.

Reivindicaciones

1. Material para almacenamiento de hidrógeno, caracterizado porque comprende los siguientes elementos: un soporte meso o microporoso (1), un compuesto de almacenamiento de hidrógeno (3), estabilizado en el interior de la estructura porosa del soporte, y un material, susceptible a calentamiento mediante aplicación de radiación electromagnética, dispersado en el soporte (2)

2. Material para almacenamiento de hidrógeno, según reivindicación 1, caracterizado porque el material descrito en la reivindicación 1, cuando el material susceptible a la radiación electromagnética es un metal u óxido metálico.

3. Material para almacenamiento de hidrógeno, según reivindicación 1, caracterizado porque el material susceptible a la radiación electromagnética es carbono incorporado la estructura del material de soporte

4. Material para almacenamiento de hidrógeno, según reivindicación 1, caracterizado porque el compuesto para el almacenamiento de hidrógeno es un hidruro metálico o químico

5. Procedimiento para la liberación del hidrógeno almacenado en el compuesto de almacenamiento de hidrógeno según la reivindicación 1, mediante la aplicación de radiación electromagnética

6. Procedimiento para la regulación de la liberación de hidrógeno del material según la reivindicación 5 caracterizado porque la radiación electromagnética se aplica en forma de microondas

7. Procedimiento para la regulación de la liberación de hidrógeno del material según la reivindicación 5, caracterizado porque la velocidad de liberación del hidrógeno se regula mediante la modificación de la potencia de la energía electromagnética aplicada al material.

Figuras

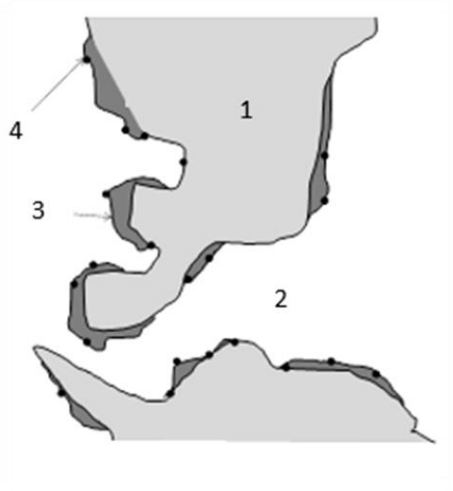

Figura 1

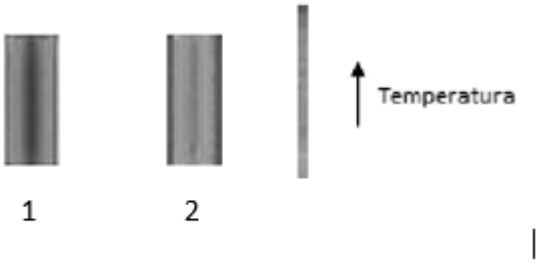

Figura 2

Figura 3

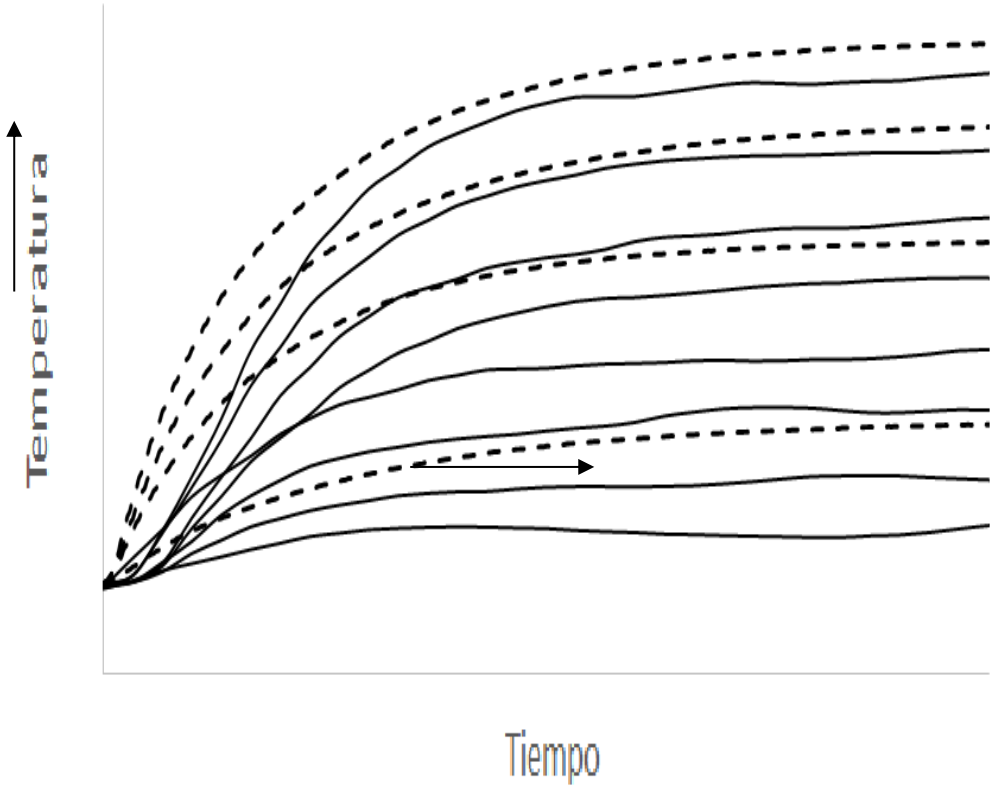

Figura 4

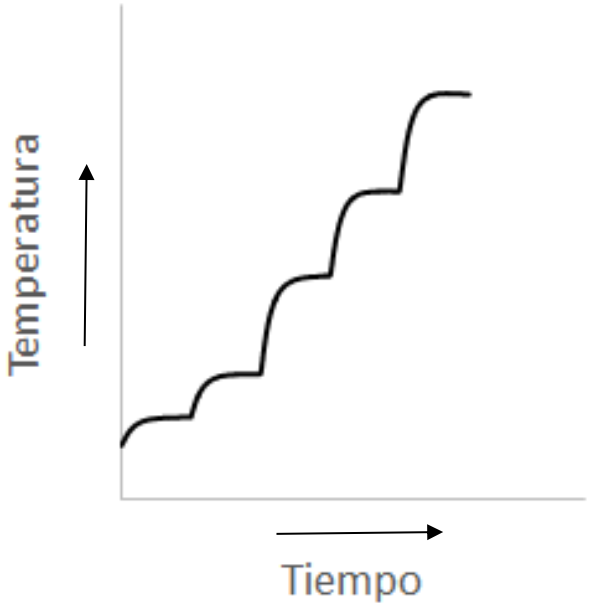

Figura 5

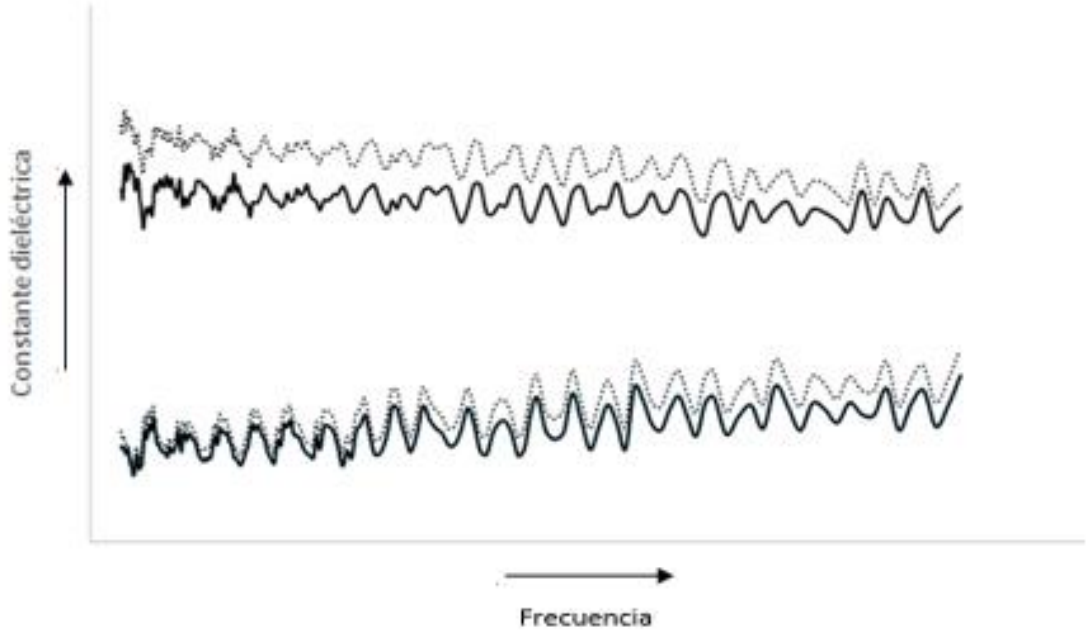

Figura 6

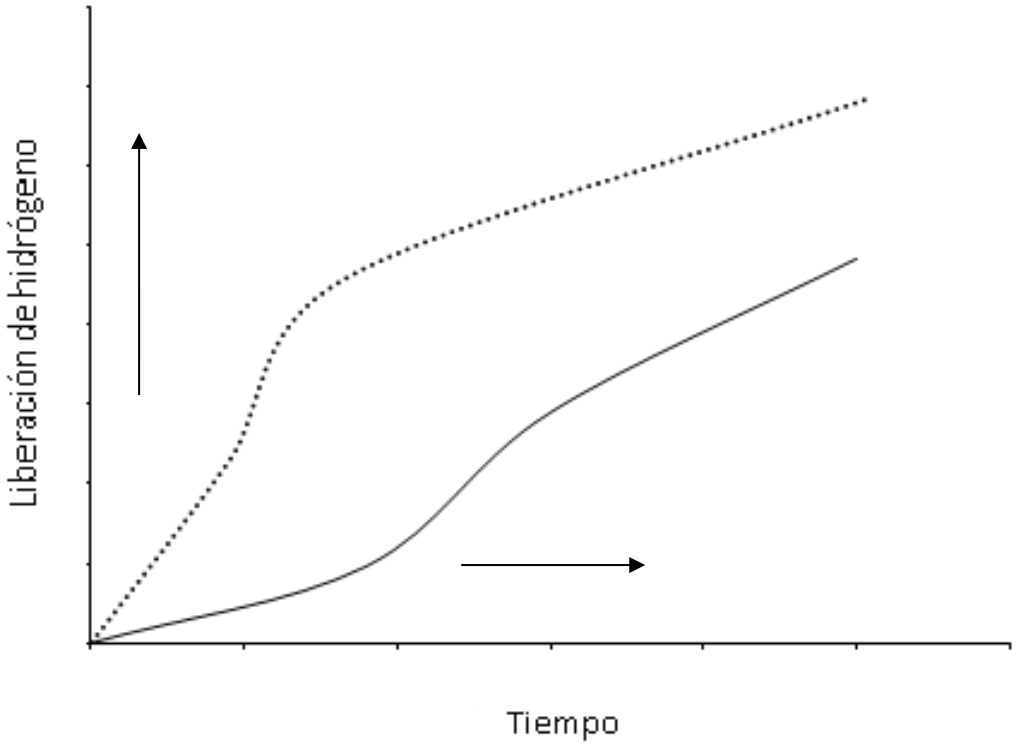

Figura 7

Resumen:

Material y procedimiento para el almacenamiento y regulación de la liberación de hidrógeno en estado sólido

La presente invención se refiere a un material que permite la regulación rápida de la velocidad de liberación de hidrógeno producida mediante termólisis de compuestos de almacenamiento de hidrógeno, caracterizado porque dicha regulación se produce mediante incorporación de dichos compuestos en un soporte poroso, el cual se ha sensibilizado a la aplicación de radiación electromagnética mediante la adición en su estructura de materiales susceptibles a calentamiento mediante aplicación de radiación electromagnética , lo cual permite un calentamiento rápido y homogéneo de todo el soporte.

Chapter 6

Plan Empresa

LIGHTENERGY

1. Presentación

En los últimos años la demanda de drones se ha disparado. Si bien la legislación actual restringe enormemente su uso recreativo, el gran potencial de esta tecnología los hace fuertes candidatos a ser utilizados en labores profesionales (fotografía, vigilancia, agricultura, topografía etc.), ahorrando tiempo y abaratando los costes. Sin embargo, estos prodigios tecnológicos presentan un gran problema; su autonomía de vuelo. Hasta la fecha, las baterías de Litio se han impuesto como las más eficientes para este fin, sobre todo debido a su bajo peso y su precio económico. Sin embargo esta solución limita las horas de autonomía a minutos. Por tanto si queremos que realmente los drones se conviertan de verdad en un instrumento alternativo a tareas actualmente realizadas con naves tripuladas, es necesario dar una solución a esa baja autonomía de vuelo.

Para superar esta barrera tecnológica, la celda de combustible de hidrógeno ha sido propuesta como alternativa. Empresas como Medavia ya están trabajando en el desarrollo de celdas de combustible de hidrógeno de bajo peso para este fin. Otras como la inglesa Intelligent Energy, ya ha desarrollado un prototipo de dron que se alimenta con esta tecnología. Sin embargo el reto no está resuelto. La autonomía de vuelo es un compromiso entre la energía almacenada y el peso de la batería. El almacenaje de hidrógeno en tanques presurizados es una alternativa en vehículos rodados (así funciona por ejemplo el comercializado Toyota Mirai); sin embargo el peso de estas bombonas lastra el objetivo de aumentar la autonomía en aplicaciones aeronáuticas. Por ello desde el grupo de Procesos a Alta Presión de la Universidad de Valladolid dirigido por la Catedrática Mª José Cocero Alonso, llevamos desde 2012 trabajando en un sistema de almacenamiento de hidrógeno más ligero y compacto. Como resultado se ha desarrollado una tecnología a base de hidruros embebidos en una matriz porosa que soluciona este problema. La tecnología pudo ser patentada gracias al programa Prometeo convocado por la Fundación General de la Universidad de Valladolid (Patente nacional 201500170). Posteriormente el proyecto fue premiado con el Premio VIVERO organizado por el Fuescyl, lo cual ha permitido que en la actualidad ya se esté desarrollando un prototipo de pila compacta de celda de combustible de hidrógeno que demuestre el enorme potencial de esta tecnología y sirva para alimentar los motores eléctricos de los drones aumentando así su autonomía y abriendo así el camino al uso de estos dispositivos en ámbitos donde hoy por sus tiempos de vuelo los hacen inutilizables

Cabe también señalar que LightEnergy contribuye al desarrollo de una economía sostenible de hidrógeno (figura 1) ya que este este puede producirse a partir de energías renovables, y emite

tan sólo vapor de agua en el momento de su consumo, por lo que elimina todo tipo de emisión contaminantes a la atmósfera.

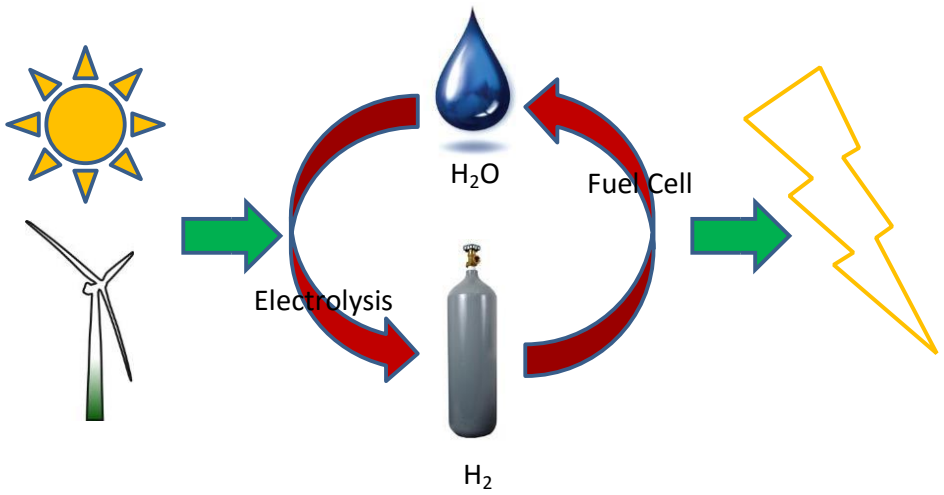

Figura 1.- Economía o sociedad del hidrógeno.

2. Demanda y oportunidades del producto

Light Energy ofrece una pila de hidrógeno para uso en drones que demanden vuelos de larga duración, cuyas características diferenciales más importantes a destacar respecto a las pilas que actualmente se utilizan para este tipo de aeronaves no tripuladas (en la mayoría de los casos, baterías química tipo LiPo) son las siguientes:

- **Compacto**
- **Ligero**
- Mayor densidad energética que se ve traducido en una **mayor autonomía de vuelo y/o mayor potencia.**
- **Seguro,** tanto mientras se encuentra funcionando el dispositivo, como durante la recarga de la que se encarga LighEnergy, evitando posibles cortocircuitos que hoy en día se producen en la recarga de pilas químicas.
- **La recarga se efectuará en segundos** ya que sólo habrá que cambiar los cartuchos de combustible frente a los largos tiempos que demandan las batería químicas para recargarse.
- Las baterías químicas tienen una vida útil mientras que los cartuchos nuevos suministrados por LightEnergy siempre están igualmente cargados.
- **Menor impacto ambiental** al utilizar el hidrógeno como combustible, que se trata de un vector energético más sostenible.

Al abrir el campo de aplicaciones con estas nuevas pilas de mayor autonomía, se podría sustituir a las aeronaves tripuladas. En estas aplicaciones, el hecho de que la tripulación se quede significa un enorme ahorro, además de un gran abaratamiento en los costes de la aeronave en sí. Además permitiría realizar actividades que no son posibles con aeronaves tripuladas debido al mayor tamaño de éstas como puede ser volar en interiores, realizar maniobras de **mayor precisión y maniobrabilidad** al poder volar a menores velocidades o acercarse más al objetivo ya que pueden volar siguiendo cualquier trayectoria. Por último, el menor tamaño también reduce necesidades logísticas al no necesitar ningún tipo de infraestructura preparada para su despegue, ahorrando de nuevo gastos de operación.

Por todo lo anteriormente expuesto, LightEnergy ve en este campo una gran oportunidad de mercado, dirigido especialmente a aplicaciones de industria civil entre las que se destacan las siguientes:

- Industria (instalaciones industriales, líneas eléctricas, torres eólicas).
- Transporte (vigilancia e inspecciones ferrocarril, carreteras, ríos).
- Construcción, inspección estructuras.
- Agricultura de precisión.
- Mantenimiento sistema eléctricos.
- Vigilancia en fronteras (tráfico de drogas).
- Mediciones.
- Monitorización bosques vírgenes.
- Búsqueda restos arqueológicos en volcanes.
- Rescates.
- Inspección de palas de aerogeneradores o huertos solares, de una manera más rápida eficaz y barata.

3. Mercado, segmento objetivo

El mercado actual del hidrógeno está sufriendo una revisión debido a sus prometedoras propiedades y ventajas que presenta como vector energético. El cambio climático, la contaminación, la dependencia de las energías fósiles y la emergente demanda de energía nos han llevado a reconsiderar la ecuación energética de nuestra sociedad. El hidrógeno, junto con la pila de combustible, proporciona una respuesta a estas cuestiones al ser un vector energético para las fuentes de energía sostenibles, ser eficaz y ser silencioso en el punto de uso.

Como puede verse en el siguiente gráfico (figura 2) extraído del Fuel Cell Technologies Market Report 2014 encargado por el US Department of Energie, el número de celdas de combustible producidas, la tecnología está en rápida expansión.

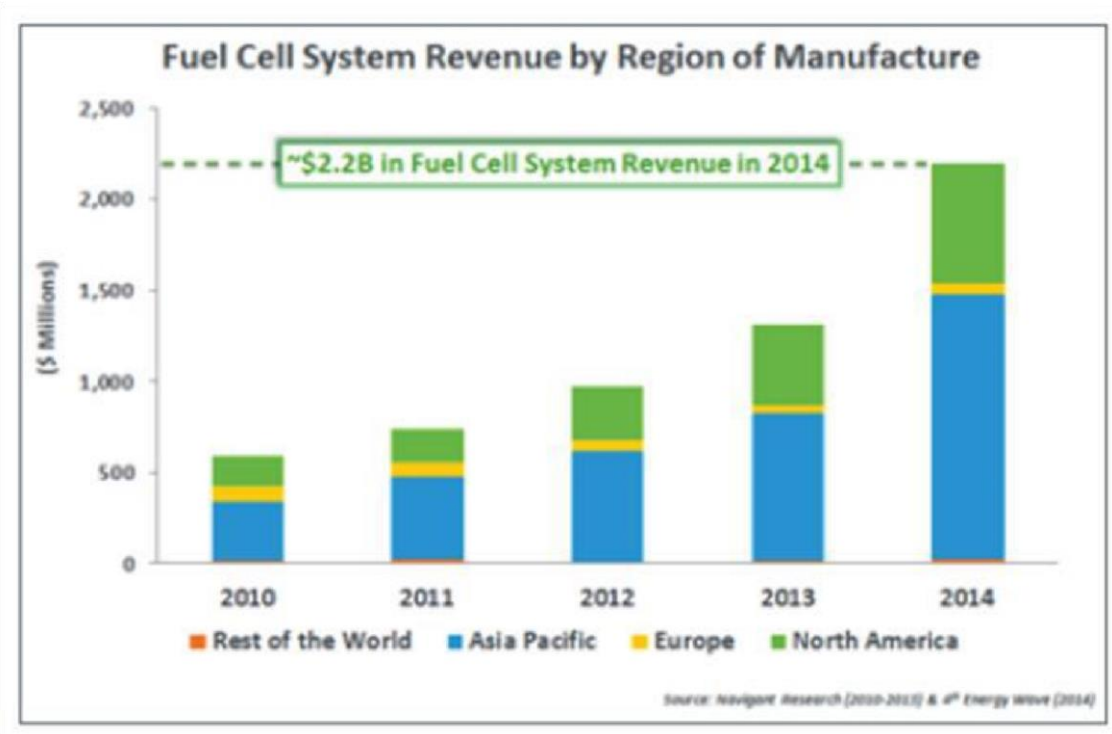

Figura 2.- Ingresos estimados en celdas de combustible durante los últimos 5 años según US Departmento de Energía.

Así puede aplicarse esta tecnología a aparatos de baja potencia (<6KW) como aviones no tripulados; media potencia (<20KW) como sistemas auxiliares de generadores o generación en lugares remotos (países en vías de desarrollo); necesidades energéticas a bordo de aeronaves; por último alta potencia (>20KW). Todas estas aplicaciones de sistemas de almacenamiento de hidrógeno generarán un mercado de unos 8000 millones de € en los próximos 10 años.

Los aviones no tripulados o drones es un mercado emergente en el que la Agencia de Seguridad Aérea (AESA) ha registrado más de 1000 operadores, exactamente, 1337 de menos de 25 kilos en el primer año y medio desde la entrada en vigor de la normativa, experimentando un crecimiento exponencial en los últimos años.

La revolución de los drones está transformando las empresas de todos los sectores de actividad, desde la agricultura hasta la industria cinematográfica. El incipiente mercado relacionado con el uso de los drones puede generar oportunidades de negocio por un valor total de más de 127.000 millones de dólares (114000 millones de euros) a nivel mundial, según el informe *Clarity from*

above elaborado por PwC. En la siguiente tabla se recoge la estimación de ingresos por sector de actividad.

Tabla 1.- Estimaciones de ingresos generados por la aplicación de drones

Estimaciones de ingresos generados por la aplicación de los drones en los diferentes sectores – (M de $)	
Infraestructura	45.2
Agricultura	32.4
Transporte	13
Seguridad	10
Entretenimiento y Medios	8.8
Seguros	6.8
Telecomunicaciones	6.3
Minería	4.4
Total	**127.3**

La Unión Europea, que trabaja ya en una normativa común para el uso de drones en el espacio aéreo europeo, calcula que en poco más de una década el 10% de la facturación del sector aeronáutico procederá de la fabricación de drones de uso civil. Un mercado que podrá superar los 15.000 millones de euros al año y que en **España** se estima que en **2050** la facturación alcance **los 20 millones de euros.**

Tratando de cazar una parte de este mercado embrionario y creciente, en España han surgido toda clase de iniciativas públicas y privadas. La Xunta de Galicia se ha convertido en uno de los principales inversores en el mercado de los drones con la puesta en marcha del proyecto Civil UAVs Inititive, por el que el ejecutivo autonómico, junto a las empresas Indra e Inaer, destinarán 115 millones al desarrollo de drones para que puedan emplearse en labores de ordenación del territorio, salvamento marítimo o extinción de incendios, polo tecnológico que entrará en funcionamiento en septiembre.

El uso y la aplicación de los drones en las diferentes actividades están permitiendo a las empresas de los diferentes sectores crear nuevas oportunidades de negocios, así como transformar sus modelos de operaciones. Un estudio del comité para la UE de la Cámara de los Lores británica afirma que en el año 2050 podría crearse unos 150.000 puestos de trabajo relacionados con los drones en Europa. Y otro informe, esta vez de la AUVSI, estima que para 2025 habrá unos 100.000 nuevos empleos relacionados con esta industria.

Los drones con mayor autonomía podrían sustituir a aeronaves tripuladas en aplicaciones en ingeniería civil. Esta última va a sufrir un gran crecimiento; ‘’los helicópteros no pueden competir

contra los drones", según ha asegurado Manuel Oñate, presidente de la patronal Aerpas y director general de EuroUSC España, una consultora especializada en formación de pilotaje. Como ejemplo, Ineco ya ha apostado por el uso de estos drones para inspección de vías de difícil acceso.

El **valor añadido** de los drones son los sofisticados equipos que pueden cargar para realizar las más diversas misiones. Los sensores y demás aparatos de alta precisión con que se les equipan son lo que hacen que el **precio de los mismos** oscile entre los 1.000 y los 500.000 euros.

En el ejército más poderoso del mundo, el norteamericano, las aeronaves no tripuladas constituyen ya 1/3 del total de la flota de aeronaves en operación. Las misiones de inteligencia, vigilancia y reconocimiento que llevan a cabo las fuerzas armadas en las que los sensores recogen la información necesaria recorriendo un vuelo preestablecido y donde el piloto no debe interactuar con la aeronave a no ser que se produzca una alerta se podrían realizar con aeronaves no tripuladas con un gran ahorro económico. También se considera prometedor utilizar este tipo de aeronaves para operaciones peligrosas de inspección de terreno o condiciones contaminadas que podrían acarrear problemas sanitarios a la tripulación del avión.

En el ámbito civil, mucho menos desarrollado que el militar, la situación es contraria. Según la Dirección General de Aviación Civil francesa, el 76% del total se realiza mediante aeronaves no tripuladas.

Actualmente, en España, la normativa para el uso de estos sistemas es muy restrictiva y sólo se permite su uso civil cuando trabaja a la vista del operador, y un máximo de veinticinco kilos de carga, si bien existen distintas iniciativas de regulación internacional que permitan la integración de los Remotely Piloted Aircraft System (RPAS) en el espacio aéreo civil.

En el ámbito de la agricultura, se han realizado trabajos (proyecto Sudoe Forrisk del grupo Tragsa,) que consideran el uso de aeronaves no tripuladas de especial interés desde el punto de vista técnico y económico sustituyendo sensores aerotransportados y las imágenes de satélite, donde la superficie de estudio sea pequeña. Además, es interesante su uso en aplicaciones de sanidad forestal para seguimientos frecuentes a escala local donde se requiere un gran nivel de detalle.

Aunque en nuestro país la industria de los **drones** no acaba de conseguir el favor de los inversores privados, a nivel internacional el sector comienza a despegar. El pasado ejercicio las startups de RPAs levantaron 475 millones de dólares, lo que supone un incremento del 301%.

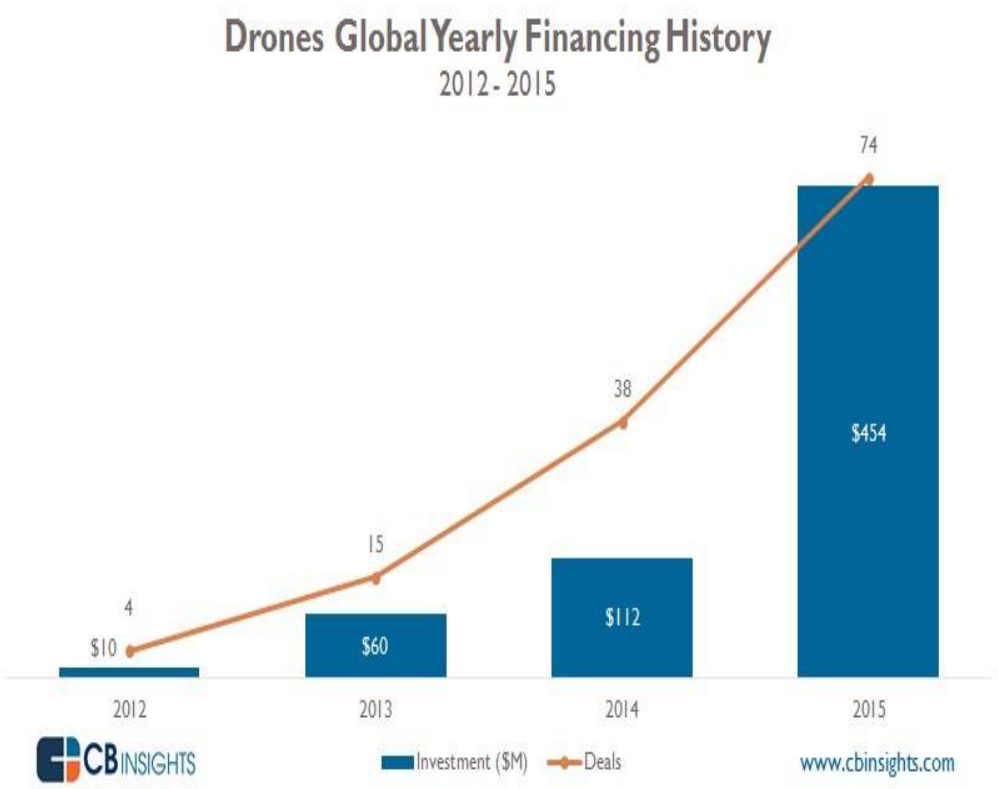

Figura 3.- Historial inversiones en drones

Teniendo en cuenta el total de drones hasta ahora registrados y su potencial crecimiento, se estima que el 30% de los drones van a ser utilizados para aplicaciones con largas autonomías de vuelo. De este 30%, se estima que en 3 años se va a captar el 4%, en torno a 20 pilas, lo que corresponde a un 1% del mercado total actual de drones. Esta estimación se dificulta debido a su exponencial crecimiento en los últimos años así como su uso en nuevas aplicaciones.

Por todo lo anteriormente expuesto LightEnergy se dirigiré a empresas de drones que demanden baterías de gran autonomía para aplicaciones de ingeniería civil principalmente.

Potenciales clientes son Drone Spain, Aeromedia, Ummaned Solutions, Multielfo, Win Inertia Tehnologies, Fulmar-Thales Group, Smartrural, Novaer o Drontecnic entre otros.

3.1 Competencia

Los mejores resultados con baterías se han conseguido con las baterías LiPo que se pueden conseguir en la mayoría de los casos mediante venta online. La capacidad de estas baterías, restringe la autonomía de vuelo en drones a no más de 30 minutos. Además estas baterías requieren de un largo tiempo para recargarse con bajos rendimientos debido a las continuas cargas y descargas.

Otra de las ventajas que presenta nuestras pilas es que las baterías LiPo requieren un trato más delicado y existe mayor riesgo de deteriorarlas irreversiblemente o producir su ignición o explosión por cortocircuito.

La empresa Inteligent Energy ya anteriormente ciatada, ha desarrollado una batería de hidrógeno que dota a las aeronaves no tripuladas de una autonomía de hasta 2 horas, permitiendo la recarga en tan sólo unos pocos minutos, utilizando hidrógeno comprimido. El peso total del sistema de combustible en este caso es de 1 kilo y medio, sólo tienen prototipo de momento, con una versión comercial estándar de 2600 dólares cuya batería es de unos 200 dólares, un precio mayor que los convencionales pero ofreciendo mayor autonomía y menor impacto ambiental.

Además, como se ha comentado, podría sustituir a aeronaves tripuladas, por lo que estos serían realmente nuestra competencia. La tecnología de LightEnergy permite almacenar el hidrógeno de forma más compacta y ligera que utilizando bombonas, por lo que se conseguiría una autonomía que aún no se ha producido con otras tecnologías. Además, se diferenciará de la competencia por el uso de una tecnología propia patentada por la Universidad de Valladolid (patente nacional 201500170), autores de la cual son los socios fundadores de esta empresa.

4. Política de producto

El modelo contempla 2 partes del producto:

Por un lado la celda de combustible, de la cual se ofertarán 3 modelos.

Las recargas de hidrógeno. Vendidas por la empresa al consumidor y suministradas mediante mensajería. Si se devuelven recargas que no hayan sido utilizadas, se devolverá el dinero. Estas serán enviadas en cajas asegurando que llegue al cliente en perfectas condiciones. Este sistema de funcionamiento por el cual el cliente deberá consumir a LightEnergy cada recarga, fidelizará a los clientes a lo largo del tiempo.

LightEnergy va a ofrecer 3 celdas de combustible que ofrecerán potencias de 200W, 500W y 1000W respectiva. Obviamente mayores potencias requerirán de mayores consumos de hidrógeno y proporcionalmente de mayores contenedores de hidrógeno para alargar su autonomía. Además desde LightEnergy y debido a la gran especialización en investigación, se ofrecerá un servicio capaz de diseñar y ejecutar pilas que se ajusten a medida a los requisitos que nuestros clientes demanden. A continuación se muestran a modo de ejemplo una de las hojas de especificaciones de las celdas de combustible que ofertará LightEnergy.

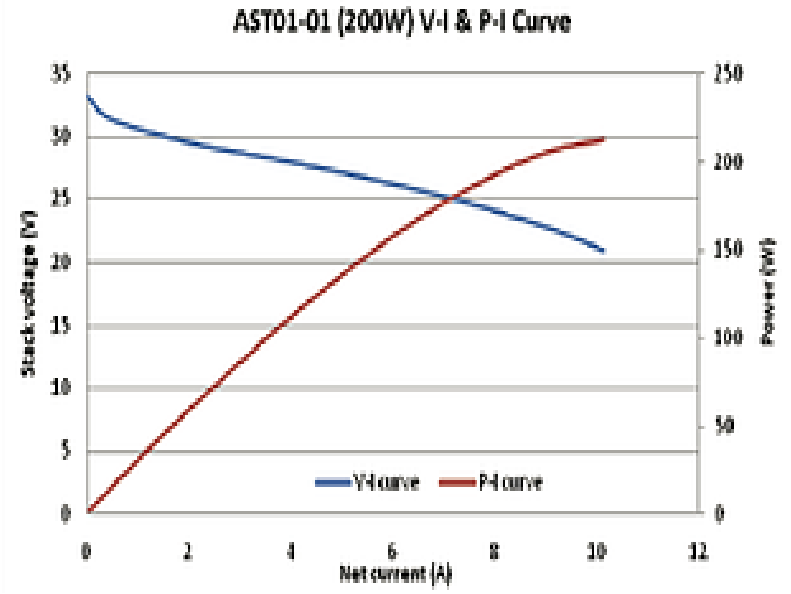

Figura 4.- Especificaciones de las celda de combustible de 200W

Debido a la alta complejidad técnica del producto, no se pretende competir mediante el precio del dispositivo frente a las baterías químicas.

La idea es que las prestaciones que se aportan y los valores diferenciales (mayor autonomía y o potencia en un material ligero) abran las puertas a la utilización de aeronaves no tripuladas en nuevas aplicaciones que compiten con el uso de aeronaves tripuladas o helicópteros como se ha detallado anteriormente.

No se pretende obtener grandes beneficios mediante la venta de pilas, las cuales se han estimado por coste de producción con un % de beneficios (factor de 1.5-1.7 dependiendo del tipo de pila). La mayoría de las beneficios se pretenden obtener de las ventas recurrentes de las recargas.

Tabla 2.- Resumen de productos y precios

Tipo pila	Potencia (W)	Precio pila (€)	Precio recarga (€)
B1	200	750	260
B2	500	1100	425
B3	1000	1500	475

Además, LightEnergy se adaptará a las necesidades del cliente como se ha comentado anteriormente, lo cual nos hará únicos en el mercado de pilas para drones.

4.1 Procesos

La pila (ensamblaje de pila así como producción y recarga de los cartuchos donde se encuentra el combustible de hidrógeno) se va a realizar en las instalaciones del Departamento de Ingeniería Química de la Universidad de Valladolid. Se pagará un alquiler por el uso de las mismas, por lo que supondrá un gran ahorro al no tener que hacer inversión inicial en instalaciones.

Uno de los factores clave a tener en cuenta en nuestro modelo de negocio es la exclusividad de la tecnología haciendo uso de la patente.

Ya pensando en el funcionamiento de los servicios de la empresa, es fundamental la logística para hacer llegar las pilas recargadas a nuestros clientes. Para ello será necesario un stock y un servicio de paquetería de respuesta rápida. La logística es un papel importante en nuestro plan de negocio, para asegurar la satisfacción del cliente con nuestro producto y que siga confiando en nosotros.

Nos podrán contactar a través de correo, teléfono o página web, donde solicitarán directamente el envío de recargas.

Otra de las actividades clave es el marketing, para que le cliente conozca el servicio que ofrecemos de baterías de hidrógeno de larga duración de vuelo, ligeras y seguras.

5. Comunicación y promoción:

La empresa tendrá página web donde se describirán los productos y servicios que proporcionamos así como los contactos y direcciones para cubrir cualquier duda o pedido.

A mayores y debido a lo selecto del producto, se expondrá el mismo en congresos y ferias específicos del sector como III Congreso sobre las Aplicaciones de los drones a la Ingeniería Civil (Civil Dron) que se va a desarrollar en el Complejo Duque de Pastrana 25-26 Enero 2017 y donde presentarán el prototipo de Intelligent Energy, Expodronica o Civildron, entre otros.

Además, una vez conseguido el prototipo, se acudirá personalmente a ofrecer nuestro producto y servicio a posibles futuros clientes. A mitad del segundo año, será tarea del director comercial, quien motivado por su salario variable en función de las ventas, conseguirá aumentar el número de clientes de la empresa.

6. Recursos humanos

LightEnergy va a estar constituido en un primer momento por 4 socios: Ángel Martín Martínez, Alexander Navarrete, Luis Miguel Sanz Moral y Miriam Rueda Noriega. Todos ellos, fundadores

y autores de la patente que van a explotar, con perfiles ingenieriles y científicos lo cual encaja con el alto nivel tecnológico de la empresa.

LighEnergy es una empresa que nace del Grupo de Alta Presión que forma parte del Departamento de Ingeniería Química de la Universidad de Valladolid en el que María José Cocero Alonso, catedrática de la Universidad de Valladolid, ha liderado el grupo de Alta Presión en los últimos 18 años.

Ángel Martín

Asesor i+D

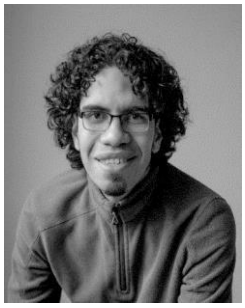

Alexander Navarrete

Asesor i+D

Miriam Rueda

Desarrollo producto

Luis Miguel Sanz

A continuación, se va a detallar el cv de cada uno de los fundadores de la empresa.

Ángel Martín completó su doctorado en la Universidad de Valladolid en el año 2006. Posteriormente fue investigador postdoctoral en la Universidad Técnica de Delft (2007), donde trabajó en el desarrollo de materiales de almacenamiento de hidrógeno basados en hidratos, y becario Alexander von Humboldt en la Universidad de Bochum (2009). En el 2011 se reincorporó a la Universidad de Valladolid como investigador Ramón y Cajal, y en la actualidad es profesor Contratado Doctor en esta universidad. Va a ser uno de los fundadores de la empresa cuya función será asesoramiento científico sin disponer de un salario proveniente de LightEnergy.

Sus áreas de especialización en investigación son los procesos a alta presión y con dióxido de carbono supercrítico, el desarrollo de materiales novedosos, y la aplicación de estos materiales al almacenamiento de hidrógeno. Entre sus contribuciones en este último campo, puede reseñarse el desarrollo de materiales porosos novedosos con propiedades mejoradas (de área superficial y porosidad, así como químicas) y el uso de estos materiales como soportes para compuestos de almacenamiento de hidrógeno y catalizadores. También ha participado en el desarrollo de una metodología “Raman operando” para monitorizar el comportamiento de estos materiales durante los procesos de almacenamiento y liberación de hidrógeno, en colaboración con el grupo del “Instituto CSIC de catálisis” dirigido por el profesor M. A. Bañares. En colaboración con el grupo dirigido por la profesora Chiara Milanese, del “Hydrogen Lab” de la Universidad de Pavia, ha analizado las propiedades de esos materiales, y en particular la

velocidad de liberación de hidrógeno, durante ciclos repetidos de carga y liberación de hidrógeno.

Con su trabajo en estos campos ha publicado más 90 artículos en revistas científicas internacionales, que han recibido más de 1500 citas, y ha sido director de seis tesis doctorales, en cooperación con importantes grupos de investigación a nivel europeo (TU Hamburg-Harburg, ETH Zurich, University of Bochum, IBET-Oeiras). También ha sido investigador principal en tres proyectos de investigación con financiación pública y proceso de selección competitivo, así como de quince contratos y convenios de investigación con diferentes empresas. Dos de estos contratos han recibido el premio "Desafío Universidad-Empresa" otorgado por la Junta de Castilla y León a las mejores colaboraciones entre el sector académico y el industrial en el ámbito de la región.

Alexander Navarrete nació en 1976 en Cali, Colombia. Se graduó como Ingeniero Químico de la Universidad Nacional de Colombia en 2001. Después de varios años a cargo de proyectos relacionados con simulación CFD, inició su doctorado en la Universidad de Valladolid en el año 2006. Allí, él desarrolló procesos basados en energía de microondas útiles para extraer productos de valor agregado a partir de plantas. Como parte del modelado matemático de los procesos, visitó brevemente la Universidad de Nottingham (UK).

Durante su estancia postdoctoral en la Universidad Tecnológica de Delft (Holanda) el año 2011, con el apoyo de la fundación Bill and Melinda Gates, desarrolló un reactor de demostración para gasificación de biomasa usando plasmas impulsados con microondas. Está interesado en el desarrollo de nuevos conceptos de procesos que usen energía renovable en conexión con nuevos materiales, usando para ello una filosofía de intensificación de procesos y estudios fenomenológicos. Durante los últimos años ha desarrollado equipos basados en estructuras micrométricas para el almacenamiento de energía renovable a través de vectores como el hidrógeno, el CO_2 y alcoholes. También va a asesorar para poder suministrar un producto con las prestaciones que el cliente desee.

Miriam Rueda finalizó Ingeniería Química en Julio 2011 en la Universidad de Valladolid realizando el proyecto fin de Carrera en la Universidad Técnica de Dinamarca (DTU) bajo la supervisión de Nicolas von Solms.

Durante el curso académico 2011/2012 realizó el Máster de Investigación en Termodinámica de Fluidos en la Escuela de Ingenierías Industriales de la Universidad de Valladolid obteniendo 9.4 de nota media. El proyecto fin de master lo desarrolló en el Grupo de Alta Presión del Departamento de Ingeniería Química y Tecnología del Medio Ambiente con ayuda de una beca UVa-Santander. Dicho proyecto fue presentado en el Seminario Internacional de Termodinámica

de Fluidos celebrado en Tarragona en junio 2012 y en 5émes Entretiens du Centre Carrier en Lyon en noviembre del mismo año.

En noviembre de 2012, recibió una beca de Formación Personal Investigador (FPIUVA) de 4 años duración (2 años beca y 2 años contrato) para realizar el doctorado dentro del Programa de Ingeniería Química y Ambiental en el grupo de Alta Presión de la Universidad de Valladolid y bajo la supervisión de Ángel Martín. Dicho proyecto ha formado parte del proyecto nacional de Investigación Fundamental no Orientada, ENE2011-24547 'Light Hydrogen Storage materials for mobile applications'. El objetivo de la tesis doctoral que se encuentra finalizando es mejorar las propiedades de diferentes hidruros mediante el uso de técnicas desarrolladas por el propio grupo. Se trata por una parte de la micronización de hidruros mediante proceso de precipitación con CO_2 supercrítico y por otro lado la estabilización de los mismos en aerogeles de sílice utilizados como soporte. Ha presentado los resultados más relevantes en varios congresos internacionales especializados en el tema. Además, ha realizado dos estancias (3 meses de duración cada una) en el Laboratorio de Hidrógeno del Departamento de Química de la Universidad de Pavía (Italia) bajo la supervisión de Amedeo Marini donde ha podido trabajar con un grupo especializado en materiales de hidrógeno en estado sólido basado en hidruros y ha podido medir las cinéticas de liberación de hidrógeno durante varios ciclos repetidos de carga. Su actitud emprendedora a lo largo de su actividad investigadora ha sido fundamental a la hora de adaptarse a las necesidades de cada momento para poder continuar su actividad profesional.

Luis Miguel Sanz, se licenció en Ingeniería Química en el año 2010 en la Universidad de Valladolid, cursando el último año en Universidad de Birmingham (UK). Posteriormente compaginó el curso de Especialista en Energías Renovables de la Universidad de Valladolid con su primer trabajo en San Gabriel Ciudad de la Educación donde impartió formación continua (2010-2011). Posteriormente realizó el máster en Investigación en Termodinámica de Fluidos (2011-2012) para posteriormente y hasta la actualidad, enrolarse en el programa de doctorado del mismo. Durante el doctorado ha trabajado en el desarrollo de materiales meso y microporosos, ligeros y susceptibles de ser calentados mediante microondas. Es experto en la utilización de fluidos supercríticos, los cuales han sido utilizados durante la síntesis de estos materiales. Estos soportes han sido propuestos como soporte de catalizadores, y de hidruros. Actualmente trabaja en la impregnación de hidruros en estas matrices porosas y su liberación mediante la aplicación de microondas. Los resultados más importantes de su investigación han sido comunicados tanto en congresos, como en publicaciones científicas. A lo largo de su tesis ha realizado 2 estancias internacionales: en Universidad de Maribor (Eslovenia), donde trabajó en la síntesis de aerogeles y en TU Delft (Países Bajos), donde realizó el diseño de reactores de

vidrio para el almacenamiento de hidruros y su posterior calentamiento aplicando microondas, realizando los primero test y simulaciones.

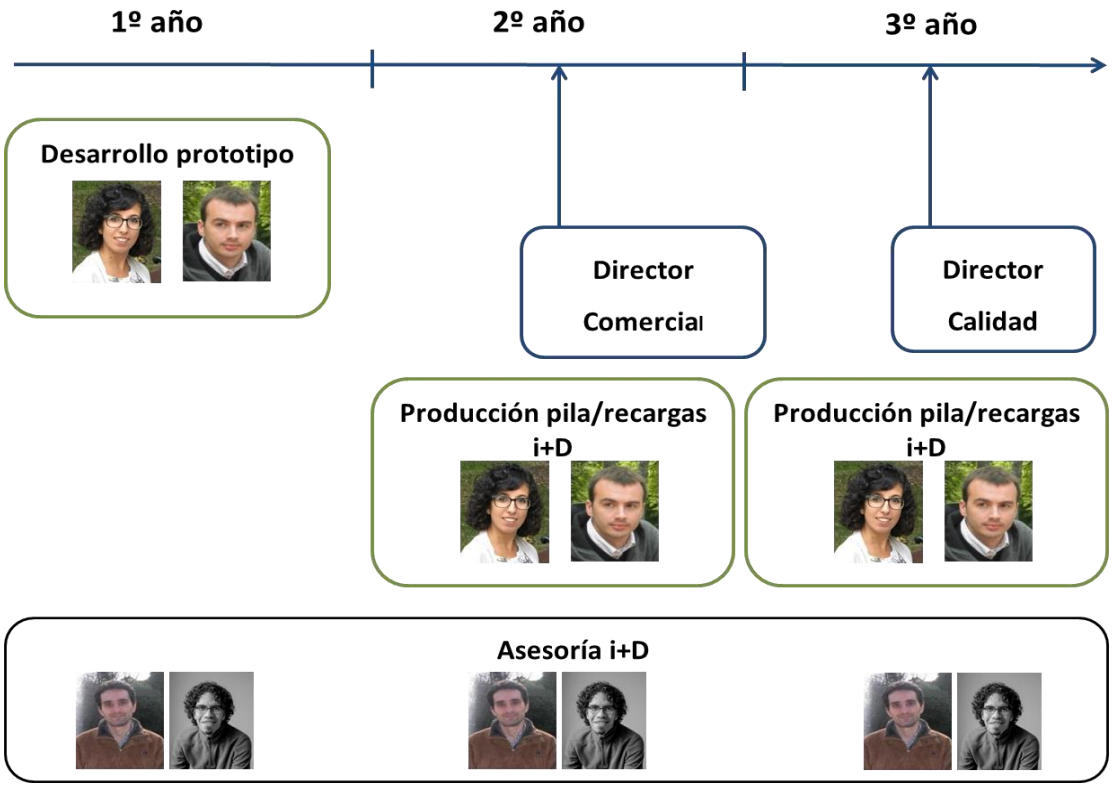

Figura 5.- organigrama funcional previsto para los 3 primeros años.

Miriam Rueda y Luis Miguel Sanz van a trabajar a tiempo completo para desarrollar el prototipo durante el primer año y producción de pilas una vez conseguidos los primeros clientes.

En el caso de Miriam Rueda, más especializada en las recargas de los combustibles de la pila basados en hidruros mientras que Luis Miguel Sanz ofrece alta experiencia a en la tecnología del microondas y síntesis de material combustible de la pila.

Ambos van a desarrollar la función comercial una vez que esté desarrollado el prototipo, para mostrarlo en ferias y congresos así como directamente en empresas de drones para captar a clientes. A mitad del segundo año, se va a contratar un director comercial cuyo sueldo va a estar constituido por una parte fija más una variable dependiente del número de ventas, para que de esta manera su función a la hora de conseguir más clientes sea más efectiva.

En este momento, Miriam Rueda se encargará de la síntesis de los materiales de combustible, pedir las materias primas y mantener el stock necesario para abastecer a los clientes mediante las recargas de las mimas.

Luis Miguel Sanz se dedicará a diseñar y amoldar nuestros servicios a las demandas de nuestros clientes, realizando los avances y modificaciones necesarias a la potencia, peso y geometría de

las pilas. También deberá proseguir con la investigación y desarrollo que permitan hacer al sistema más eficiente y barato, lo cual se traducirá en un incremento en la autonomía de las pilas y en su venta.

Además, debido al aumento de producción estimado en el tercer año, se va contratar un director de calidad a la mitad del tercer año para asegurarnos de que un aumento de producción no supone una pérdida de calidad del producto.

La figura.5 presenta un esquema del organigrama funcional previsto para los 3 primeros años.

7. Localización y edificaciones

Se incluyen también en este apartado las funciones que Light Energy va a externalizar.

A partir del segundo año en el que LighEnergy ya empieza a producir, se va a externalizar la función de un contable (200€/mes).

Además, se tendrá en cuenta la necesidad de un abogado (500€/año) a partir del segundo año, que corresponde con la creación de la empresa.

La oficina de LighEnergy en el primer año va a ser ocupada por 2 empleados (Miriam Rueda y Luis Miguel Sanz). El espacio va a ser de en torno a 23 m^2 ubicado en el Centro de Transferencia de Tecnologías Aplicadas del Parque Científico de la Universidad de Valladolid, en el Campus Miguel Delibes de Valladolid.

Es un espacio para la innovación abierta que facilita el encuentro entre la investigación y el mundo empresarial. El CTTA alberga a empresas que demandan investigaciones y desarrollos de la UVa, spin-off recién constituidas o en fase de lanzamiento así como unidades mixtas de investigadores-empresas, por lo que se cree muy conveniente que resida en este edificio puesto que va a ser una empresa que nace de la Universidad de Valladolid. El precio fijado es de 12€/m^2, por lo que se estima que va a contar con un gasto fijo de unos 300€/mes.

En 3 años se estima que la plantilla va a ser duplicada, por lo que trabajarán 4 personas en estas oficinas.

Los equipos utilizados para la síntesis y análisis de materiales serán alquilados por horas al Grupo de Procesos a Alta Presión de la Universidad de Valladolid.

Se ha estimado que se va a utilizar 8 días/mes, con un gasto de 1200€/mes, pudiendo ampliar estos días con el previo consentimiento del Grupo de Alta Presión, en el que están desarrollando dicha tecnología.

8. Económico-Financiero

A continuación se presenta el plan económico-financiero que se ha estimado para los 3 primeros años de LightEnergy, sociedad creada durante el segundo año.

8.1 Ventas

Tabla 3.- Estimación ventas durante los 3 primeros años

		2AÑO		3AÑO	
	precio/ud	**uds vendidas**	**total €**	**uds vendidas**	**total €**
B1	750	2	1500	3	2250
B2	1100	4	4400	6	6600
B3	1500	1	1500	3	4500
R1	260	50	13000	150	39000
R2	425	80	34000	300	127500
R3	475	10	4750	60	28500
TOTAL			**59150**		**208350**

Como puede verse en la tabla 3, se va a comenzar a vender a partir del segundo año, ya que como se ha comentado el primer año se va a dedicar a desarrollar el prototipo y darnos a conocer.

Las siglas B1, B2 y B3 corresponden a los tres tipos de pilas que ofrece LightEnergy, siendo R1, R2 y R3 sus respectivas recargas.

La estimación de ventas en el segundo año es baja debido a la dificultad de penetrar en el mercado, pero en el tercer año, el efecto de añadir un comercial a la plantilla de LightEnergy se ve reflejado en un crecimiento en la captación de clientes.

8.2 Compras

Las compras del primer año corresponden al material utilizado en el desarrollo del producto mínimo viable y diferentes prototipos.

En el segundo año, se especifica el coste de cada una de las partes que integran la celda de combustible y las materias primas necesarias para sintetizar las recargas. Se puede comprobar que las unidades compradas son superiores en número que en las ventas con el fin de generar un pequeño stock de producto en la empresa.

Una vez conocidas las compras y las ventas, se conoce el **margen bruto (M.B)** que corresponde a **32590€ y 153150€** para el segundo y tercer año respectivamente.

Tabla 4.- .Estimación compras durante los 3 primeros años

1AÑO		**2AÑO**			**3AÑO**			**PRODUCTO**
Microondas	1000	4	400	1600	3	400	1200	B1
Batería	100	6	600	3600	6	600	3600	B2
Celda	120	3	1000	3000	3	1000	3000	B3
Contenedor	700	80	60	4800	150	60	9000	R1
Sistema control	300	102	100	10200	300	100	30000	R2
Hidruro+soporte	500	24	140	3360	60	140	8400	R3
TOTAL €	**2720**			**26560**			**55200**	

8.3 Otros Gastos de Explotación(O.G.E)

En primer lugar, los alquileres corresponden al espacio físico de la oficina, utilización de los equipos de la Universidad de Valladolid, así como análisis externos del producto. Este gasto no se tiene en cuenta durante el primer año ya que durante este periodo se sigue trabajando bajo la financiación del Ministerio de Economía y Competitividad.

En cuanto a la licencia, la cantidad está calculada como un 2% de las ventas.

El suministro es 0 ya que el alquiler de las oficinas y laboratorio está incluido.

El gasto comercial deriva de los desplazamientos a congresos y/o ferias, sobre todo en el primer y segundo año, mientras que en el tercero se centra más en gastos directos del propio comercial.

El gasto del abogado se ha tenido en cuenta en la constitución de la empresa el segundo año y su asesoramiento y/o servicio durante el tercero. No se contempla realizar auditorías durante estos 3 primeros años.

En lo que confiere a la gestoría, sus servicios se contratar a partir de la constitución de la empresa en el segundo año, que corresponden a 300€/mes.

La creación de la página web supondrá el gasto de 800€ mientras que su mantenimiento será de 200€.

La mensajería ha sido calculada teniendo en cuenta el número de ventas y teniendo en cuenta que se ofrece un servicio de suministro urgente.

Tabla 5.- Estimaciones O.G.E durante los tres primeros años

	1año	**2año**	**3año**
Alquileres	0	18000	18000
Licencia	0	1500	5200
Suministro	0	0	0
Comerciales	2500	10000	10000
Abogado	0	500	500
Auditores	0	0	0
Gestoría	0	2400	2400
Página web	800	200	200
Mensajería	0	3100	7170
TOTAL (€)	**3300**	**35700**	**43470**

8.4 Amortizaciones

LightEnergy va a hacer una inversión correspondiente a la compra de 2 ordenadores, 1 impresora, 3 mesas y 6 sillas durante el segundo año, mientras que en el tercero se va a invertir en otro ordenador, 1 mesa y 2 sillas más (director de calidad).

Estas amortizaciones mostradas en la tabla 6, corresponden a las inversiones realizadas en el segundo año. Para su cálculo, se ha considerado un 25% para material informático y un 10% para mobiliario. El material invertido en el tercer año se empezará a amortizar en el cuarto año.

Tabla 6.- Estimaciones amortizaciones durante los tres primeros años

	Amortizaciones 3 año
3 pcs	450
1 impresora	25
3 mesas	90
6 sillas	30
TOTAL (€)	**595**

8.5 Gasto personal

Tabla 7.- Estimaciones gasto personal durante los tres primeros años

Personal	1 año	2 año	3 año
Luis Miguel Sanz	0	26000	26000
Miriam Rueda	0	26000	26000
Director comercial	0	7100	17200
Director calidad	0	0	13000
TOTAL (€)	**0**	**59100**	**82200**

El gasto en personal comienza en el momento en que se constituye la empresa (segundo año). Desde el principio, 2 de los socios fundadores estarán contratados a tiempo completo (i+D).
En la segunda parte del segundo año se incorpora el comercial. Este cobrará una parte fija (13000€/año) más un 2% de las ventas conseguidas.
Finalmente, se incorporará un director de calidad en la segunda mitad del tercer año para garantizar que se cumplan las especificaciones del producto a pesar del aumento en la producción.

8.6 Cuesta de explotación

Tabla 8.- Cuenta explotación resumen durante los tres primeros años

	1 año	2 año	3 año
Ventas	0	59150	208350
Compras	2720	26560	55200
O.I.E	6000	6000	0
O.G.E	3300	35700	43470
Amortizaciones	0	0	595
G.Personal	0	59100	82200
O.Resultados	-	-	-
B. EXPLOTACIÓN	**-20**	**-56210**	**27480**

En el caso de otros ingresos de explotación (O.I.E) se han tenido en cuenta el premio recibido de Vivero, 6000€ para el desarrollo de prototipo durante el primero año, así como otros 6000€ para la creación de la empresa.

De la cuenta de explotación (tabla 8), se calculan las necesidades de financiación siendo de 60000€ (segundo año). Esta necesidad es cubierta por la aportación en el momento de creación de la empresa (15000€/socio).

Aunque no se alcanza el break-event, puede observarse que la tendencia es positiva y aunque no se ha especulado en un margen temporal más amplia se estipula que incluso en el cuarto año este acontecimiento será alcanzado.

Esta última tabla los valores resumen del plan económico-financiero de LightEnergy, concluyendo que el **EBITDA** del tercer año es de un 13%, valor atractivo para la naturaleza tecnológica de la empresa y el mercado en el que se encuentra y que nos da una idea de que va a ser rentable el negocio, según las estimaciones asumidas.

Tabla 9.- Resumen del económico financiero

	1 año	**2 año**	**3 año**
Ventas	0	59150	208350
G.Explotación	6020	124410	180870
B.Explotación	-20	-56210	27480
C.Financiero			
G.Financiero			
R.A.O	-20	-56210	27480
Extraordinarios	0	0	0
B.NETO	-20	-56210	27480
Impuesto Sociedades	0	0	6870
RESULTADO EJERCICIO	**-20**	**-56210**	**20610**

9. Forma jurídica

Sociedad Limitada (S.L) formada por 4 socios al 25% cada uno de ellos. La sociedad será creada en el segundo año del plan, tras haber conseguido el desarrollo de un prototipo. Hasta entonces se continuará trabajando bajo la financiación del Ministerio de Economía y Competitividad y de la Universidad de Valladolid.

DAFO

Fortalezas

- Tecnología novedosa.
- Tecnología en proceso de ser patentada (solicitud de Patente Nacional 201500170).
- Equipo humano con conocimiento suficiente para llevar a cabo el proyecto a nivel tecnológico.
- Personal cualificado en I+D con know-how.
- Resultados prometedores validados a nivel laboratorio.
- Pila ecológica, como subproducto se obtiene agua. De este modo, eliminaríamos gases. de efecto invernadero que contribuyen al calentamiento global y cambio climático.

Debilidades

- Nivel de madurez de la tecnología (TRL4).
- Falta de prototipo y primera prueba de concepto para poder mostrar en ferias y posibles futuros clientes.
- Falta de personal con experiencia en finanzas y comercialización de la tecnología.
- Falta marca reconocida.

Oportunidades

- El mercado de las pilas de hidrógeno muestra un crecimiento exponencial.
- Tendencia a la restricción en las emisiones de efecto invernadero por parte de los gobiernos.
- Se están tomando medidas para mejorar la calidad del aire en los núcleos urbanos.

Amenazas

- Hay muchos grupos de investigación y empresas trabajando en estos sistemas luego las alternativas son muchas. Existen empresas ya explotando el almacenamiento de hidruros (no su descomposición mediante microondas).
- Hay sectores del mercado donde hoy por hoy por las infraestructuras ya creadas y la apuestas hechas por multinacionales, hace difícil entrar a corto plazo.
- La patente aún no está aprobada y de serlo tan sólo proporciona protección a nivel nacional.

- La falta de reconocimiento en la marca.

Conclusions

First of all, different mesoporous and microporous light materials have been synthetized. On the one hand, silica aerogel were prepared using supercritical for its drying. These experiments were performed in a high pressure view cell. This has allowed to optimize the drying conditions, reducing the time required for drying by maximizing the carbon dioxide flow and hence making the maximum advantage of the advective transfer mechanism during the first stages of the drying, and showing that after a period this flow can be reduced without affecting the drying velocity, since the process comes to a period when diffusion completely governs drying. Size variations of gels have been followed studying the video captures. It has been observed that a noticeable aerogel shrinkage only takes place during CO_2 decompression at the end of drying process. Damages to aerogels during this decompression step seem to be governed by the mechanical stresses caused by CO_2 expansion. Further studies seeking a quantitative relationship between the diffusion rate of CO_2 out of the pores of the aerogel, the decompression rate and the extent of aerogel shrinkage would be useful to confirm this hypothesis. Furthermore, although at the operating conditions considered in this work methanol and carbon dioxide are completely miscible, a transient interface at the beginning of the drying process has been observed both between bulk CO_2 and methanol phases and inside the alcogel. The formation of this interface does not appear to have a detrimental effect on the integrity of the aerogel. This result can be due to the similarity between the densities of methanol and CO_2 at the operating conditions, and the reduced composition gradients at the interface due to the miscibility between the two phases, that contribute to reduce capillary forces. On the other hand a hybrid C/SiO_2 aerogel has been synthesized. The resultant material kept interesting textural properties and the addition of carbon to the matrix has modified the global dielectric properties of the matrix, making it susceptible to be heated by microwaves.

The next step was controlling the chemical nature of the synthesized materials. The treatment of dry silica aerogels with solutions of different precursors in supercritical carbon dioxide enabled a successful surface functionalization of the aerogels. Varying the operating pressure or the functionalization reagent, it was possible to control the degree of funcionalization, allowing to achieve a gradual variation of the hydrophobicity of the aerogel in a wide range that was extended from highly hydrophilic aerogels, to hydrophobic aerogels with an equivalent behavior as those synthesized using hydrophobic precursors in the sol–gel step. The treatment with supercritical solutions of functionalization agents did not cause apparent morphological variations of the monoliths, and allows a highly homogeneous functionalization of aerogel monoliths. However, after the functionalization, significant reductions of the specific surface area, and particularly of the pore volume, were observed. That was probably

due to a partial filling or blocking of pores by the silane coating. In the case of the C/SiO_2 aerogels the silanization reduced significantly the presence of oxide groups on the surface.

Then, the C/SiO_2 aerogels were used to hold Ethane 1,2-diaminoborane inside its pores. The encapsulation of the hydride has allowed to reduce the response time during the thermolysis and has minimized the second decomposition step typical of the pure compound. After it the system was heated up by using microwaves, improving the heating rate in comparison with the oven test. In addition this heating rate could be easily controlled by tuning the power of the electromagnetic field. What is more, the system just heat up the sample, not the container. Therefore the thermal inertia was reduced in comparison with traditional heating, and the temperature started to drop as soon as the microwave was stopped, allowing to control the hydrogen flow.

Another task was the development of catalyst by using silica aerogels as support. Different routes have been used to impregnate silica aerogels with Pd. The load of the metal could be tuned by controlling the concentration of Pd in the different impregnation media but at the same time the achievable concentration was limited by the solubility of the precursor. Well distributed particles were obtained with wet impregnation and supercritical impregnation but agglomeration was observed on the catalyst prepared by direct synthesis. The test of the catalysts in the hydrogenation of D-glucose have proven that the influence of the concentration of metal and the size of the metallic particles are important. In addition, the chemistry of the support, which was modified depending on the way in which the support was impregnated, and the presence of carbides, seem to play an important role on activity and selectivity.

Finally a business model prepared from the products developed during the work, proving the viability of the project.

Resumen

Desarrollo y funcionalización de aerogeles para aplicaciones en catálisis y confinamiento de hidruros

El vertiginoso crecimiento de la población mundial y la concentración de la misma en torno a grandes núcleos urbanos, presentan retos importantes para la raza humana.
La contaminación atmosférica es un problema grave en muchas ciudades de nuestro planeta. El tráfico intenso e incesante, junto con las incontroladas emisiones de nuestras fábricas, deterioran la calidad del aire hasta límites preocupantes. En muchas ocasiones, los niveles de partículas superaran el límite de seguridad para la salud humana establecido por la OMS. Lo que es más, esta institución ha clasificado el humo emitido por los motores diésel como cancerígeno para los seres humanos.

Otro aspecto a tener en cuenta es el crecimiento del peso tanto de la energía solar y como de la eólica en el mix energético, así como el acuerdo COP21, dispuesto a allanar el camino para una nueva familia de tecnologías basadas en energías renovables. Como estas formas de energía renovables son de naturaleza fluctuante, es necesario el desarrollo de técnicas que permitan su almacenamiento en los periodos de exceso de oferta, para después utilizarlo durante los periodos de demanda. Por otro lado el uso directo de esta energía en aplicaciones móviles no es posible, por lo que se demanda de un vector energético de alta densidad energética.

Se han barajado muchas opciones, pero el hidrógeno es una de las alternativas más prometedoras para alcanzar una sociedad energéticamente sostenible. El hidrógeno además de ser un buen vector energético, evita la emisión de contaminantes durante su uso en combustión o en celdas de combustible. Para su almacenamiento se están utilizando sistemas basados en el hidrógeno comprimido, licuado o en materiales sólidos. Hasta la fecha el gas comprimido se impone en aplicaciones rodadas, habiéndose creado ya importantes estructuras en Japón y la costa oeste de USA, donde numerosos modelos de vehículos ya circulan por sus calles utilizando este sistema. En comparación con los depósitos de gas y de almacenamiento de líquidos, los hidruros sólidos pueden almacenar grandes cantidades de hidrógeno en pequeños volúmenes, que se libera por una reacción química reversible mediante su calentamiento. Esta alternativa puede ser interesante en aplicaciones donde el peso toma un papel importante, y en particular en las relacionadas con la aeronáutica.

Uno de los desafíos tecnológicos que limitan el desarrollo de hidruros para el almacenamiento de H_2 es la transferencia de calor dentro de los tanques de almacenamiento. Grandes esfuerzos se han hecho para superar este desafío. Sin embargo, este problema puede evitarse si la energía de calentamiento se suministra directamente al material, y no por la transferencia de calor a través del tanque de almacenamiento. La aplicación de microondas ofrece esta posibilidad.

Por otro lado otra forma de mejorar la descomposición cinética de hidruros es el nanoconfinamiento de los mismos en materiales micro o mesoporoso. Al confinar el hidruro en el interior del soporte poroso, el tamaño de partícula de hidruro está restringido al tamaño de

los poros; se limita así su tamaño y se evita la aglomeración del mismo, lo puede tener un efecto adverso en la cinética de descomposición. También se han identificado que algunos soportes como el carbono o la sílice interactúan químicamente con diferentes hidruros, desestabilizándolos y mejorando aún más la cinética de descomposición.

Además, la matriz porosa puede ser diseñada para proporcionar propiedades adicionales al compuesto. En particular, se puede modificar para mejorar la absorción de la energía de microondas, y por lo tanto combinar las ventajas principales de las dos mejoras anteriormente expuestas: nanoconfinamiento y calentamiento por microondas.

En esta tesis se han desarrollado aerogeles con el fin de servir como soporte de catalizador y como matriz para los hidruros.

En primer lugar (***capítulo 1***) se ha desarrollado la síntesis y secado supercrítico de aerogeles de óxido de silicio, utilizando un proceso sol-gel. Tetrametilortosilicato se utilizó como precursor. Tras la formación de un gel por hidrólisis y policondensación de este precursor, se realizó su secado haciendo uso de la tecnología del dióxido de carbono en estado supercrítico (T = 45°C; P = 10.5 MPa). El proceso de secado con CO_2 supercrítico de los aerogeles se realizó en una celda visual, lo cual permitió la captura de imágenes durante este proceso. Esto posibilitó optimizar las condiciones de secado. Se observó que en las primeras fases, la convección tiene un papel predominante; esto quiere decir que un aumento del flujo de CO_2 permite la más rápida extracción del disolvente retenido en los poros durante las primeras etapas de secado. Transcurrido un tiempo, este flujo puede ser reducido sin afectar a la velocidad de secado, ya que el proceso entra en un período en que la difusión del disolvente a través de los poros del gel gobierna el proceso.

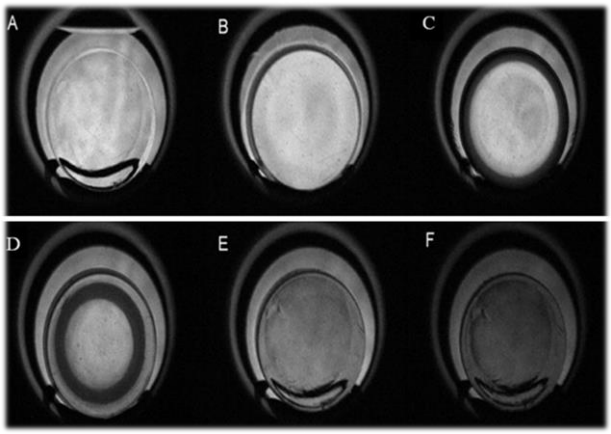

Figura 1: capturas de los aerogeles durante el secado supercrítico (vista axial): (a) Antes de la presurización (inmerso en metanol); (B) después de la presurización; (C) después de la conexión de la bomba de recirculación; (D) durante el lavado supercrítico (formación de corona); (E) después del secado supercrítico y (F) después de la despresurización.

Por otra parte, el cambio de las dimensiones del gel como consecuencia del proceso de secado es un parámetro importante que debe controlarse y minimizarse. Por ello, las variaciones de tamaño de los geles fueron seguidas estudiando las capturas de vídeo. Se observó que una contracción notable de los aerogeles sólo tiene lugar durante la descompresión del CO_2 al final del proceso de secado. Los daños a los aerogeles durante esta etapa de descompresión parecen estar provocados por las tensiones mecánicas causadas por la expansión del CO_2. Un estudio en profundidad podría llevar a cuantificar la relación entre la velocidad de difusión de CO_2 en los poros del aerogel, la velocidad de descompresión y la contracción del aerogel. Además, aunque en las condiciones en las cuales se llevaron a cabo los secados, el metanol y el dióxido de carbono son completamente miscibles, una interfaz de las fases se pudo observar tanto en el exterior como en el interior del aerogel. La formación de esta interfaz no parece tener un efecto perjudicial sobre la integridad del aerogel. Este resultado puede ser debido a la similitud entre las densidades del metanol y del CO_2 en las condiciones de secado y los reducidos gradientes de composición en la interfaz debido a la miscibilidad entre las dos fases, que contribuyen a reducir la tensión capilar.

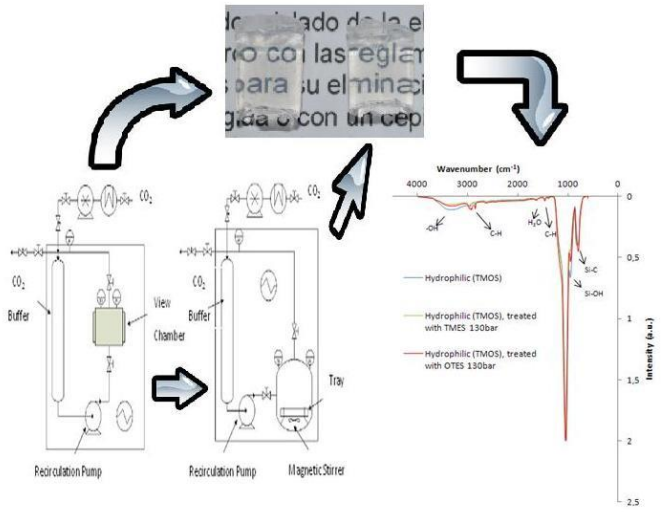

Figura 2. Equipos utilizados durante el secado y funcionalización así como los aerogeles resultantes y la variación de sus espectros infrarrojos.

El siguiente paso (***capítulo 2***) fue el control de la química de superficie de los aerogeles de óxido de silicio mediante la regulación de su afinidad por el agua. Tetrametilortosilicato o una mezcla de este con trimetiletoxisilano se utilizaron como precursores. Como en el capítulo anterior, tras las etapas de hidrólisis y policondensación se realizó el secado supercrítico con dióxido de carbono (T = 45°C; P = 10.5 MPa). Los aerogeles hidrofílicos resultantes se sometieron a

diferentes tratamientos para transformar su superficie en hidrofóbica. La funcionalización se logró mediante el uso de dióxido de carbono supercrítico como medio solvente para diferentes reactivos con efecto silanizante: trimetiletoxisilano, octiltrimetoxisilano y clorotrimetilsilano. La influencia de la presión de trabajo y la concentración de reactivo durante la funcionalización se analizaron mediante espectroscopia de infrarrojos y la exposición de los aerogeles tratados a condiciones de humedad saturada con el fin de estudiar el incremento de su masa durante esta exposición. Mediante la modificación de las condiciones de funcionalización, la concentración de grupos silanol en superficie pudo variarse gradualmente hasta los valores extremos de los aerogeles sintetizados como hidrofóbicos en la fase de gelificación. Sin embargo, después de la funcionalización, se observaron reducciones significativas de la superficie específica, y en particular del volumen de poro. Esto es probablemente debido a un llenado parcial o el bloqueo de los poros por el revestimiento del silanizante.

Después de su síntesis y posterior funcionalización, los aerogeles estaban listos para ser utilizado en diferentes campos. Rutas eficaces para obtener productos de mayor valor añadido requieren el diseño de catalizadores eficientes. Por lo tanto el desarrollo de estructuras catalíticas novedosas obtenidas por la integración de nanopartículas metálicas distribuidas de manera uniforme en una matriz mesoporosa y con alta superficie específica como son los aerogeles, se presenta como una alternativa prometedora (***capítulo 3***). Así nanopartículas de Pd se incorporaron a aerogeles de óxido de silicio mediante el uso de tres técnicas diferentes: la síntesis directa, la impregnación húmeda y la impregnación supercrítica de los aerogeles previamente secados. Los materiales resultantes se caracterizaron para analizar las diferencias en función de la técnica aplicada para su impregnación. Absorción atómica, isotermas de adsorción de nitrógeno, difracción de rayos X, espectroscopia infrarroja y microscopía electrónica de transmisión, se llevaron a cabo con el fin de caracterizar los catalizadores resultantes. La concentración de metal se varió desde 0.13% a 1.61% en peso. Esto se logró mediante la modificación de la concentración de la suspensión (nanopartículas de Pd-polivinilpirrolidona utilizadas en la síntesis directa) o de la solución del precursor metálico (paladio acetilacetonato), tanto en el disolvente orgánico como en el dióxido de carbono supercrítico. La caracterización mostró una buena distribución de partículas en los materiales sintetizados mediante impregnación húmeda e impregnación supercrítica; por el contrario, grandes aglomerados pudieron identificarse en el caso del catalizador preparado por síntesis directa. Finalmente, se observaron diferencias significativas en la concentración de grupos silanol en la superficie de los catalizadores. Estos materiales se emplearon en la hidrogenación de D-glucosa como reacción modelo, observándose diferencias importantes en el rendimiento del catalizador en función de la técnica de síntesis empleada para prepararlo.

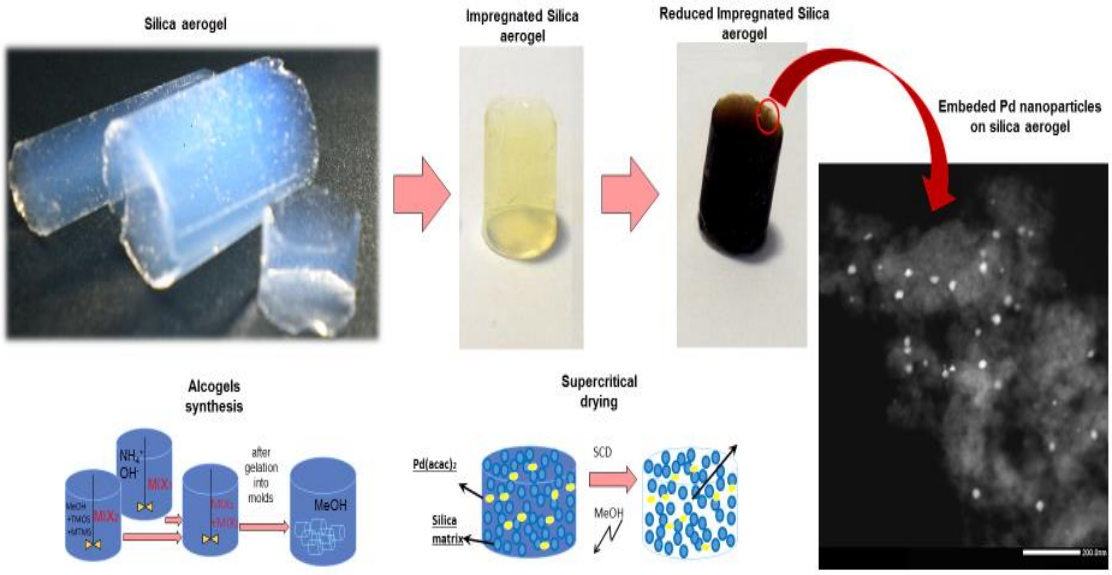

Figura 3. Proceso de síntesis e impregnación con Pd de los aerogeles.

Por último se estudió el uso de aerogeles como soporte para hidruros (***capítulo 4***). El nanoconfinamiento de estos compuestos ha demostrado mejorar la cinética de descomposición y reducir su temperatura de termólisis. Por el contrario, en algunos casos el uso de una matriz podría reducir la conductividad térmica, creando gradientes de temperatura significativos a lo largo de la muestra. Para eliminar esta limitación, se sintetizaron aerogeles de carbono/óxido de silicio, manteniendo unas propiedades físicas muy interesantes (386 m^2/ g y 1,41 cm^3/g) que dejan espacio de poro para el confinamiento de un hidruro, y variando las propiedades dieléctricas globales del complejo, haciéndolo susceptible a calentamiento por microondas. Esta idea está protegida por una patente nacional (***capítulo 5***). A continuación se impregnó etano 1,2-diaminoborano en la matriz (en concentraciones del 11 a 31% en peso) utilizando el método de impregnación húmeda. El compuesto obtenido fue caracterizado y se llevaron a cabo pruebas de liberación de hidrógeno haciendo uso de calentamiento mediante horno y mediante microondas. La utilización de microondas ha permitido la mejora de la velocidad de calentamiento en comparación con el calentamiento con horno. Además, esta velocidad de calentamiento puede ser fácilmente controlada mediante la regulación de la potencia del campo electromagnético. Lo que es más, el sistema simplemente calienta la muestra, no el contenedor; por lo tanto la inercia térmica se reduce en comparación con el calentamiento tradicional, y la temperatura empieza a bajar tan pronto como el microondas se detiene, lo que permite controlar el flujo de hidrógeno con un reducido tiempo de respuesta. Además se realizó una simulación numérica del dispositivo bajo la influencia de un campo de microondas para lograr

una mejor comprensión del proceso. Los resultados mostraron el gran potencial de esta tecnología.

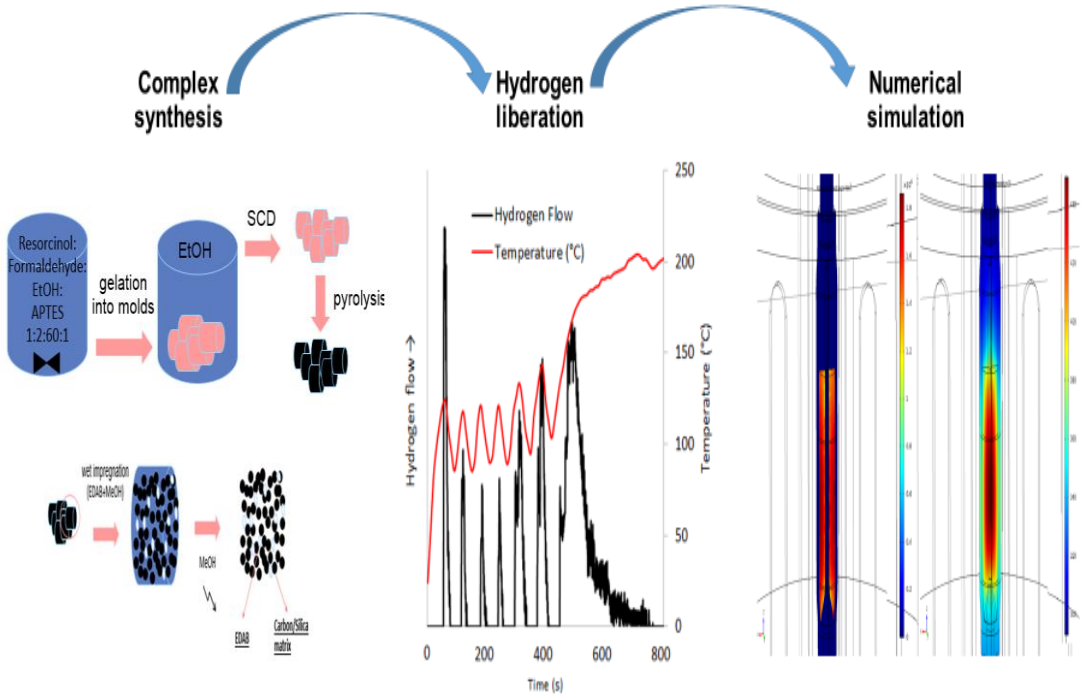

Figura 4. Síntesis del compuesto, liberación de su hidrógeno contenido mediante pulsos de microondas y simulación del calentamiento de la muestra.

Por último, la viabilidad económica de la comercialización del producto obtenido en esta última etapa de la tesis fue explorada mediante el desarrollo de un modelo de negocio (***capítulo 6***) que ofrece pilas de diferentes potencias mediante el uso de hidruros para el almacenamiento de hidrógeno y celda de combustible para transformarlo en electricidad.

Figura 5. Logotipo y nombre de la empresa propuesta.

Quiero comenzar dando las gracias a Ángel Martín y Mª Dolores Bermejo, que junto a Mª José Cocero confiaron en mí y me han dado la oportunidad de conocer el mundo de la investigación. Además de guiarme y ayudarme han sido para mí un ejemplo de humildad y constancia. No debo olvidarme de Alexander Navarrete, de quien he aprendido otro punto de vista de la ciencia, más alejada del sin duda mejorable sistema que existe y más cercano a la verdadera pasión y vocación científica. Nunca olvidaré las conversaciones que hemos mantenido, y espero que sean el preludio de muchas más. Ha sido un lujo trabajar con vosotros.

Tampoco puedo dejar de mencionar al resto de profesores del grupo de investigación, a todos mis compañeros y a los técnicos, sin duda sin ellos el trabajo hubiera sido mucho más arduo y los objetivos alcanzados mucho menores. De ellos también he aprendido la necesidad de trabajar con un buen equipo que no falle ni en lo profesional, ni en lo humano.

En la última parte de mi tesis he podido también entrar en contacto con el mundo del emprendimiento, (que no es solo una actividad sino también una actitud ante la vida), y la necesidad de explorar el potencial de los resultados que obtenemos en la investigación. Sin duda valores que se deberán tener en cuenta por todos en tiempos no muy lejanos. Gracias en especial a todos los miembros de Un-Em, a Javier Cid y a Pedro Ignacio por vuestro tiempo, atención y dedicación.

I would like to acknowledge Prof.Dr. Željko Knez, head of the Laboratory of Separation Processes and Product Design (University of Maribor, Slovenia), for the possibility to carry out a research collaboration in his group. I would also like to acknowledge Dr. Zoran Novak and Tanja Fajfar for their support and kindness.

I am also grateful to Prof.Dr. Andrzej Stankiewicz for giving me the possibility of doing a research collaboration in his group Intensified Reaction & Separation Systems (Delft University of Technology**,** Netherlands) and Dr. Georgios Stefanidis and Dr. Guido Sturm for their guidance during my stay.

Me gustaría también agradecer al Ministerio de Economía y Competitividad del Gobierno de España que a través del proyecto ENE2011-24547 ha financiado toda la investigación realizada.

Llegado a este momento de mi vida me vienen también a la cabeza los pasos dados hasta antes de llegar a la investigación, y que sin duda marcaron mi carácter y valores. Toda mi educación con todos los profesionales que me han ayudado y mis padres, siempre volcados con sus hijos. Después en el colegio San Gabriel tuve mi primer trabajo como profesor. Allí tuve la suerte de coincidir con grandes personas como su director Enrique García, de quien admiré su ilusión por el trabajo y por aportar a la sociedad. Y a Mario, quien lejos de buscar una vida cómoda mantenía aún su curiosidad por seguir creciendo y abordar nuevos retos. Sin duda sois ejemplos para mí.

Dejando la formación y los trabajos quiero mencionar a mis amigos, que a pesar de no ser numerosos, son de verdad. John Lennon dijo una vez que ser honesto puede que no te dé muchos amigos, pero te dará los amigos adecuados. Siempre me han escuchado y ayudado en lo que han podido. Gracias a todos, podéis siempre contar conmigo.

Como no mencionar a Esther, mi compañera en los buenos y en los malos momentos. También debo a la tesis que nuestros caminos se hayan cruzado. Me siento muy afortunado de poder compartir mi vida con alguien tan especial.

Quiero terminar dando las gracias a mi familia. Sin duda no sería la persona que soy sin ellos. Siempre han dejado todo por mí, por aconsejarme, por ayudarme…no miento si digo que me considero una persona privilegiada por tenerlos a mi lado.

Compañeros, profesores, amigos, familia, Padre: GRACIAS!!!

Luis Miguel Sanz Moral (Aranda de Duero -Burgos, 1986) started the studies of Chemical Engineer at the University of Valladolid in 2004. In the academic course of 2009-2010, she spent 9 months at the University of Birmingham (Birmingham, United Kingdom) in the frame of the Erasmus Program. At the return from England, he graduated (June, 2010), and afterwards, he started to work as teacher of job training, getting in contact with several companies demands. Simultaneously his curiosity and environmental consciousness make him study the Specialist in Renewable Energies title of the University of Valladolid. Few months later, in November 2011, he gave up her job in order to start a PhD in the High Pressure Processes Group of the Department of Chemical Engineering (University of Valladolid). His PhD was focused in preparation of novel materials to store hydrogen in solid state and to intensify the energy requirements for this porpoise. In 2011, he was at the Laboratory of Separation Processes and Product Design (University of Maribor, Slovenia). During a month he could learn from their experience in aerogel synthesis. And in 2014, he was at the Intensified Reaction & Separation Systems group (Delft University of Technology**,** Netherlands) during 4 months. There he got in contact with the importance of the process intensification.

The synthesis of aerogels of different nature, its surface functionalization and metal and/or hydride deposition inside its pores along with the energy intensification of the release of hydrogen from impregnated hydrides, are the main topics which have been investigated by the author. Lastly he became aware of the importance of the need of the research results industrial valorization and transfer.

ACADEMIC TRAINING

- Chemical Engineer at the University of Valladolid, 2004-2010.
- 9 months at the University of Birmingham (Birmingham, United Kingdom) in the frame of the Erasmus Program, 2009-2010.
- Specialist in Renewable Energies title of the University of Valladolid, 2010-2011.
- Official Master in Investigation in Fluid Thermodynamics, 2011-2012. Final master project: Silica aerogels synthesis and functionalization.

STAYS IN FOREIGN RESEARCH INSTITUTES

- Laboratory of Separation Processes and Product Design (University of Maribor, Slovenia), in 2011 (1 month). Topic: Synthesis of silica aerogels.
- Intensified Reaction & Separation Systems group (Delft University of Technology**,** Netherlands), 2014 (4 months). Topic: Development of a system for the hydrogen release from hydrides by applying microwaves.

SUPERVISOR OF RESEARCH PROJECTS

- Fabian Holtz, Master Thesis. Topic: Investigation into dry and wet impregnation techniques of metal hydrophilic silica aerogels and –phobic.

LIST OF PUBLICATIONS

- **Sanz-Moral L.M.**, Rueda M., Nieto A., Novak Z., Knez Z., Martín Á.. Gradual hydrophobic surface functionalization of dry silica aerogels by reaction with silane precursors dissolved in supercritical carbon dioxide. Journal of Supercritical Fluids, 2013, 84, 74-79.
- **Sanz-Moral L.M.**, Rueda M., Mato R., Martín Á.. View cell investigation of silica aerogels during supercritical drying: Analysis of size variation and mass transfer mechanisms. Journal of Supercritical Fluids, 2014, 92, 24-30.
- Rueda M., **Sanz-Moral L.M.**, Nieto-Márquez A., Longone P., Mattea F., Martín Á.. Production of silica aerogel microparticles loaded with ammonia borane by batch and semicontinuous supercritical drying techniques. Journal of Supercritical Fluids, 2014, 92, 209-310.

- Rueda M., **Sanz-Moral L.M.**, Martín Á.. Micronization of Magnesium Acetate by the Supercritical Antisolvent Process as a Precursor for the Production of Magnesium Oxide and Magnesium Hydride. Crystal Growth & Design, 2014, 14, 4768–4776.
- Navarrete A., Muñoz S., **Sanz-Moral L.M.**, Brandner J.J., Pfeifer P., Martín Á., Dittmeyer R., Cocero M.J. Novel windows for "solar commodities": a device for CO_2 reduction using plasmonic catalyst activation. Faraday Discussions, 2015, 183,249.
- Mustapa A.N., Martin Á., **Sanz-Moral L.M.**, Rueda M., Cocero M.J.. Impregnation of medicinal plant phytochemical compounds into silica and alginate aerogels. Journal of Supercritical Fluids, 2016, 116, 251-263.
- **Sanz-Moral L.M.**, Romero A., Holz F., Rueda M., Navarrete A., Martín Á.. Tuned Pd/SiO_2 aerogel catalyst prepared by different synthesis techniques. Journal of the Taiwan Institute of Chemical Engineers, 2016, 65, 515–521.
- Rueda M., Sanz-Moral L.M., Segovia J.J.,Martín Á.. Enhancement of hydrogen release kinetics from ethane 1,2 diamineborane (EDAB) by micronization using Supercritical Antisolvent(SAS) precipitation. Chemical Engineering Journal, 2016, 306, 164–173.
- Rueda M., **Sanz-Moral L.M.**, Girella A., Cofrancesco P., Milanese C., Martín Á.. Reversible hydrogen sorption in the composite made of magnesium borohydride and silica aerogel. International Journal of Hydrogen Energy, 2016, 14, 15245–15253.

SUBMITTED

- **Sanz-Moral L.M.**, Navarrete A., Sturm G., Link G., Stefanidis G., Rueda M., Martín Á.. Release of hydrogen from nanoconfined hydrides by application of microwaves. Advanced Energy Materials, 2016, submitted.

PATENTS

- Luis Miguel Sanz Moral, Miriam Rueda Noriega, Alexander Navarrete Muñoz, Ángel Martín. **Patente Nacional 201500170.** Material y procedimiento para el almacenamiento y regulación de la liberación de hidrógeno en estado sólido.
- Luis Miguel Sanz Moral, Miriam Rueda Noriega, Alexander Navarrete Muñoz, Ángel Martín. **Patente Nacional solicitada.** Material poroso o en celosía con vacío en sus poros para reducir su peso.

CONTRIBUTIONS TO CONGRESSES

ORAL COMUNICATIONS

- **Sanz Moral L.M.**, Martín Á., Cocero M.J.. Silica Gels Development and Functionalization. 4th International Seminar on Engineering Thermodynamics of Fluids. 23-24 July 2012, Tarragona (Spain).
- **Sanz Moral L.M.**, Martín Á., Cocero M.J.. Silica aerogels gradual surface functionalization. 6th International Symposium on High Pressure Processes Technology. 8-11 September 2013, Belgrade (Serbia).
- **Sanz Moral L.M.**, Rueda M., Martín Á., Cocero M.J.. View cell investigation of silica aerogels during supercritical drying: Analysis of size variation and mass transfer mechanisms. International Seminar on Aerogels – 2014. 6-7 October, Hamburg (Germany).
- Navarrete A., Muñoz S., **Sanz-Moral L.M.**, Brandner J.J., Pfeifer P., Martín Á., Dittmeyer R. and Cocero M.J.. Novel windows for "solar commodities": a device for CO_2 reduction using plasmonic catalyst activation. Carbon Dioxide Utilisation: Faraday Discussion. 7-9 September 2015, Sheffield (United Kingdom).
- Rueda M. , **Sanz-Moral L.M.**, Martín Á.. Enhanced hydrogen storage material by stabilization of ammonia borane nanoparticles in microparticles of silica Aerogel. 2015 E-MRS Fall Meeting and Exhibit. 15-18 September 2015, Warsaw (Poland).
- Martín Á., Navarrete A., Muñoz S., **Sanz-Moral L.M**., Brandner J.J., Pfeifer P., Cocero M.J.. CO_2 reduction using plasmonic catalyst activation employing catalyst nanoparticles dispersed into transparent aerogels. IV Iberoamerican Conference on Supercritical Fluids ProSCiba. 28 March-1 April 2016, Viña del Mar (Chile).
- **Sanz-Moral L.M.**, Romero A., Holz F., Rueda M., Navarrete A., Martín A. Tuned Pd/SiO_2 aerogel catalyst by different synthesis techniques. 5° Encontro Português de Jovens Químicos (PYCheM) e 1° Encontro Europeu de Jovens Químicos (EYCHeM). 26-29 April 2016, Guimarães (Portugal).
- **Sanz-Moral L.M.**, Rueda M., Navarrete A., Romero A., Nieto A., Martín Á.. Síntesis y funcionalización de aerogeles para su uso en catálisis y almacenamiento de hidrógeno. II Encuentro de Jóvenes Investigadores de la Sociedad Española de Catálisis. 27-29 June 2016, Ciudad Real (Spain).
- Muñoz S., Navarrete A., **Sanz-Moral L.M.**, Martín Á, Cocero M.J.. Improvement of the kinetics of hydrogen release from hydrides confined in silica aerogel. II Encuentro de

Jóvenes Investigadores de la Sociedad Española de Catálisis. 27-29 June 2016, Ciudad Real (Spain).

- **Sanz-Moral L.M.**, Navarrete A., Sturm G., Link G., Stefanidis G., Rueda M., Martín Á.. Hydrogen from solids by microwave influence. 3rd Global Congress on Microwave Energy Applications - CPCD. 25-29 July 2016, Cartagena (Spain).
- Rueda M., **Sanz-Moral L.M.** , Girella A. , Cofrancesco P. , Milanese C., Martín Á.. Improvement properties in the composite magnesium borohydride infiltrated in silica aerogel. 5th International Symposium on Metal-Hydrogen Systems. 7-12 August 2016, Interlaken (Switzerland).
- **Sanz-Moral L.M.**, Navarrete A., Sturm G., Link G., Stefanidis G., Rueda M., Martín Á.. Microwave for H_2 release from 1,2-diaminoborane infiltrated in C/SiO_2 aerogel. 5th International Symposium on Metal-Hydrogen Systems. 7-12 August 2016, Interlaken (Switzerland).
- Muñoz S., Navarrete A., **Sanz-Moral L.M.**, Martín Á., Dittmeyer R., Cocero M.J.. Carbon dioxide hydrogenation by means of plasmonic resonance activation. 22nd International Congress of Chemical and Process Engineering (CHISA). 27-31 August, Prague (Czech Republic).

POSTER COMUNICATIONS

- **Sanz Moral L.M.**, Martín Á., Cocero M.J.. Size variation of silica aerogels during SCD. 6th International Symposium on High Pressure Processes Technology. 8-11 September 2013, Belgrade (Serbia).
- **Sanz Moral L.M.**, Rueda M., Cocero M.J., Martín Á.. MgH_2/Pd Nanoparticles embeded in silica aerogel monoliths. 14th International Symposium on Metal-Hydrogen Systems: Fundamentals and applications. 20-27 July 2014, Manchester (United Kingdom).
- Rueda M., **Sanz Moral L.M.**, Martín Á., Cocero M.J.. Micronized MgH_2 and MgO by supercritical anti solvent process . 14th International Symposium on Metal-Hydrogen Systems: Fundamentals and applications. 20-27 July 2014, Manchester (United Kingdom).
- Rueda M., **Sanz Moral L.M.**, Martín Á., Cocero M.J.. Hydrogen storage by stabilizing magnesium hydride in microparticles of silica aerogel. International Seminar on Aerogels – 2014. 6-7 October, Hamburg (Germany).
- **Sanz-Moral L.M.,** Holz F., Rueda M., Romero A., Navarrete A, Cocero M.J., Martín Á.. Pd nanoparticles embeded in SiO_2 aerogels as catalyst for H_2 liberation from hydrides.

International Summer School "Nanosciences Ile-de-France". 21-26 June 2015, Étiolles (France).

- **Sanz-Moral L.M.,** Rueda M. , Navarrete A, Stefanidis G., Sturm G. Martín Á.. Carbon/Silica composite as matrix for ethane 1,2-diamineborane. 2015 E-MRS Fall Meeting and Exhibit. 15-18 September 2015, Warsaw (Poland).
- Muñoz S., Navarrete A., **Sanz-Moral L.M.**, Brandner J.J., Pfeifer P., Martín Á., Dittmeyer R. y Cocero M.J.. Conversion of carbon dioxide into useful products by means of plasmonic catalyst activation. VIll Reunión de Expertos en Tecnologías de Fluidos Comprimidos (FLUCOMP). 16 – 18 September 2015, Cádiz (España).
- Martín Á., Navarrete A., Rueda M., **Sanz-Moral L.M.**, Romero A.. Improvement of the kinetics of hydrogen release from hydrides confined in silica aerogel. IV Iberoamerican Conference on Supercritical Fluids ProSCiba. 28 March-1 April 2016, Viña del Mar (Chile).

PRIZES

- **Premio Prometeo convocatoria 2013** (organizado por la Fundación General de la Universidad de Valladolid), Liberación rápida de H_2 desde hidruros en soportes porosos mediante aplicación de microondas.
- **2° Premio Vivero 2016** (organizado por la Fundación Universidades y Enseñanzas Superiores de Castilla y León -FUESCYL)), **"HIDROWAVE"** Microondas para la liberación de H_2 almacenado en estado sólido para uso como combustible en diferentes vehículos.
- **Premio Doctor TC 2015**: CONVOCATORIA PARA APOYAR LA FINALIZACION DE TESIS DOCTORALES RELACIONADAS CON NECESIDADES EMPRESARIALES (organizado por la Fundación General de la Universidad de Valladolid).
- **Premio YUZZ VALLADOLID** al mejor plan de empresa "LIGHTENERGY" (organizado por el Centro Internacional del Santander Emprendimiento –CISE)
- **Premio Prometeo convocatoria 2016** (organizado por la Fundación General de la Universidad de Valladolid), Material poroso o en celosía con vacío en sus poros para reducir su peso.